TRIBHUVAN UNIVERSITY

INSTITUTE OF ENGINEERING

DEPARTMENT OF CIVIL ENGINEERING

FINAL YEAR PROJECT on

OBSERVATION OF CHANGE IN STORAGE OF KULEKHANI RESERVOIR USING STANDARD OPERATING POLICY

Submitted by:

Alija Subedi (076BCE014)

Biplov Nepal (076BCE058)

Dip Sagar Gnawali(076BCE071)

Hemanta Adhikari(076BCE078)

Kabindra Sharma Chapagain(076BCE083)

Saurab Baral(076BCE157)

Supervisor:

Prof.Dr.Bhola Nath Sharma Ghimire

Baisakh, 2081

TRIBHUVAN UNIVERSITY

INSTITUTE OF ENGINEERING

DEPARTMENT OF CIVIL ENGINEERING

FINAL YEAR PROJECT on

OBSERVATION OF CHANGE IN STORAGE OF KULEKHANI RESERVOIR USING STANDARD OPERATING POLICY

IN PARTIAL FULFILLMENT OF THE REQUIREMENT FOR THE AWARD OF BACHELOR DEGREE IN CIVIL ENGINEERING

(Course Code: CE755)

Submitted by:

Alija Subedi (076BCE014)
Biplov Nepal (076BCE058)
Dip Sagar Gnawali(076BCE071)
Hemanta Adhikari(076BCE078)
Kabindra Sharma Chapagain(076BCE083)
Saurab Baral(076BCE157)

Supervisor:

Prof.Dr.Bhola Nath Sharma Ghimire

Baisakh, 2081

TRIBHUVAN UNIVERSITY

INSTITUTE OF ENGINEERING

DEPARTMENT OF CIVIL ENGINEERING

CERTIFICATE

This is to certify that this project work entitled **"**Observation of change in storage of Kulekhani Reservoir using Standard Operating Policy**"** has been examined and declared successful for the fulfillment of academic requirements towards the completion of a Bachelor's Degree in Civil Engineering.

………………………

Supervisor

Prof.Dr.Bhola Nath Sharma Ghimire

……………………

HOD,Department of Civil Engineering

Prof.Dr. Gokarna Bahadur Motra

…………………..……

External Examiner

Prof.Dr. Prem Chandra Jha

………………..………

Internal Examiner

Asst. Prof. Suresh Manandhar

COPYRIGHT [©]

The author of this project report has agreed that the Department of Civil Engineering Pulchowk Campus and Pulchowk Campus Library can make it freely available for further inception.

The plagiarism and publication of the thesis for financial gain without the approval of the supervisor of this project, the Department of Civil Engineering, and author's written permission is strictly prohibited.

The authors have agreed to copy the report for which permission may be granted by the supervisor, or in his absence; the department of Civil Engineering, Pulchowk Campus.

Request to make a copy or any other use of the material in whole or part should be addressed to:

Head of Department

Department of Civil Engineering

Pulchowk Campus

Institute of Engineering

Lalitpur, Nepal

ACKNOWLEDGEMENT

Abstract

The Kulekhani Hydropower Plant has seen fluctuation in power supply due to variance in power production throughout the year. During the dry season discharge through Kulekhani reservoir catchment streams has significantly decreased which ultimately varies in storage level of the reservoir. Therefore, this study aims to assess the hydrological and numerical models for analyzing efficient power supply policies. For the selection of hydrological models, non-linear regression model was used for the calculation of the discharge. The simulated discharge was compared with observed discharge, obtained precise data was calibrated and model performance was validated with calibrated parameters. The result showed the coefficient of determination 0.89, NSE 0.85 and PBIAS -12.94% for calibration period and coefficient of determination 0.94, NSE 0.72 and PBIAS 14.96% for validation period. The Standard Operating Policy (SOP) was used for balancing demand, supply and delivery of energy production. The SOP algorithm was used to observe the change in head variation of the reservoir and simulate the reservoir operation from 2010-2022. The simulation showed that the energy demand was fulfilled for most of the time except for the few months. Forecasted precipitation from CMIP6 tool was used to forecast future discharge and the SARIMAX model was used to forecast the future power generation from January,2023 to December,2029 using best fitted parameter (0,1,2) and (1,2,2,12) with minimum AIC value. The result showed that there is a gradual decline in the power production for the future. Forecasted discharge and forecasted energy generation was again used to simulate the future storage level of the reservoir.

Table of Contents

LIST OF TABLES

LIST OF FIGURES

ABBREVIATIONS

AIC	Akaike Information Criterion
ARIMA	Autoregressive Integrated Moving Average
CMIP6	Coupled Model Intercomparison Project Phase 6
CRMSD	Centralized Root Mean Squared Deviation
DEM	Digital Elevation Model
EQM	Empirical Quantile Mapping
GCM	Global Climate Models
KGE	King Gupta Efficiency
Masl	Meters above sea level
MBE	Mean bias error
MME	Multi-model ensemble
MOO	Multi-Objective Optimization
MWh	MegaWatt-hour
OLR	Outgoing Longwave Radiation
QM	Quantile Mapping
RCP	Representative Concentration Pathway
RMSE	Root mean square error
SARIMA	Seasonal Autoregressive Integrated Moving Average
SOP	Standard Operating Policy
SRES	Special Report on Emissions Scenarios
SSP	Shared socioeconomic pathways
SST	Sea Surface Temperature

1. Introduction

1.1 Background

Reservoir operations refer to managing the flow of river water over time while storing excess water and using it during times when water is scarce. Such studies are critical in guaranteeing a dependable water supply for all needs, including municipal, irrigation, hydropower generation, flood control, and recreation. They answer the question of when and how much water to release, which is beneficial for planning and operation under a particular time scale. (K. Srinivasan, 1999)

Simulation models are constructed with historical data of river inflows, and the performance is assessed relative to the reservoir`s operating rules. Different performance parameters can be used, including economic indicators and release-based information. Although, it is more preferable that the benefit be scaled to a monetary term when objectively evaluating the project, non-monetary goals such as social equity and environmental sustainability are also important. Different release policies are applied depending on the project's context. The Standard Operating Policy is a simplistic model often used in planning models. The policy is designed to release the current demand and confer no importance for the value of water for the following time-season. (Stedinger, 1984)

In recent times, there has been an increase in demand of energy in our country. The current ROR and peak ROR hydropower projects meet demand during wet season. The energy produced by these projects can't meet demand during dry season. Therefore, the storage type projects are essential in our country to meet the energy demand. Nepal also requires enhance method of reservoir operation policy and optimization policies for existing storage projects and future storage projects. Research on reservoir operation policies have been extensively conducted, but there is a significant lack of research regarding the release policies.

1.2   Problem Statement

Maximum energy consumption is the crucial factor for varying power demand. Population growth affects the per capita consumption of energy leading to insufficient power. Thus, optimum power production with appropriate reservoir storage level is necessary. Storage type power plants generate electricity during peak hour and there hasn't been any operating policy till date. Therefore, it is necessary to observe the change in head of the reservoir which requires a computer algorithm to analyze the reservoir operation which ultimately helps in developing a suitable reservoir operation policy and optimization of the reservoir.

1.3   Objectives

The main objective of this project is to simulate the power production of the Kulekhani reservoir which is listed as follow:

- To observe the change in storage and power production of the Kulekhani reservoir using Standard Operating Policy

- To forecast future power generation from year 2023 to 2029

1.4   Scope of the Study

The scope of the study comprises the following:

- Study and analysis of the historical trend of rainfall.

- Study of Volume-Elevation-area graph.

- Identification and analysis of Hydrological model

- Study and analysis of the Standard Operating Policy

- Power generation forecasting using SARIMAX models

- Simulation of future storage level

1.5   Limitations of the study

Although the model is highly correlated with the recorded data, the model is not an exact representation of the actual operation. The limitation can be enlisted under following points

- Infiltration losses are not incorporated in this model.

- The operation hour data is essential for the exact determination of power demand. The operation hour data was not available which is an important limitation.

- The DEM resolution of Kulekhani reservoir available for this project is 5x5 m. The model would perform better if the resolution was even better.

2   Study Area

The Kulekhani watershed lies in the north-eastern part of Makwanpur District in the Central Development Region. Tribhuwan Highway passes from upper part of basin. The catchment area is drained to Palung khola from the west to the east and many tributaries flowing from the north, the south, and the west merge into Palung khola. The elevation varies from 1534m at the dam crest to 2621m at the peak of Simbanjang of Mahabharat Range.

The four hydrological stations of Kulekhani catchment area are Daman, Chisapani, Markhu of Makawanpur district and Dhunibesi of Dhading district. It extends from northeast to south of Chisapani. West region of catchment area i: e (Daman) has an elevation of 2265m at the peak of Mahabharat Range. Latitude and Longitude of four hydrological stations are enlisted as;

Table 2.1 Latitude and Longitude of four hydrological stations

SN	Index No.	Name of Stations	Latitude	Longitude
1	905	Daman	27.604389N	85.09197E
2	904	Chisapani	27.559732N	85.1386E
3	915	Markhu	27.6190N	85.1496E
4	1038	Dhunibesi	27.68819N	85.22131E
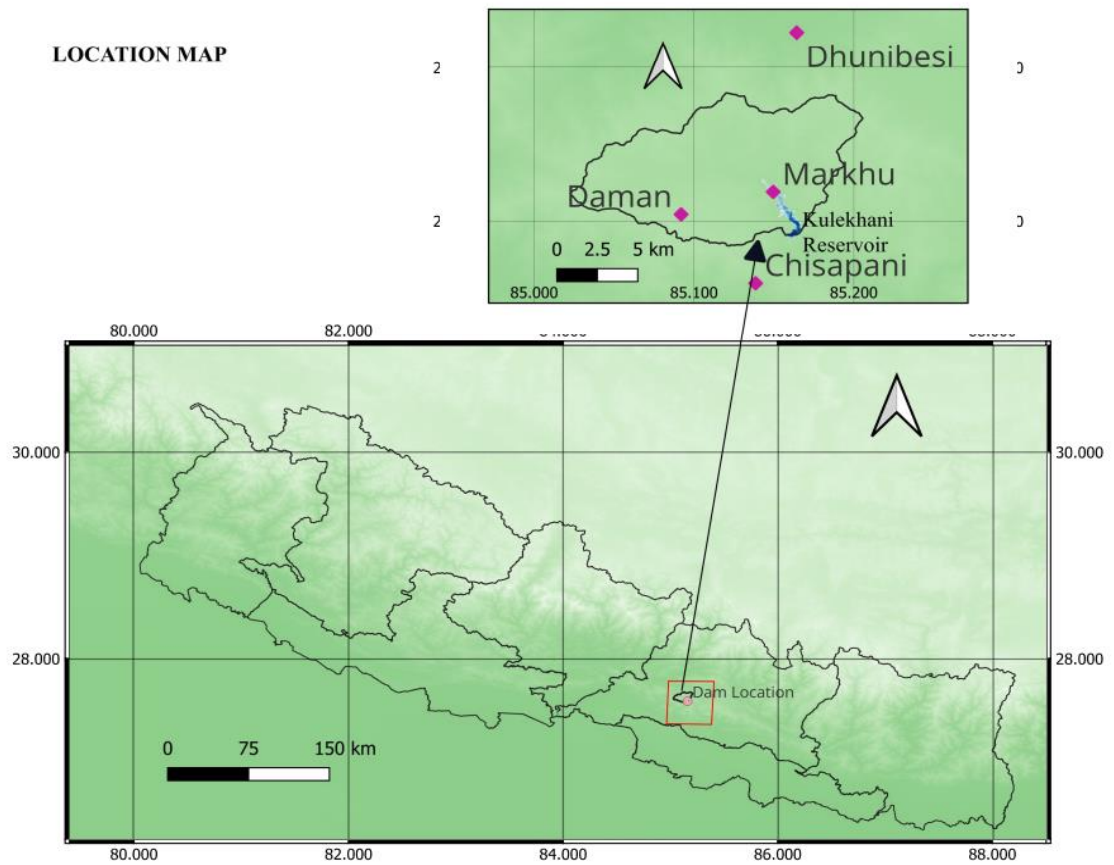
Figure 2.1 Location Map of Kulekhani Catchment Area

2.1 Major Features

The main structure of the Kulekhani-I Hydroelectric Power Station is a dam with a spillway and two radial gates and a water intake system. Water taken from the reservoir is passed through a headrace tunnel, a surge tank and penstock pipe to an underground power house near Bhimphedi. Power generated is evacuated from its switchyard through two 29 km long double circuit 66Kv transmission line to Hetauda substation.

Although the planet is constructed for peak hour generation, the shortfall in energy forced this power station to run even during off-peak hours. In 1990, the old and existing conventional type of excitation system, which was giving problems from time to time, was replaced by a brushless excitation system, under the financial assistance from the OECF of Japan. Replacement of two 72KV MOCB by SF6 gas circuit breaker was also done. (NEA Annual Report, 2022)

This power station was generating power as per requirement till 1993, when a disaster took place due to unprecedented flood, sweeping away the penstock at Jurikhet river crossing and filling up the reservoir by the unexpected volume of 52 million cubic meter silt. NEA with consultant Nippon Koei of Japan refurbished the damaged infrastructure by constructing a new sloping intake check dam, installing a new telemetering system and taking the penstock underground below bed- rock at Jurikhet. A 16 Km long road connecting the powerhouse to the dam and reservoir area was also part of this rehab project. (NEA Annual Report, 2022)
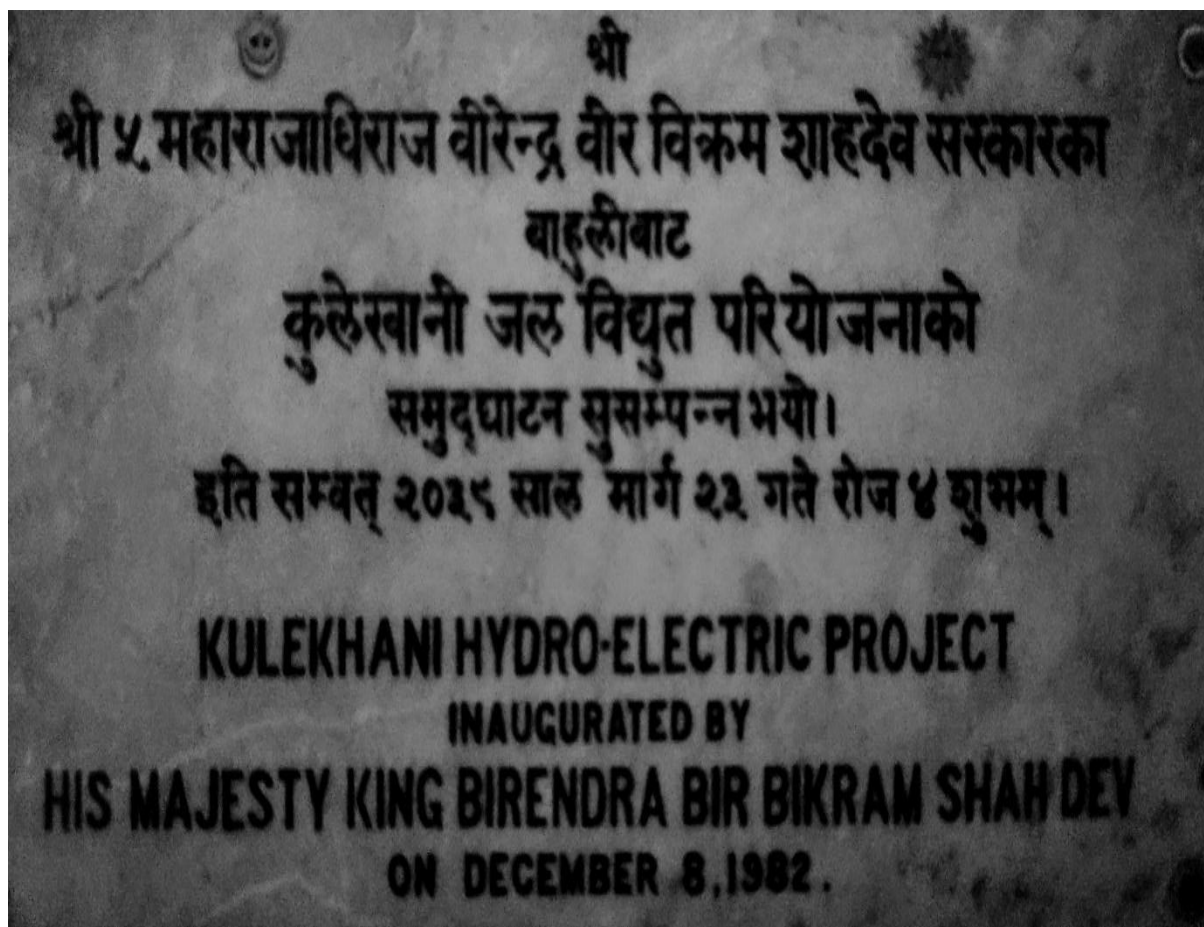
Figure 2.2 Inauguration of Kulekhani Hydropower Project

(NEA, 2022)

3 Literature review

3.1 Hydrological Model

Hydrological modeling is used to answer environmental transport questions where water excess, scarcity, or dissolved or solid content is of primary importance. The most effective model is the one that achieves results closely resemble reality employing minimal parameters and complexity.

Regression Equation is highly regarded for its capabilities in hydrology. The Regression Model outperformed another model (HEC-HMS) in Kulekhani Catchment to simulate the runoff.

3.2 Standard Operating Policy

The functioning of dam reservoirs is an important factor in water management research and planning. It aims to establish guidelines for the efficient operation of reservoir to meet water supply, flood control, and other environmental objectives. The research compared the three policies for improving reservoir performance: the standard operation policy (SOP), the Hedging Rule (HR), and the Multi-Objective Optimization (MOO). (K. Srinivasan, 1999)

This involves several key factors aimed at managing water resources effectively, various steps are followed to maintain SOP for reservoir operations such as;

1. Water release protocol (Based on downward demand, inflow rates, and anticipated water condition.
2. Forecasting and monitoring (Policy relies on weather forecasts, streamflow data, and hydrological models to anticipate inflows to the reservoir.
3. Multi-objective optimization (Optimization techniques and decision support systems are set to find solutions that maximize benefits across these objectives

while considering constraints such as reservoir storage capacity and operational limitations.

4. Maintenance of reservoir infrastructures along with flood management.

5. Establishing different protocols for managing the Kulekhani reservoir during the dry season, including water conservation measures, and public communication strategies.

6. Policy should specify the parameters to be monitored, including water levels, inflows, outflows, and other weather conditions.

3.3 Precipitation and Climate Projection

CMIP6, a Global Climate Model, which is for simulation of earth's past climate and predict how it may change in the future. CMIP6 model showcase notable enhancements compared to CMPIP5. The improvements include higher spatial resolution enabling finer-scale regional features. (Bourdeau-Goulet, 2021)

CMIP6 lacks fine resolution needed to capture regional features accurately. Therefore, it is necessary to downscale modeled output and to correct for any biases that may arise. (Jakob Themeßl et al., 2011) examined the effectiveness and concluded that the QM methods can be the most effective methods in correcting the biasness. QM's results were accurate (Laon et al., 2013). Quantile-based method, Empirical Quantile Mapping (EQM) has been used for downscaling and correcting biasness. The package 'qmap' is used in R to perform EQM.

GCMs proposed by Almazroui et al. (2020) and Mishra et al. (2020) for South Asia have been selected for the daily precipitation and maximum and minimum temperature.

3.4 Power Generation Forecasting

Power forecasting is predicting future electricity generation or consumption levels based on historical data, current conditions and relevant influencing factors. This

forecasting is significant for energy grid operators, utility companies, and energy traders to efficiently manage the production, transmission, and distribution of electricity, optimize resource allocation, and ensure grid stability.

There are various methods for power generation forecasting such as; time series analysis, where historical data of power generation are analyzed to identify patterns and trends. The SARIMAX model considers both seasonal and non-seasonal components. Therefore, it is used to forecast non-stationary dataset of power generation. Such hybrid models can combine time series with machine learning for better performance of the model.

4 Methodology
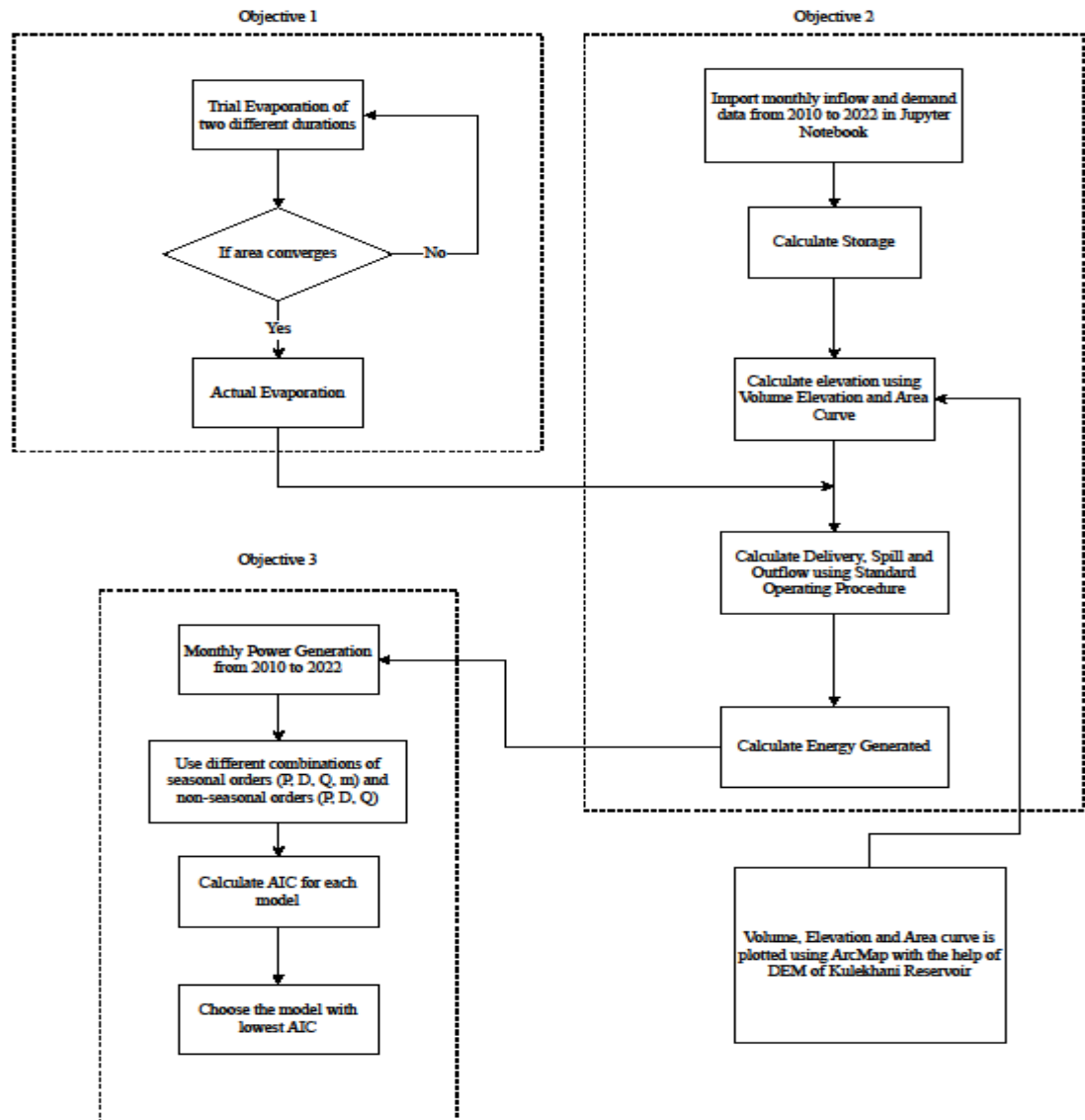
Figure 4.1 Methodology Framework of the Research

4.1 Catchment Parameters

Table 4.1 Characteristics of Kulekhani Watershed (Extracted from QGIS)

Catchment area, km^2	124
Longest stream length, km	18.6
Highest point of longest stream, m	2155
Lowest point of longest stream, m	1537
Catchment highest point, m	2566
Catchment lowest point, m	1498
Longest stream slope, %	3.32
Concentration time, hours	2.33
Snow Covered Area, km^2	0
Elevation difference between remotest point and outlet, m	618
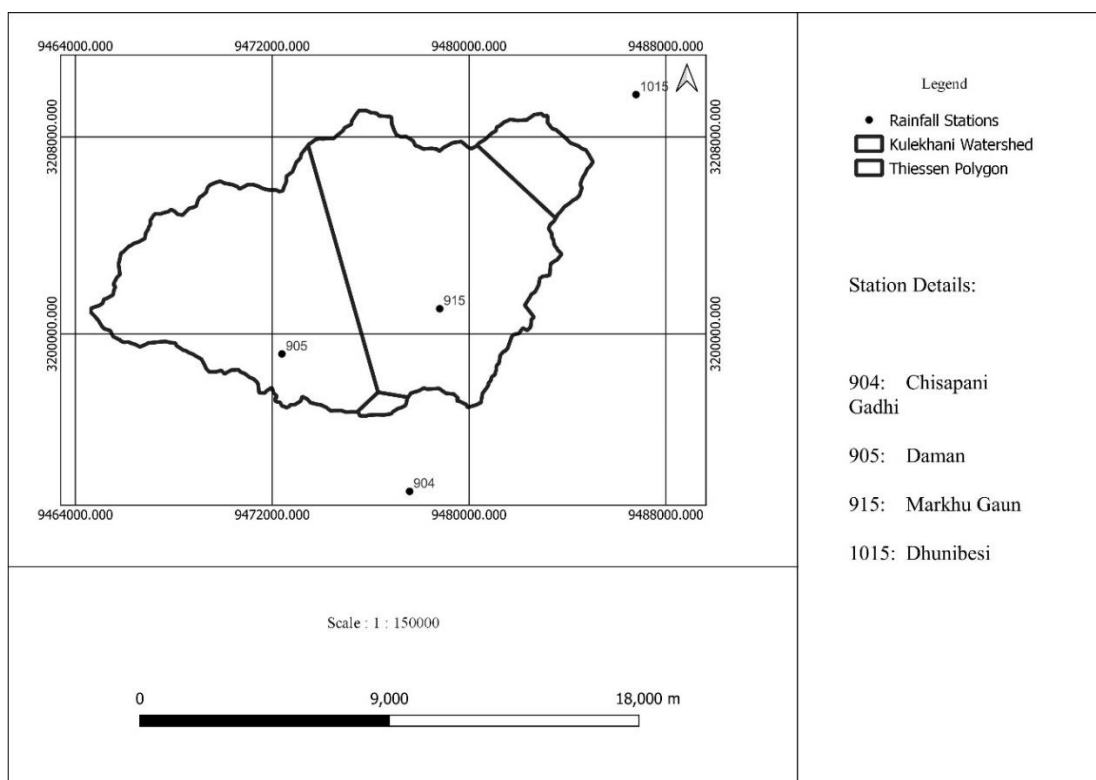
Figure 4.2 Kulekhani Catchment with Thiessen Polygon

All the catchment parameters shown above were calculated using QGIS v3.22.12.

The raster data "Digital Elevation Model" was downloaded from SRTM, a plugin in QGIS. The resolution of the raster data was 30m. (Saephan, 2022)

4.2 Rainfall analysis of Representative Stations

The Daily rainfall data of stations Daman, Chisapani Gadhi, Dhunibesi and Markhu Gaun was obtained from Department of Hydrology and meteorology (DHM). Among them Chisapani Gadhi, Dhunibesi and Markhu gaun station lies inside the catchment area of Kulekhani reservoir whereas Daman station lies outside but in the vicinity. Data consisted of daily cumulative rainfall from 1957 AD to 2023 AD.

4.2.1 Calculation of Missing Rainfall data

The stations were missing some of the data at different time interval due to several reasons such as absence of the observer, instrumental failure etc, which were find out using normal ratio method. In this method, the rainfall values at surrounding station are weighed by the ratio of normal annual rainfall. For the calculation using normal ratio method, we checked for the continuity of daily data for 30 years' time period, which was found to be from 1977/4/13 to 2007/4/13. The normal annual data for all 4 stations is shown in the Table 4.2

Table 4.2 Normal Annual Rainfall of Stations (Nepal, 2024)

S.N	STATION NUMBER	STATION NAME	NORMAL ANNUAL RAINFALL (mm)
1	0905	Daman	1724.3
2	0904	Chisapani Gadhi	2125.1
3	0915	Markhu Gaun	1439.5
4	1038	Dhunibeshi	1611.6

Here the annual normal rainfall at the surrounding gauges differs from the normal annual rainfall of the station under consideration by more than 10% so Arithmetic Average Method couldn't be used. (K.N. Dulal)

$$P_x = \frac{1}{m}\left(\frac{N_x}{N_1}P_1 + \frac{N_x}{N_2}P_2 + \cdots + \frac{N_x}{N_m}P_m\right)$$

Where,

P_x - Rainfall of missing station.

N_x – Normal annual rainfall at station X.

$N_1, N_2, \ldots N_m$ - Normal annual rainfall at the m surrounding stations.

m- Numbers of surrounding stations

$P_1, P_2 \ldots P_m$ - Precipitation at the surrounding stat

Using the above equation, we calculated missing rainfall data wherever required.

4.2.2 Check for Homogeneity

Homogeneity checks of rainfall data are essential to ensure the accuracy and reliability of the data. These checks involve assessing the data for errors, outliers, and inconsistencies that could arise due to various factors such as instrumentation errors, data transmission issues, or changes in the environment. If the data are not found to be homogenous, the dataset cannot be used. Therefore, homogeneity check is important.

Yearly cumulative data were calculated from the daily rainfall data which were later on used to check for consistency.

Using Cumulative Deviations Method:
(Buishand, 1982) provided a method of testing the homogeneity of rainfall data based

on adjusted cumulative deviations of the observed data from the mean. The null hypothesis of this test is that data are independent and randomly distributed. The cumulative sum has been defined as:

$$S_0^* = 0; \quad S_k^* = \sum_{i=1}^{k}(Y_i - Yavg) \quad , \qquad k = 1, 2, \ldots, n$$

Where,

$Y_i \forall \; i \in [0, n]$ represents the observed rainfall data and Y is the mean of the observations.

For a homogeneous record, it can be noted that the terms fS_k^* or each k fluctuate around zero. Rescaled adjusted partial sums are obtained by dividing the S_k^* 's by the sample standard deviation σ_y:

$$S_k^{**} = \frac{S_k^*}{\sigma_y} , \; k = 0,1,2 \ldots .n ,$$

Departures from homogeneity are explained by a statistic Q defined as follows by (Buishand, 1982):

$$Q = max \mid S_k^{**} \mid$$

Higher values of Q indicate that the data points are not from the same population. Critical values of the test statistic can be found in the Table 4.3:

Table 4.3 Percentage points of Q/√n (Buishand, 1982)

n	Q/√n		
	90%	95%	99%
10	1.05	1.14	1.29
20	1.10	1.22	1.42
30	1.12	1.24	1.46
40	1.13	1.26	1.50
50	1.14	1.27	1.52
100	1.17	1.29	
∞	1.22	1.36	

The yearly rainfall data for our study period i.e 1993-2022 was obtained as below (Refer Table A-1 for calculation steps):

Table 4.4 Homogeneity check from cumulative deviation method

$$S_k^{**}$$

	|S**|		
Year	Daman	Chisapani Gadhi	Markhu	Dhunibesi
1993	0.8	1.0	1.9	0.2
1994	0.4	0.8	1.2	0.4
1995	0.4	1.0	2.2	0.5
1996	0.1	1.3	2.0	0.5
1997	0.7	2.3	2.3	1.8
1998	0.5	2.8	3.0	5.6
1999	1.8	4.3	5.2	6.7
2000	3.1	5.3	5.6	6.2
2001	3.4	4.7	5.6	6.7
2002	5.3	6.2	7.4	7.9
2003	4.8	7.2	7.8	7.8
2004	5.4	7.5	7.9	7.1
2005	4.9	7.7	7.6	6.6
2006	5.0	5.0	7.3	6.3

Observation of change in storage of Kulekhani Reservoir using Standard Operating Policy
by Alija, Biplov, Dip Sagar, Hemanta, Kabindra, Saurab

23

Year	Daman	Chisapani Gadhi	Markhu	Dhunibesi
2007	5.7	6.9	7.8	5.8
2008	4.1	5.3	6.4	4.6
2009	2.8	3.9	5.7	4.0
2010	1.5	2.7	5.2	4.5
2011	2.2	2.5	5.6	4.7
2012	2.0	1.8	4.8	5.1
2013	1.7	1.5	4.3	4.3
2014	0.0	0.7	2.3	2.7
2015	1.0	0.3	0.7	1.5
2016	2.1	1.0	0.5	0.4
2017	2.6	1.2	1.3	0.2
2018	2.9	1.5	2.2	0.3
2019	2.6	1.3	1.3	0.5
2020	1.7	0.7	0.4	0.3
2021	0.3	0.3	0.1	0.6
2022	0.0	0.0	0.0	0.0
Q =	5.67	7.75	7.92	7.94
Q/√(n) =	1.04	1.41	1.45	1.45

Based on the above calculations of all the stations, the Q-statistic was computed for a significance level of 1% (i.e., a confidence interval of 99%). This value are found to be lower than the critical value for a sample size of 30. So, the null hypothesis is accepted and the available data are found to be homogeneous. (Omar M. A. Mahmood Agha, 2017)

4.3 Design Flood Estimation of Kulekhani Catchment

4.3.1 Log-Excel Method

Rainfall Analysis of four Rainfall stations were done: (904-Chisapani Gadhi, 905-Daman, 915-Markhu Gaun, 1038-Dhunibesi). The plots for every respective station are shown below. The plots represent extreme rainfall in mm at ordinate and time period in years at abscissa. (Refer Table A-2 for calculated value of design rainfall using Log-Excel Method of four stations)

The chart shows a scatter plot with a logarithmic trendline. The y-axis is labeled "Extreme Rainfall (mm)" ranging from 0.0 to 500.0. The x-axis is labeled "Time in years" on a logarithmic scale from 1 to 100. The trendline equation is:

$$y = 120.25\ln(x) + 53.074$$
$$R^2 = 0.9787$$
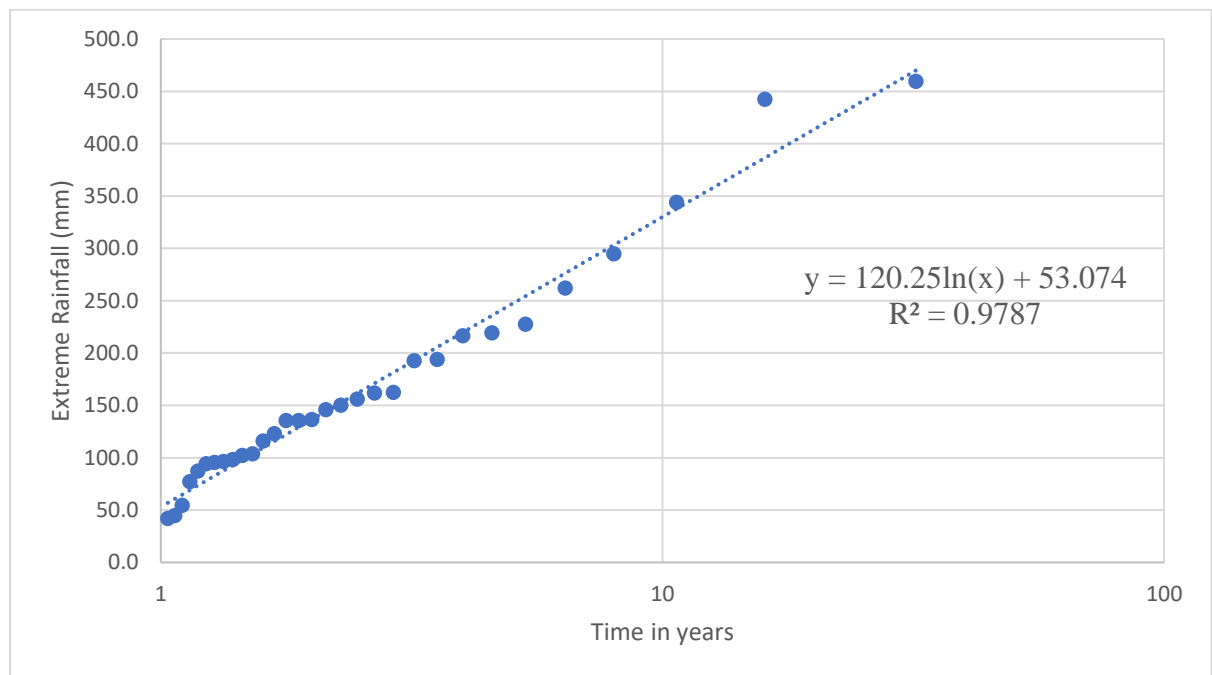
Figure 4.3 Rainfall analysis of Chisapani Gadhi Rainfall Station
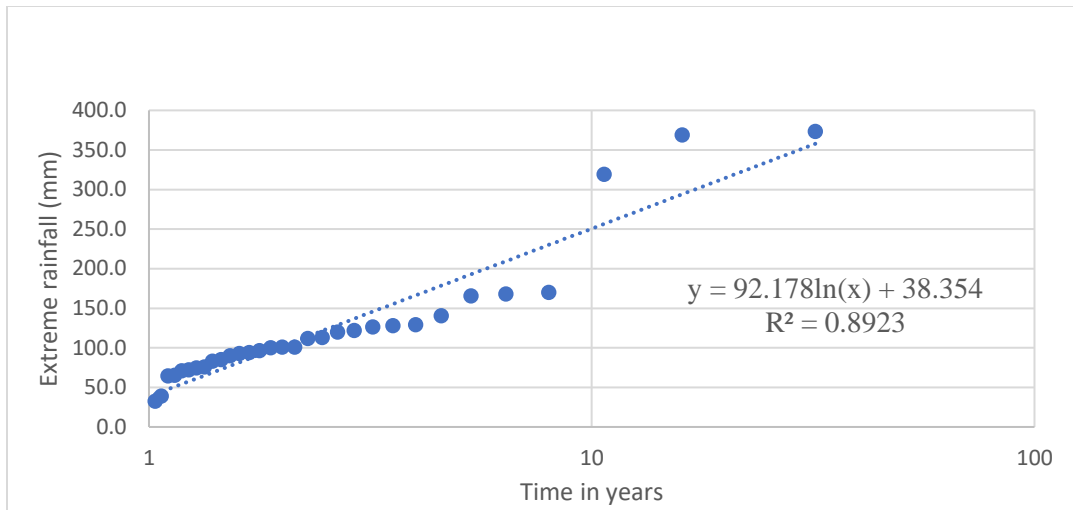
Figure 4.4 Rainfall Analysis of Daman Station using Log-excel Method
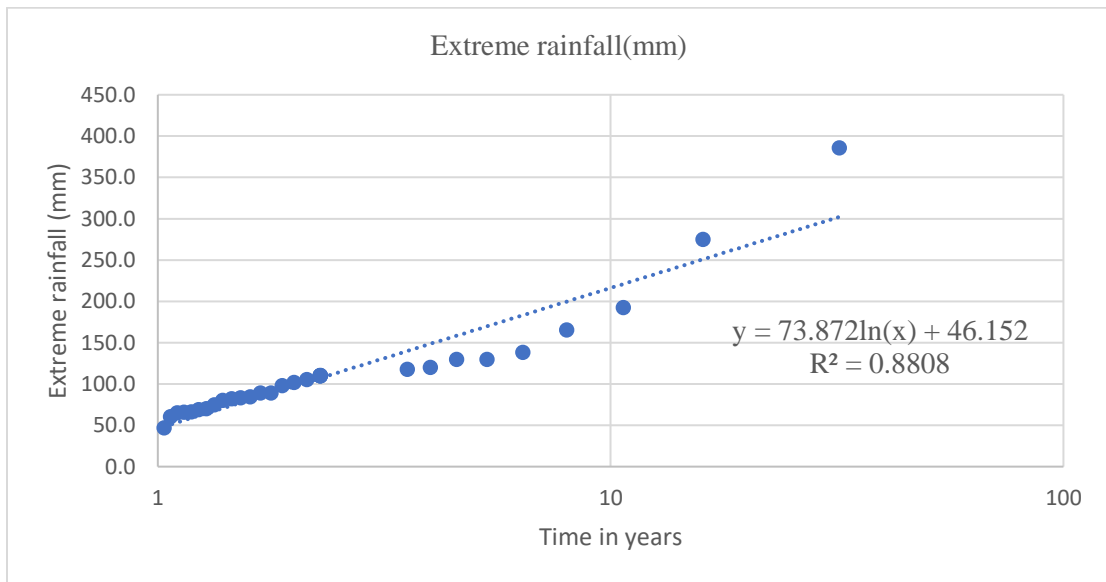
Figure 4.5 Rainfall Analysis of Markhu Gaun Station using Log-excel Method
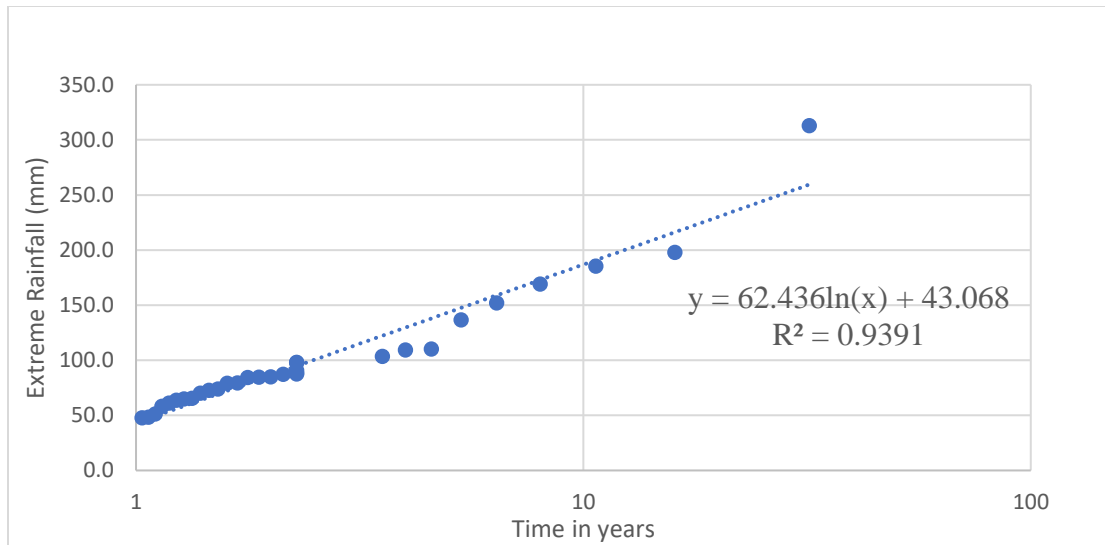
Figure 4.6 Rainfall Analysis of Dhunibesi Station using Log-excel Method

Table 4.5 Computation of Weighted Mean of Design Rainfall using Log-excel
Method

Weighted Mean of Design Rainfall from 4 stations:					
Return Period	Chisapani Gadhi	Daman	Markhu Gaun	Dhunibesi	Weighted Mean Rainfall
Weighted rainfall	0.009	0.45	0.495	0.045	1
10	329.96	250.60	216.25	186.80	231.189
50	523.49	398.96	335.14	287.29	363.065
100	606.85	462.85	386.35	330.56	419.860
200	690.20	526.74	437.55	373.84	476.656
500	800.38	611.20	505.24	431.05	551.735
1000	883.73	675.10	556.44	474.33	608.531
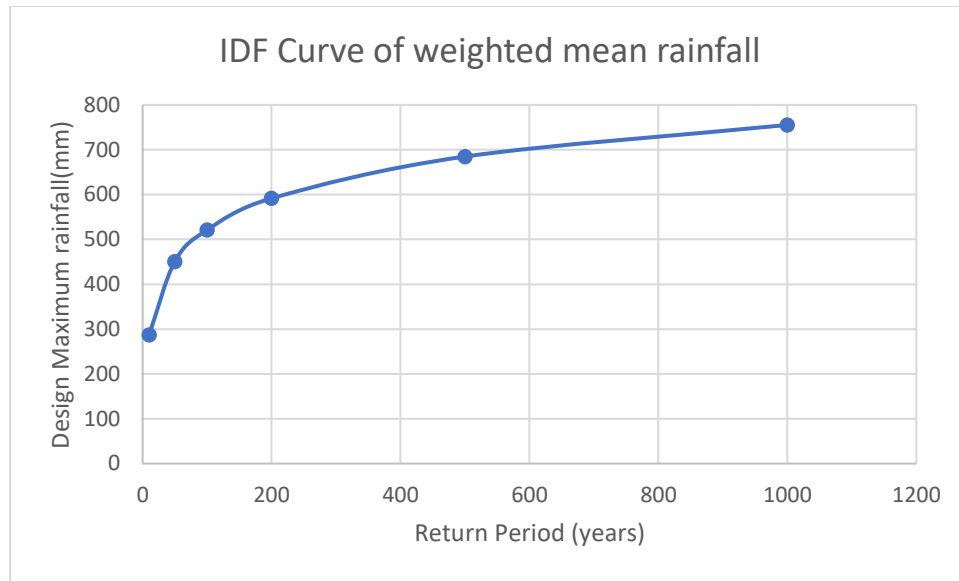
Figure 4.7 IDF Curve of weighted mean rainfall

Calculating time of concentration using Kirpich formula; (Kirpich, 1940)

$t_c = 0.01947 \times L^{0.77} \times S^{-0.385} = 0.01947 \times (18600)^{0.77} \times (0.03323)^{-0.385}$

$= 140.04$ minutes

$= 2.33$ hours

where,

L= Channel Flow Length = 18600

S = Slope of catchment = 0.03323

This 24-hour maximum rainfall has been converted into rainfall intensity by Mononobe's method as: (Chalid, 2020)

$$I = \left(\frac{R_{design}}{24}\right) \times \left(\frac{24}{D}\right)^{2/3}$$

where,

R design = Design maximum rainfall

D= duration

The discharge is calculated using Rational method

$$Q = C \times I \times A$$

where,

C= runoff coefficient = 0.35 (assumed)

A= catchment area = 124 Km^2

I = maximum rainfall intensity

Table 4.6 Design rainfall using Mononobe's method and discharge using Rational method

Return Period(years)	10	50	100
Design Rainfall(mm)	231.189	363.065	419.86
24hrs Rintensity (mm/hr)	9.63	15.127	17.5
Maximum Rintensity(for tc) (mm/hr)	45.6	71.61	82.82
$Q_{T, m3/s}$	**549.733**	**863.298**	**998.441**

Observation of change in storage of Kulekhani Reservoir using Standard Operating Policy
by Alija, Biplov, Dip Sagar, Hemanta, Kabindra, Saurab

29

4.3.2 Gumbel's method:

This is one of the most widely use extreme value prediction methods. Following key formula were used for this study.

$$X_T = \bar{X} + K\sigma_{n-1} \qquad\qquad \sigma_{n-1} = \sqrt{\frac{\Sigma(X-\bar{X})^2}{N-1}}$$

$$K = \frac{y_t - y_n}{Sn} \qquad\qquad y_t = -[\ln\ln(\frac{T}{T-1})] \qquad \text{(Rijal, 2014)}$$

Where,

X_T = Value of variate x at return period T

X = Mean of variate X

K = frequency factor

σ_{n-1} = Standard deviation of sample size N

Y_T = Reduced variate

S_n = Reduced standard deviation

Y_n = Reduced mean

Table 4.7 Flood Analysis using Gumbel method

(DhavalDwivedi, 2019)

Gumbel Method						
				Y_T	S_n	Design Rainfall
	For 31 years			0.5371	1.1159	(mm)
Stations	Chisapani Gadhi		Daman	Markhu Gaun		Dhunibesi
Weightage Factor	0.009		0.45	0.495		0.045
X mean	166.9		125.6	114.2		100.5
Standard Deviation	103.71		83.26	67.11		54.94
Return Period	Y_T	K_T	X_T			
10	2.251	1.535	326.13	253.431	217.235	184.851
50	3.901	3.015	479.62	376.658	316.561	266.163
100	4.601	3.641	544.51	428.753	358.551	300.539
200	5.295812143	4.264461101	609.17	480.6590313	400.388	334.789
500	6.213607264	5.086931861	694.47	549.1379468	455.584	379.976
1000	6.907255071	5.708535774	758.93	600.8926886	497.2998	414.126
Design Rainfall for 10 years return period(R_{10}) =						232.828
Design Rainfall for 50 years return period(R_{50}) =						342.487
Design Rainfall for 100 years return period(R_{100}) =						388.846
Design Rainfall for 200 years return period(R_{200}) =						435.032
Design Rainfall for 500 years return period(R_{500}) =						495.975
Design Rainfall for 1000 years return period(R_{1000}) =						542.031
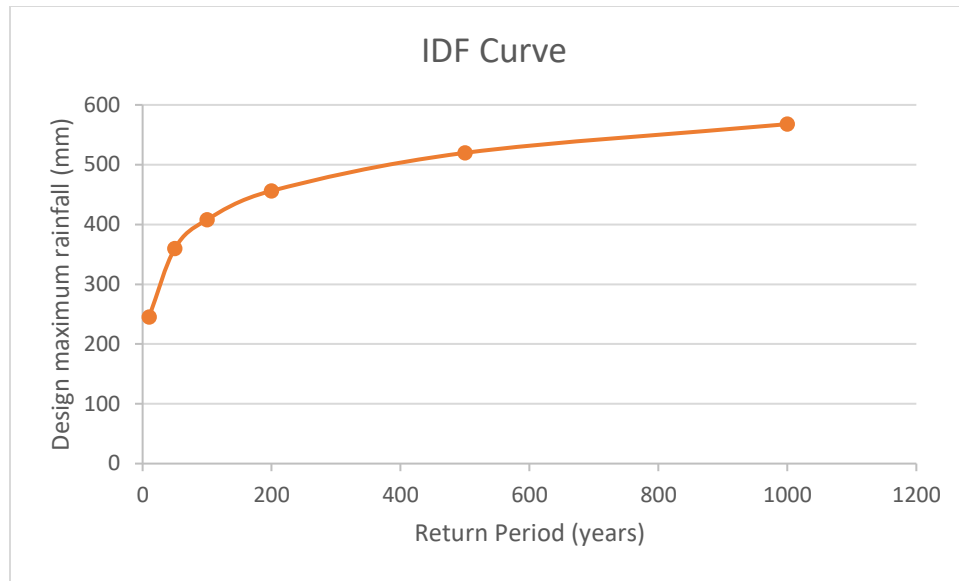
Figure 4.8 IDF curve using Gumbel Method

This 24-hour maximum rainfall has been converted into rainfall intensity by Mononobe's method as: (Chalid, 2020)

$$I = \left(\frac{R_{design}}{24}\right) \times \left(\frac{24}{D}\right)^{2/3}$$

where,

R design = Design maximum rainfall

D= duration

The discharge is calculated using Rational method

$$Q = C \times I \times A$$

where,

C= runoff coefficient = 0.35 (assumed)

A= catchment area = 124 Km^2

I = maximum rainfall inrtensity

Observation of change in storage of Kulekhani Reservoir using Standard Operating Policy
by Alija, Biplov, Dip Sagar, Hemanta, Kabindra, Saurab

32

Table 4.8 Design rainfall using Gumbel's Method and discharge using Rational method

Return Period(years)	10	50	100	200	500	1000
Design Rainfall(mm)	232.8	342.5	388.85	435	495.9	542
24hrs Rintensity (mm/hr)	9.7	14.27	16.2	18.125	20.66	22.58
Maximum Rintensity(for tc) (mm/hr)	45.92	67.55	76.7	85.8	97.64	106.91
Q_T (m³/s)	**553.59**	**814.352**	**924.66**	**1034.366**	**1177.1**	**1288.86**

Comparison of discharge from Rational method using Gumbell's design rainfall and log excel method

Table 4.9 Design Flood Discharge of different return period

Return Period (years)	Rational (Gumbel) (m3/s)	Rational (Log Excel) (m3/s)
10	553.59	549.733
50	814.352	863.298
100	924.66	998.441

Since, comparing the design maximum discharge obtained from design maximum rainfall obtained from Gumbel's method and log-excel method we found that design maximum discharge from log-excel method is more than that from Gumbel's method so we adopt the design maximum discharge from log-excel method. The design discharge calculated from Log Excel method for 50 years return period is 863.298 m³/s which is less than that of peak discharge estimated by JICA 1340 m³/s. (JICA, Disaster Prevention Study in the Central Development Region of Nepal, 1993)
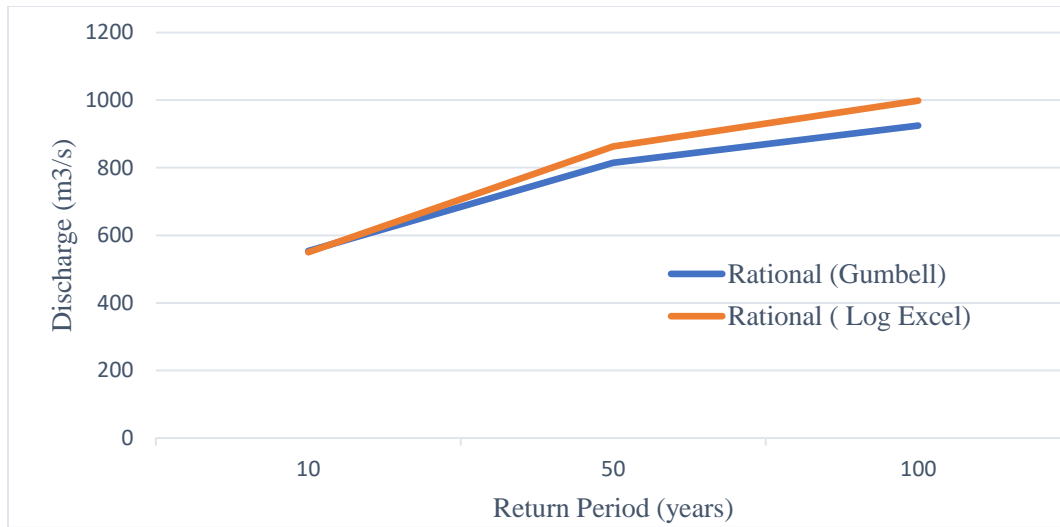
Figure 4.9 Comparison of design flood discharge of Gumbel and Log excel method

4.4 Hydrological modelling using Regression Equation

Regression analysis allows for investigating the relationship between variables. The variables are dependent and independent variables. Independent variable has impact on the dependent variable. (Montgomery DC, 2012)

In our analysis, we used non-linear equation to find out the relationship between the precipitation and the runoff. The parameters were calibrated using the discharge data provided by Department of Hydrology and Meteorology from the year 1972 to 1975. Later, the parameters were validated using the discharge data provided by Department of Hydrology and Meteorology from the year 1976 to 1977.

The equation obtained after calibration and validation was:

$$Q_t = a + (Q_{t-1})^b + c\left(\frac{P}{100}\right)^n$$

Where,

P = precipitation in mm,

Q_t = runoff in m³/s at time 't'

Q_{t-1} = runoff in m³/s at time 't-1'

a, b, c and n are the constants.

The values of the constants were calibrated by using MS Excel and assigned after number of iterations.

4.4.1 Model Performance

The performance of the calibrated and validated model was checked using the three statistical indices: the coefficient of determination (R^2), the percentage volume error and the Nash-Sutcliffe efficiency (NSE). (Refer Figure A-1 and A-2 for calibration and validation)

The coefficient of determination gives the proportion of variance in discharge data that is predictable from the independent variables in the model. It varies from 0 to 1, with higher values indicating best result. It can be calculated as:

$$R^2 = \frac{\Sigma\left(Q_0 - \underline{Q_0}\right) * \left(Q_s - \underline{Q_s}\right)}{\sqrt{\Sigma(\left(Q_0 - \underline{Q_0}\right)^2 * \left(Q_s - \underline{Q_s}\right)^2)}}$$

Where, Q_0 is observed discharge, $\underline{Q_0}$ is average discharge, Q_s is simulated discharge and $\underline{Q_s}$ is an average simulated discharge.

The percentage volume error is the ratio of difference between the calibrated and observed volume to the observed volume. A lower value of percentage volume error indicates good fit. It is expressed as:

$$Percentage\ volume\ error = (V_c - V_o)\ /V_o$$

The Nash-Sutcliffe Efficiency (NSE) (Nash and Sutcliffe 1970) provides a measure of how well a model's prediction matches the observed data. It is expressed as:

$$NSE = 1 - \frac{\Sigma(Q_0 - Q_c)^2}{\Sigma\left(Q_0 - \underline{Q_0}\right)^2}$$

Where, Q_0, Q_c, and $\underline{Q_0}$ are observed discharge, calibrated discharge and average observed discharge respectively.

The general performance rating of stream flow calibration indicates 0.75 to 1 NSE and R^2 as very good, 0.65 to 0.75 as good, 0.5 to 0.65 as satisfactory, and less than 0.5 as unsatisfactory values. PBIAS, the value less than 10% is considered to be very good calibration results, 10% to 15% as good, 15% to 25% percent as satisfactory, greater than 25% as unsatisfactory results. (Moriasi, 2007)

4.5 Estimation of the trial evaporation of Kulekhani Reservoir

70% of the daily mean evaporation record at Chisapani Gadhi is adopted, taking into the difference in altitude between the observatory station and the reservoir basin, as tabulated below:

Table 4.10 Mean Daily Evaporation of Kulekhani reservoir (JICA, JICA KULEKHANI III HPP, 2003))

Unit (mm/day)

	Jan	Feb	Mar	Apr	May	Jun	Jul	Aug	Sep	Oct	Nov	Dec
Daily Evaporation	2.46	3.89	6.31	10.62	11.71	8.17	2.74	2.71	2.67	3.33	2.96	2.15
70% value	1.72	2.18	4.42	7.43	8.20	5.72	1.92	1.90	1.87	2.33	2.07	1.51

The evaporation was estimated from year 2010-2022. We estimated the surface area

(a_1) of the reservoir based on the current volume (storage$_1$). We iteratively simulate the water balance in a reservoir until a convergence criterion is met. We set the initial values "a" and "b" for (area$_1$) and (area $_2$) respectively and calculated the average area "c" from area$_1$ and area$_2$. Then we estimated the evaporation using average area "c" and evaporation coefficient "K". Then we added the inflow to the current storage to get the available water in the reservoir. We checked if available water is more than demand. If yes, we set delivery to demand, otherwise set delivery to available water. After that we calculated the updated storage considering inflow, delivery, and evaporation. We checked for the spill of water from the reservoir, If updated storage exceeds capacity, spill is calculated as the excess and storage is set to capacity, otherwise spill is zero and storage is set to the updated value which is (storage$_2$). We used polynomial regression function to fit a curve to the volume-area data and predicts the area (area$_2$) corresponding to (storage$_2$). After that we did the convergence check by comparing the difference between last two area predictions (b and area$_2$). We exit the loop if the difference is smaller than a threshold (0.0001 in this case). And, if not converged, update variables (a, b, etc.) and repeat the calculations. The code doesn't explicitly have an output, but it iteratively prints values until convergence. The final values of (area$_2$) and (storage$_2$) represent the converged state of the reservoir under the given conditions. (Refer Annex-A for actual code)

The key points of the code are:

1. The code simulates reservoir operations considering inflows, demand, evaporation, storage capacity, and energy generation.

2. It uses polynomial regression to model relationships between reservoir variables.

3. It iterates through time steps to calculate daily values of key variables.

4. Outputs include a dataframe with detailed results and a prediction of water level for a given storage.

4.6 Precipitation and Climate Projection

4.6.1 Global Climate Model

Global Climate Models, according to Intergovernmental Panel on Climate Change (IPCC), are the numerical models which can precisely represent the physical process that occurs in the cryosphere, land surface, ocean and atmosphere. Newton's law of motion, thermodynamic equation, mass conservation, etc. (Edwards et al., 2011) are the fundamental equations which are considered as the building block of these models. A group of people working together has led to development of project Coupled Model Intercomparison Project (CMIP) and its latest available model CMIP6 has been used.

4.6.2 Model Selection

There are many approximations taken during the development of models leading to uncertainties within the output of models. Also, selection of all models is not possible as well as practicable. GCMs must be selected for strong climate and precipitation projection. GCM Model are selected from approaches below:

- Validation Approach

- Image Formation Approach

Validation Approach (Nyunt et al., 2016)

- In this approach, we determine the model's capacity to represent the mesosphere and climatic characteristics of the local region which has an impact on the seasonal change and amount of precipitation in basin area.

- Two domains, Local and Regional domain, are considered. Wind, SST are taken in regional domain while Outgoing Longwave Radiation (OLR), rainfall are taken in the local domain. Data are taken using monthly mean spatial correlation (S_{corr}) and root mean square error (RMSE) in past years.

$$S_{corr} = \frac{\sum_{i=1}^{N}(X_i - \bar{X})(Y_i - \bar{Y})}{\sqrt{\frac{1}{N}\sum_{i=1}^{N}(X_i - \bar{X})^2(Y_i - \bar{Y})^2}}$$

$$E_{RMS} = \sqrt{\frac{1}{N}\sum_{i=1}^{N}(X_i - Y_i)^2}$$

The GCM model which has higher Scorr value and and lower RMSE value than the mean value receives point 1. If either of two requirements is met, score of 0 is given and if none of the requirements is met, score of -1 is given. The model of higher aggregate score is selected.

Image Formation Approach (Hamed et al., 2022)

- Precipitation, maximum temperature (Tmax) and minimum temperature (Tmin) are represented by three colours Red, Green and Blue (RGB) respectively in order to construct an image which serves as a reference for observed historical climate.

- Same is done for result obtained from GCM simulation.

- Comparison of simulated image with reference image is possible

- For the evaluation of similarities between simulated and reference image, King-Gupta Efficiency (KGE) measure is applied.

Every band generates a unique grayscale image. The image represents the brightness of each pixel. The most widely used pixel format is known as a "byte image," which uses an 8-bit integer with a value between 0 and 225 to represent the brightness of each pixel. Climate variables were rescaled to an 8-bit integer using equation

$$Y_N = \frac{[X_N - \min(X)] \times 255}{\max(X) - \min(X)}$$

Where X_N stands for climate variable, Y_N stands for transformed value, max(X) and min(X) for the variable's maximum and minimum readings. For the formation of image, this procedure is repeated for each band and combined. Similarity between the image is measured by KGE equation

$$KGE = 1 - \sqrt{\left((r-1)^2 + \left(\frac{\mu_s}{\mu_{ref}} - 1\right)^2 + \left(\frac{\sigma_s/\mu_s}{\sigma_{ref}/\mu_{ref}} - 1\right)^2 \right)}$$

The reference image's mean and standard deviation are represented by μref and σref respectively while simulated image's mean and standard deviation are represented by μs and σs respectively. The value of KGE ranges from 1 to -∞, where 1 represents the perfect match.

4.6.3 Scenarios of climate projection

The first climate change scenarios, IS92, were released by Intergovernmental Panel on Climate Change (IPCC) in 1992 followed by The Special Report on Emissions Scenarios (SRES) in 2000. For the enhancement of SRES, Representative Concentration Pathways (RCPs, 2007) and SSPs were subsequently introduced.

RCPs

Many factors need to be taken into account when predicting how future global warming would impact climate change. While future greenhouse gas emission remains the crucial factor, technological advancements, population growth, regional and local economic situations must all be considered. Based on all considerations, the RCP gives starting points and projected emissions until the year 2100.

Table 4.11 RCP Scenarios, along with radiative forcing (Wayne, 2013)

Name	Radiative forcing	CO2 equi (ppm)	Temp Anomaly (°C)	Pathways
RCP8.5	8.5 Wm2 in 2100	1370	4.9	Rising
RCP6.0	6 Wm2 post 2100	850	3.0	Stabilization without overshoot
RCP4.5	4.5 Wm2 post 2100	650	2.4	Stabilization without overshoot
RCP 2.6 (RCP3PD)	3 Wm2 before 2100, Declining to 2.6 Wm2 by 2100	490	1.5	Peak and decline

SSPs

For the realistic projection for climate change research, a best scenario is represented by merging the future radiative forcing and its related climatic impact and alternative socioeconomic growth. The four different RCPs on the first dimension of the matrix depict climatic outcomes, while the Shared Socioeconomic Pathways (SSPs) on the other dimension define potential reference expectations about anticipated socioeconomic development in the absence of climate policy or climate change (O'Neill et al., 2014).

When the future radiating forcing is combined with socio-economic pathways, we get updated scenarios.

Table 4.12 SSP Scenarios, along with the challenges associated (O'Neill et al., 2014)

SSP	Challenges	Illustrative starting points for narratives
SSP1	Low for mitigation and adaptation	Sustainable development proceeds at a reasonably high pace, inequalities are lessened, technological change is rapid and directed toward environmentally friendly processes, including lower carbon energy sources and high productivity of land
SSP2	moderate	An intermediate case between SSP1 and SSP3.
SSP3	High for mitigation and adaptation	Unmitigated emissions are high due to moderate economic growth, a rapidly growing population, and slow technological change in the energy sector, making mitigation difficult. Investments in human capital are low, inequality is high, a regionalized world leads to reduced trade flows, and institutional development is unfavorable, leaving large numbers of people vulnerable to climate change and many parts of the world with low adaptive

SSP	Challenges	Illustrative starting points for narratives
SSP4	High for adaptation low for mitigation	A mixed world, with relatively rapid technological development in low carbon energy sources in key emitting regions, leading to relatively large mitigating capacity in places where it mattered most to global emissions. However, in other regions development proceeds slowly, inequality remains high, and economies are relatively isolated, leaving these regions highly vulnerable to climate change with limited adaptive capacity.

There has been huge improvement in CMIP6 than its preceding CMIP5 as there is incorporation of higher spatial resolutions which is important in assessment of local impacts. There is incomplete knowledge of the atmospheric condition of the Earth and many approximations have been made in numerical modeling which results in variation in output for different GCMs model for same input (Jain et al., 2018). Hence, multi-model Ensemble (MME) is used to minimize the uncertainty associated with different models (Ahmed et al., 2020; Hughes et al., 2014). In our study, we utilized downscaled and bias-corrected precipitation outputs from five GCMs (Access, Earth, Miroc, Mpi and Mri) within CMIP6. The selection of these models was based on the availability of precipitation data at the required temporal scale. Bias correction was applied to enhance the accuracy of the model outputs.

4.6.4 Downscaling and Bias Correction

Global Climate Models are powerful tools that simulate the Earth's climate system on the large scale. It may lack fine resolution needed to capture regional features accurately. It is therefore necesaary to downscale modeled output in order to obtain relevant information at smaller scales and improve the applicability of global climate model projections for specific regions. GCMs often projects with a biasness such as excessive rainfall, extreme early or late occurrence of rainfall and so on. It overpredicts

number of rainfall days and underpredicts extreme rainfall. It is result of their lack of understanding of Earth Climate as well as many approximations taken. It is important to correct this biasness before the application of the output results from the model. (Jakob Themeßl et al., 2011) examined the effectiveness and concluded that the QM methods can be most effective methods in correcting the biasness. QM's results were accurate (Laon et al., 2013). Quantile-based method, Empirical Quantile Mapping (EQM) has been used for downscaling and correcting biasness. The package 'qmap' is used in R to perform EQM.

GCMs proposed by Almazroui et al. (2020) and Mishra et al. (2020) for South Asia have been selected for the daily precipitation and maximum and minimum temperature listed in the table. GCMs were downloaded from https://aims2.llnl.gov/search/cmip6/ while SSP245 was used.

Table 4.13 Five models of climate change scenario

S.N.	Model Name	Country	Latitude resolution (Deg)	Longitude resolution (Deg)	Research Center
1	ACCESS-Cm2	Australia	1.2500	1.875000	Australian Community Climate and Earth System Simulator (ACCESS)
2	EC-EARTH3	Europe	0.7018	0.703125	European Community Earth (EC Earth)
3	MIROC6	Japan	1.4000	1.400000	Japan Agency for Marine-Earth Science and Technology, Atmosphere and Ocean Research Institute, National Institute for Environmental Studies (MIROC), Japan

S.N.	Model Name	Country	Latitude resolution (Deg)	Longitude resolution (Deg)	Research Center
4	MPI-ESM1-2-HR	Germany	0.9351	0.937500	Max Planck Institute for Meteorology (MPI)
5	MRI-ESm2-0	Japan	1.1215	1.125000	Meteorological Research Institute (MRI)

Evaluation of QM results:

Like any other modelling procedure, the result obtained from the QMs should be validated with the historical observed data. Normalized standard deviation, linear correlation coefficient and centralized root mean squared deviation (CRMSD) are the three evaluation tools that can be used with Taylor diagram to verify the outputs (Liang et al., 2017; K.E. Taylor et al., 2001).

$$R = \frac{\frac{1}{N}\sum_{i=1}^{N}(X_i^o - X_i^{-o})(X_i^m - X_i^{-m})}{\sigma^o \sigma^m}$$

$$\sigma_* = \frac{\sigma_m}{\sigma_0}$$

$$CRMSD = \left(\frac{1}{N}\sum_{i=1}^{N}[(X_i^o - X_i^{-o})(X_i^m - X_i^{-m})]^2\right)^{0.5}$$

Where, σ_o and σ_m are the standard deviations of the observed and modeled datasets respectively. N represents the number of available historical data. R is a dimensionless coefficient which varies from -1 to +1. According to Taylor (1990), the increasing correlation between X^m and X^o results in the boundary value of -1 or +1 of the

dimensionless coefficient R. σ_*, a dimensionless factor, represents the identical property between observed and simulated outputs. The performance of model depends upon value of R and CRMSD. R value closer to +1 and CRMSD value closer to 0 represents a model with better and increased performance. (Jolliff et al., 2009)

The Mean Bias Error (MBE) is another performance evaluating criterion which checks the biasness size and direction. Positive value on MBE represents over-estimation while negative value represents under-estimation. The value zero represents lack of biasness in the datas. Mathematical representation includes (Willmott and Matsuura, 2005):

$$MBE = \frac{\sum_{i=o}^{N}(X_i^o - X_i^m)}{N}$$

Performance Evaluation of Bias Correction

CMIP6 model outputs downloaded from the https://aims2.llnl.gov/search/cmip6/ were used. Raw datas cannot be utilized directly to predict future because of the discrepencies between observed historical datas and the GCMs output. Hence bias correction is required. QUANTILE MAPPING has been very efficient method in bias correction for enhancing the performance of GCMs (Berg et al., 2012). The parameters (Precipitation, Tmax and Tmin) for the GCM outputs and historical observed datas from 1990 to 2014 were compared before and after bias correction. Nash-Sutcliffe coefficient (NSE), Percentage Bias (PBIAS) and R^2 are calculated before and after bias correction to observe the performance.

Nash-Sutcliffe Coefficient

$$NSE = 1 - \frac{\sum_{i=1}^{n}(x_i - \bar{y}_{i)}{}^2}{\sum_{i-1}^{n}(x_i - \bar{x})^2}$$

The value ranges from 1 to -∞, the value 1 represents a perfect model performance while the value 0 represents poor performance of the model. -∞ represents that the mean of the observed data is a better predictor of the dependent variable than the model.

Percentage Bias Coefficient

$$Pbias = \frac{\sum_{i=1}^{n}(y_i - x_i)}{\sum_{i=1}^{n}(x)}$$

The value ranges from - ∞ to +∞, where values below 0 indicate underestimation of model compared to observed values, values greater than 0 indicate overestimation of model compared to observed values and 0 indicates perfect agreement between model and observation.

Coefficient of Determination

$$R^2 = \frac{\sum_{i=1}^{n}(y_i - \bar{x})^2}{\sum_{i=1}^{n}(x_i - \bar{x})^2}$$

The value of R^2 ranges from 0 to 1 while higher value represents better agreement with the observed data.

y = modeled value

$\bar{y}$ = mean of modeled values

n = number of values

x = observed value

$\bar{x}$ = mean of observed values

4.7 Volume, Elevation and Area of Kulekhani Reservoir

A Volume-Elevation-Area (VEA) curve, also known as a storage-discharge relationship or storage-discharge curve, is a graphical representation that illustrates the relationship between the water storage volume, the corresponding water surface elevation (or level), and the discharge (flow rate) of water in a reservoir or water body. It's an essential tool in hydropower engineering and for the management of storage-type hydropower systems, such as dams and reservoirs. Here's why it's important:

1. Hydropower Generation Planning: In hydropower engineering, understanding the VEA curve is crucial for planning and optimizing the operation of hydropower plants. It helps determine how the flow of water and the elevation of the reservoir's water level influence the amount of electricity that can be generated. Operators can use this information to schedule when to release water for power generation to meet demand and maximize efficiency.

2. Reservoir Management: VEA curves are critical for managing reservoirs efficiently. By analyzing the curve, operators can make informed decisions about when to store water during periods of excess supply (e.g., during heavy rainfall or low electricity demand) and when to release water for power generation or other purposes (e.g., irrigation or flood control) during periods of high demand or low water availability.

3. Flood Control: In addition to power generation, many reservoirs serve as flood control mechanisms. Understanding the VEA curve helps authorities anticipate the impact of heavy rainfall or snowmelt and decide when to release water from the reservoir to prevent downstream flooding while maintaining a safe water level.

4. Environmental Impact Assessment: When building or modifying hydropower facilities, it's essential to assess their environmental impact. The VEA curve can be 10 used to estimate how changes in water levels and discharge rates will affect the surrounding ecosystem, including aquatic life, water quality, and vegetation.

5. Sediment Management: Reservoirs tend to accumulate sediment over time, which can reduce their storage capacity and affect downstream ecosystems. The VEA curve can aid in managing sediment by indicating when and how much water to release to flush out sediment, thereby prolonging the useful life of the reservoir.

6. Infrastructure Design: Engineers use VEA curves when designing dams, spillways, and other infrastructure associated with hydropower projects. The curve helps in determining the dimensions and specifications of these structures to handle the expected variations in water level and discharge.

7. Water Supply: Storage-type hydropower reservoirs often serve as a source of freshwater for domestic, agricultural, and industrial purposes. The VEA curve helps in managing water supply, ensuring that there is enough water for various needs while maintaining power generation capabilities.
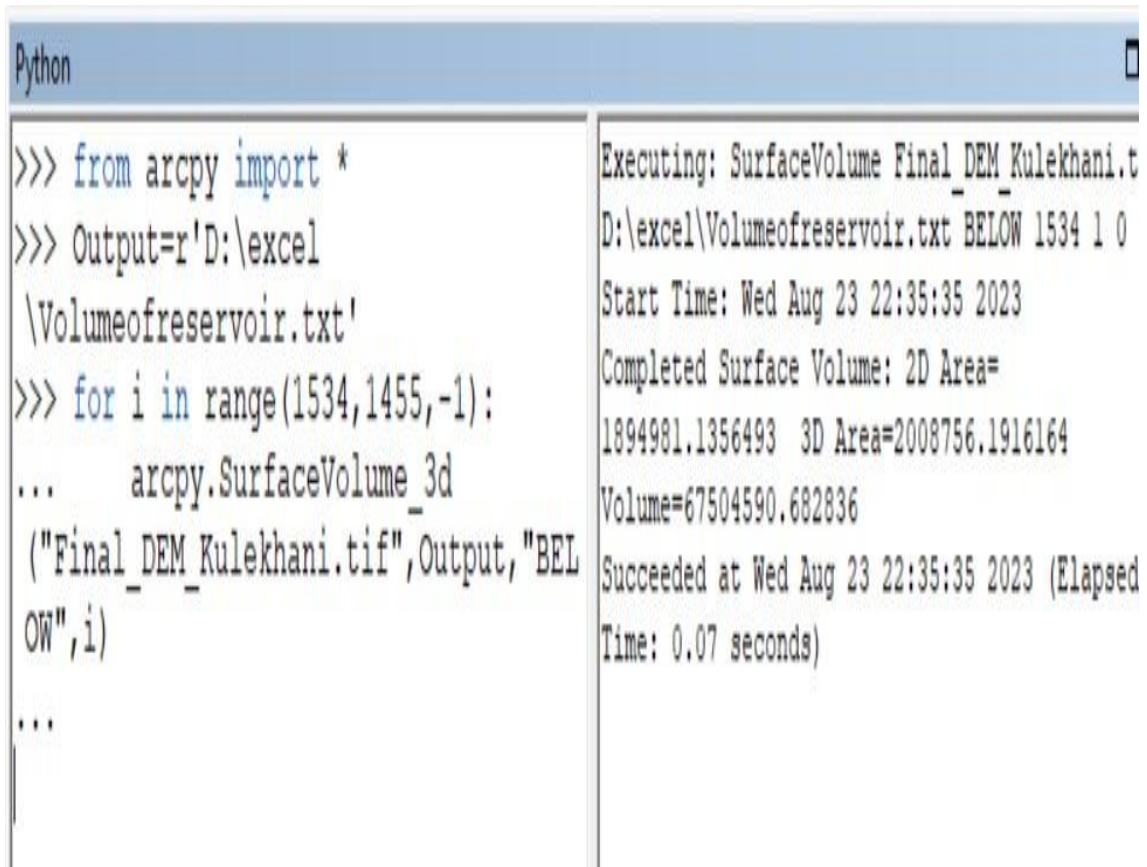
The Volume-Elevation-Area curve is a critical tool for hydropower engineers and managers to make informed decisions about reservoir operation, power generation, flood control, and environmental conservation in storage-type hydropower systems. It provides a comprehensive understanding of the relationship between water storage, elevation, and discharge, facilitating efficient and sustainable management of these complex water resources.

Here, in our project, the curve used for the reservoir operation on power production variation due to change in head of water in Kulekhani Reservoir.

Data analysis and Processing:

The Digital Elevation Model (DEM) file was provided by Nepal Electricity Authority (NEA). So, to calculate the Volume, Elevation and Area values and plot it for a final curve, we used the built-in function available in the ArcMap (10.8.2). The raster file was imported and the built-in function "SurfaceVolume_3d" was used to calculate volume, elevation and surface area from elevation 1534m to 1456m with contour

interval of 1m. For looping, the python program was used in ArcMap.


```
Python                                                               □
>>> from arcpy import *          Executing: SurfaceVolume Final_DEM_Kulekhani.t
>>> Output=r'D:\excel            D:\excel\Volumeofreservoir.txt BELOW 1534 1 0
\Volumeofreservoir.txt'          Start Time: Wed Aug 23 22:35:35 2023
>>> for i in range(1534,1455,-1): Completed Surface Volume: 2D Area=
...     arcpy.SurfaceVolume_3d   1894981.1356493  3D Area=2008756.1916164
("Final_DEM_Kulekhani.tif",Output,"BEL Volume=67504590.682836
OW",i)                           Succeeded at Wed Aug 23 22:35:35 2023 (Elapsed
...                              Time: 0.07 seconds)
```

Figure 4.10 Python Programming to calculate Surface Volume and Area 2D

Thus, the VEA curve is an important progression for our project. With the help of this curve, volume of the reservoir can be calculated for any value of elevation. This analysis will aid in upcoming tasks for our project, i.e., standard operating procedure.

4.8 Standard Operating Policy
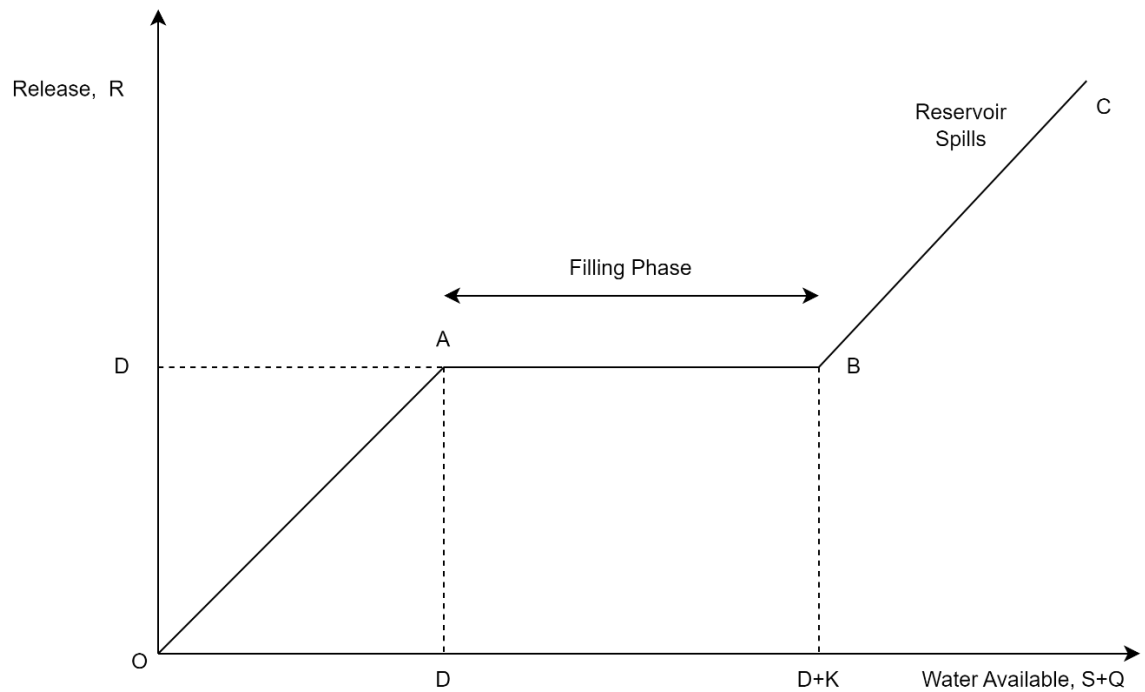
Figure 4.11 Standard Operating Policy (Rijal, 2014)

The x-axis is representing available-water and the y-axis is representing the release. D is the demand and K is the capacity of the reservoir. The available-water is defined as the sum of beginning storage in the reservoir and the inflow during the period.

Where,

D = Demand

R = Release

K = Capacity

S = Storage

Q = Inflow

E = Evaporation

O = spillage

t = time (month)

As per SOP, OABC is a release policy

Along OA: Release = Water Available, reservoir will be empty after release

AB: Release = Demand; excess water is stored in the reservoir

At A: Reservoir is empty after release

B: Reservoir is full after release

Along BC: Release = Demand + excess of availability over the capacity (spill)

While evaporation loss is included,

The SOP becomes like:

$$R_t = D_t, \qquad\qquad if \ S_t + Q_t - E_t \geq D_t$$

$$= S_t + Q_t - E_t \qquad\qquad \text{Otherwise}$$

Demand is constant and if the available-water is less than demand all the available-water is released. Otherwise, the Release amount of water is the sum of storage and inflow and minus the evaporation loss.

$$O_t = (S_t + Q_t - E_t - D_t) - K \qquad \text{if positive}$$

$$= 0 \quad \text{Otherwise}$$

There is spill in the reservoir if the sum of the storage and inflow minus the evaporation loss, demand of water for hydropower production and the capacity of the reservoir is positive and if that is negative there is no spill of water from the reservoir.

$$S_{t+1} = S_t + Q_t - E_t - R_t - O_t \ , \text{After getting values of } R_t \text{ and } O_t \text{ from above}$$

The storage of the next month can be found out by adding the storage and inflow of the previous month and subtracting the evaporation loss, release of water from the reservoir and spill of water from the reservoir in the previous month. A computer program is built up using this concept which is explained below. (Refer Annex for code)

We imported libraries like: pandas for data manipulation and analysis, numpy for numerical computation, and sys to Provide access to system-specific parameters and functions. Then we loaded the daily inflow data and reservoir volume-elevation-area data from the excel file. We converted the discharge values from cubic meters per second to million cubic meters. We used polynomial regression function to predict values based on relationships in reservoir data. We performed a polynomial regression to predict the Elevation-values based on Volume-values from a given VEA curve. Similarly, we performed a polynomial regression to predict the Elevation-values based on Area-values from the given VEA curve. Similarly, we performed a polynomial regression to predict the area-values based on volume-values from the given VEA curve. The simulation setup was based on user-provided initial water level to calculate the initial storage of the reservoir. The maximum storage capacity was set to 67.5 million cubic meters. Reservoir simulation function simulates reservoir operation for each time step which is:

- Calculate reservoir height and area based on storage.

- Calculate demand based on energy requirement and elevation.

- Estimate evaporation losses.

- Determine delivery based on available water and demand.

- Calculate spill if storage exceeds capacity.

- Update storage for the next time step and calculate outflow and energy generated.
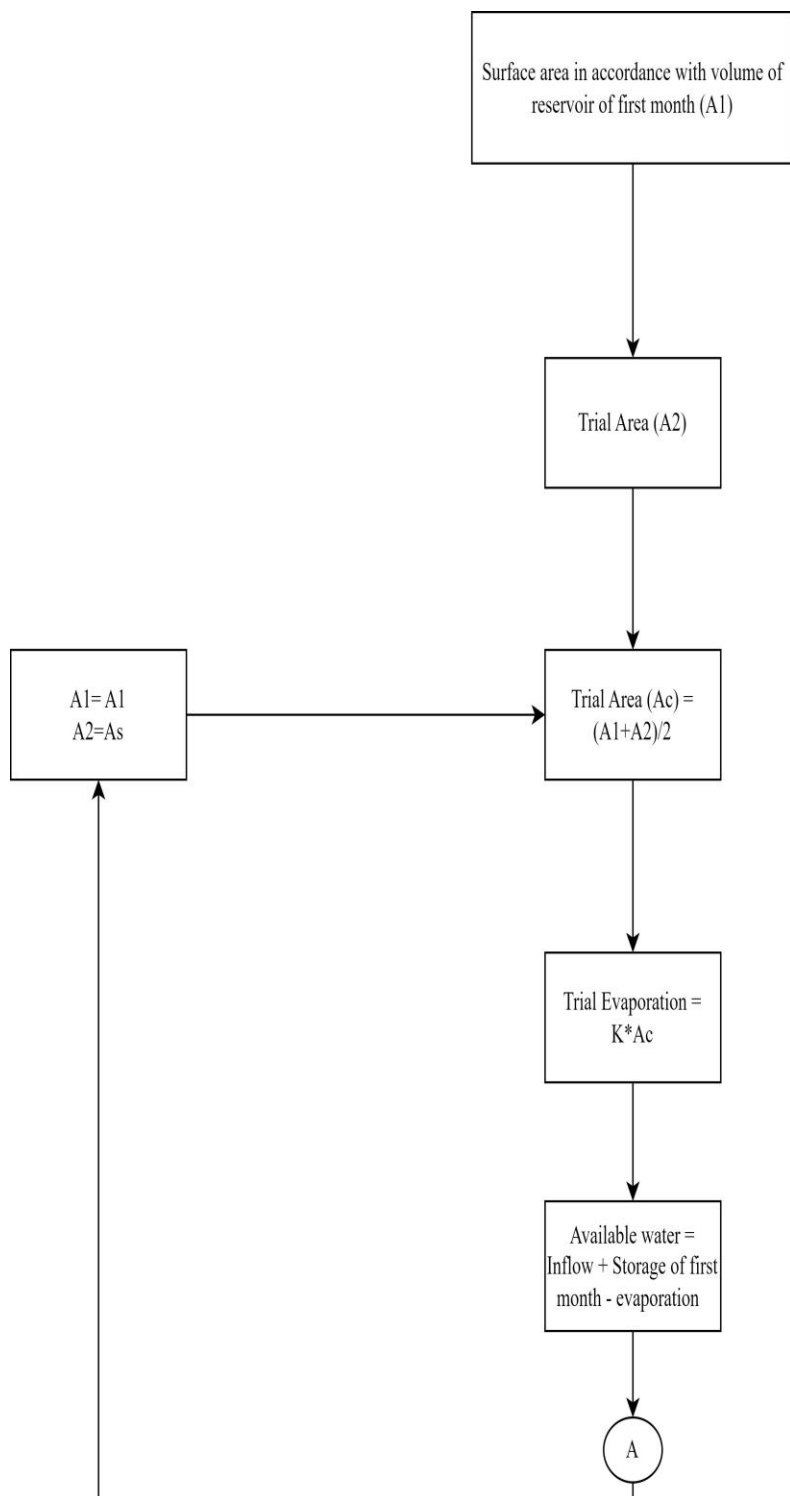
Figure 4.12 Flowchart of Standard Operating Policy
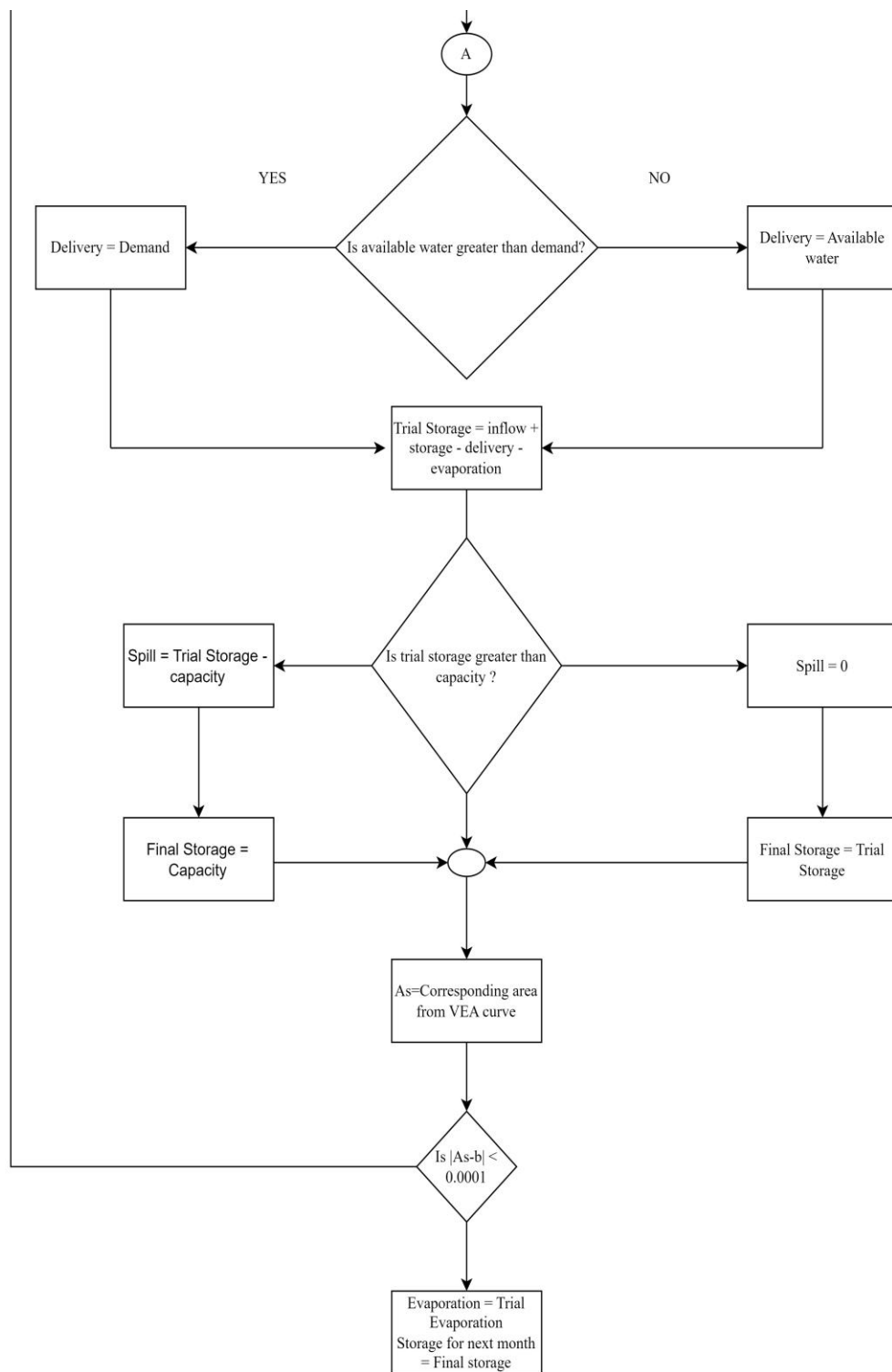
Figure 4.12 Flowchart of Standard Operating Policy

4.9   Power Forecasting

Power forecasting is predicting future electricity generation or consumption levels based on historical data, current conditions, and relevant influencing factors. It helps in managing reservoir levels by predicting inflow, outflow, and optimal storage levels, ensuring a steady supply of electricity without compromising environmental or operational constraints.

However, power forecasting is inherently uncertain due to factors such as weather variability, market dynamics, and unforeseen events.

In this study, we utilized the SARIMAX (Seasonal Autoregressive Integrated Moving Average with Exogenous Variables) model, an advanced time series forecasting technique, to predict future power output based on historical data.

SARIMAX consists of two components seasonal and non-seasonal components. Seasonal component accounts for recurring patterns that occur over fixed intervals, such as daily, weekly, or yearly cycles. It is denoted by P, D, Q, s where P is Seasonal Autoregressive Order, D is Seasonal Differencing Order, Q is Seasonal Moving Average Order and s is Seasonal period. Non seasonal component captures the trend and irregular fluctuations in the time series data. It is represented by the order p, d, q whereas p is order of autoregressive, d is differencing and q is moving average.

Before initiating SARIMAX model, monthly energy data from January, 1989 to December, 2022 was imported in Jupyter Notebook. SARIMAX class was imported from stats model library. The model was best fitted for (0,1,2) for non-seasonal components and (1,2,2,12) for seasonal components with minimum AIC value 6407.45. A forecast was generated using fitted model from January, 2020 to December, 2022. Available power generation data and forecasted power generation were plotted on same graph for visualization. Another forecast was generated for a longer period, from January, 2022 to December, 2029. It was then plotted with original data for

comparison.

The non-seasonal component captures trends and short-term fluctuations in the data. The seasonal component captures seasonal patterns and dependencies occurring every 24 hours, representing daily cycles in power generation. The Python code utilizes libraries like pandas, statsmodels, and matplotlib to perform time series forecasting on power generation data. The code utilizes several necessary libraries for data manipulation (pandas), numerical computations (NumPy), statistical modeling (statsmodels), data visualization (matplotlib),(Warnings) to manage warnings, and (Itertools) to provide tools for working with iterators.

```python
import warnings
import itertools
import pandas as pd
import numpy as np
import statsmodels.api as sm
import matplotlib.pyplot as plt
plt.style.use('fivethirtyeight')
```

The code reads an Excel file named "Power_generation_1991-2022.xlsx" using pd.read_excel. The (index_col) parameter sets the "Datetime" column as the index, and parse_dates ensures the dates are parsed correctly. The code sets the frequency of the index to monthly (MS) which means month start using (df.index.freq='MS'). This ensures the time series is treated as monthly data. We ploted the loaded data for visualization using (df.plot()) to understand trends and seasonality. The code defines a grid of potential parameters for the Seasonal ARIMA model. These parameters include:

- p: The order of the autoregressive (AR) model, which captures the effect of past values on the current value.

- d: The degree of differencing, which removes non-stationarity in the data.

- q: The order of the moving average (MA) model, which accounts for past forecast errors.

- P, Q, and S: The seasonal equivalents of p, q, and the seasonal period (here, S=12 for monthly data).

The code uses (itertools.product) to generate all possible combinations of these parameters within a specified range (0 to 2 in this case). The code iterates through a subset of parameter combinations and fits a Seasonal ARIMA (SARIMA) model for each combination using sm.tsa.statespace.SARIMAX. The model is fit to the provided power generation data (df). The code selects the best model based on a metric like AIC (Akaike Information Criterion). The code uses (results.plot_diagnostics) to visualize model diagnostics such as residuals and autocorrelation plots. These plots help assess if the model assumptions are met and identify any potential issues.

The **Akaike information criterion (AIC)** is a mathematical method for evaluating how well a model fits the data it was generated from. In statistics, AIC is used to compare different possible models and determine which one is the best fit for the data. AIC is calculated from:

- the number of independent variables used to build the model.

- the maximum likelihood estimates of the model (how well the model reproduces the data).

The best-fit model according to AIC is the one that explains the greatest amount of variation using the fewest possible independent variables. (Bevans, 2023)

5   Results and Discussions

5.1   Result from VEA curve
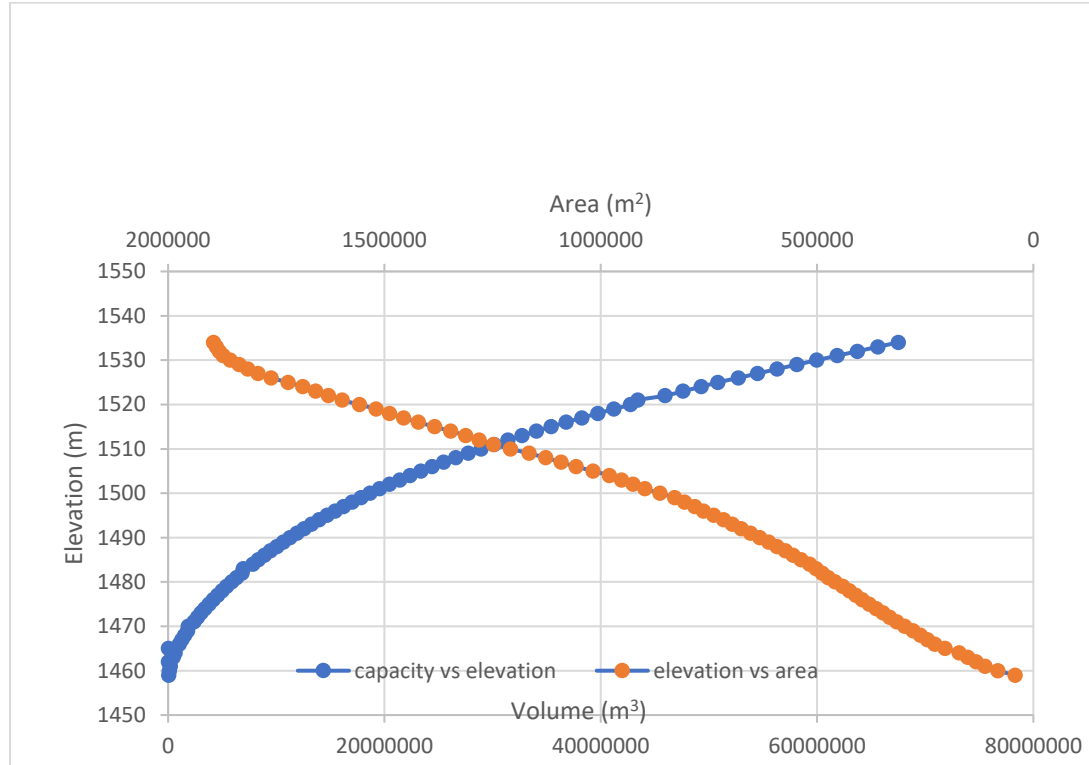
Figure 5.1 Plot on Capacity, Elevation and Area of the Reservoir (Refer Table B-1)

The elevation of crest level of the dam is 1534m. From the analysis, storage at 1534m elevation is 67.505 million cubic meters. The dead storage of the reservoir is 1459m and the corresponding storage is 0.06Millions cubic meters as per the data.   The maximum storage generated from the source file is similar to the storage calculated by NEA. Some differences are seen in the volume calculated from the source file and NEA's website. It is because of the data calculated in different time period. The maximum reservoir volume mentioned in the official source of NEA is 62.3Millions cubic meters at 1530Masl in 2005 whereas, as per our analysis, the capacity at 1530Masl is 59.98Millions cubic meters. Such difference in volume may be due to the

collection of sediments in the reservoir. However, the data obtained from the source file is highly correlated to the official data. So, we will continue with data for now.

5.2 Code results

The provided code sets up a reservoir simulation to model daily operations based on inflows, demand, evaporation, and storage constraints. It captures the dynamics of water management under varying conditions. Using the Volume, elevation and area curve and rainfall data it takes the daily inflow data frame, initial storage and storage capacity as inputs. It leverages polynomial regression and iterative calculations to estimate daily values for key reservoir parameters. It uses an iterative approach to achieve convergence in evaporation calculations. It performs the reservoir operation simulation for each day by

- Calculating reservoir height and area based on storage

- Calculating demand based on energy requirement and elevation.

- Estimating evaporation losses.

- Determining delivery based on available water and demand.

- Calculating spill if storage exceeds capacity.

- Updating storage for the next time step.

- Calculating outflow and energy generated.

This code provides a comprehensive simulation of reservoir behavior, capturing the dynamics of water management under varying conditions. The detailed outputs enable analysis of daily operations and the impact on key metrics like water level, storage, and energy generation. (Refer page 97 for computer code)

5.3 Calibration and Validation using Regression Model

For calibration, we used the river discharge data (Station No: 565) from year 1972 to 1975 provided by Department of Hydrology and Meteorology. The coefficient of determination (R^2) was found to be 0.89. The Nash Sutcliffe Efficiency was found to be 0.85. The PBIAS was found to be -12.94%. The general performance rating of stream flow calibration indicates 0.75 to 1.0 NSE and R^2 as very good, 0.65 to 0.75 as good, 0.5 to 0.65 as satisfactory, and less than 0.5 as unsatisfactory values. For PBIAS, the value less than 10% is considered to be very good calibration results, 10% to 15% as good, 15% to 25% percent as satisfactory, greater than 25% as unsatisfactory results. Therefore, the calibrated model was acceptable for further analysis. (Refer Figure A-1, Figure A-2, Table A-3 and Table A-4)

The model was used for the year 1976 and 1977 for validation. The coefficient of determination (R^2) was found to be 0.94. The Nash Sutcliffe Efficiency was found to be 0.72. The PBIAS was found to be 14.96%. Therefore, the model was validated as per calculated model performance and model was adopted. In short,

Table 5.1 Model performance parameters

Model performance parameters	Calibration	Validation
R^2	0.89	0.94
NSE	0.85	0.72
PBIAS %	-12.94	14.96
Peak discharge observed (m^3/s)	26.3	7.96
Peak discharge calculated (m^3/s)	27.36	11.38
Peak discharge observed time	July, 1972	June, 1976
Peak discharge calculated time	July, 1972	June, 1976

5.4 Results from CMIP6

Table 5.2 NSE, PBIAS and R^2 of precipitation before and after applying bias correction

Station	Tool	ACCESS-Cm^2		EC-EARTH3		MIROC6		MPI-ESM1-2-HR		MRI-Esm^2-0	
		Before Bias	After Bias	Before Bias	After Bias	Before Bias	After Bias	Before Bias	After Bias	Before Bias	After Bias
905	NSE	-7.68	1	-4.38	0.99	-1.98	1	-5.21	0.99	-3.57	1
	PBIAS	34.9	0.2	27.1	1.4	20.7	0.6	30.2	0.8	25.3	0.7
	R^2	0.95	0.97	0.91	0.93	0.96	0.97	0.92	0.95	0.98	0.99
904	NSE	0.98	1	0.98	0.99	0.97	1	0.99	1	0.99	1
	PBIAS	2.2	1.3	-9	7.6	-2.1	1.3	-6.5	1.8	-5.5	1.3
	R^2	0.97	0.97	0.93	0.9	0.96	0.98	0.91	0.95	0.98	0.97
915	NSE	0.21	0.97	0.52	0.73	0.49	0.98	0.46	0.63	0.49	0.98
	PBIAS	48.5	5.2	32.2	24.5	42.3	6	35.6	17.8	37.3	4.6
	R^2	0.98	0.98	0.97	0.8	0.99	0.98	0.97	0.7	0.99	0.98
1038	NSE	-0.99	0.67	-0.86	0.37	-0.73	0.66	-0.84	0.35	-0.88	0.67
	PBIAS	31.4	28.4	17	40	25.9	28.2	20	39.5	21.5	28.6
	R^2	0.14	0.81	0.1	0.7	0.14	0.81	0.12	0.68	0.11	0.82

Table 5.3 NSE, PBIAS and R^2 of maximum temperature (Tmax) before and after applying bias correction

Station	Tool	ACCESS-Cm^2		EC-EARTH3		MIROC6		MPI-ESM1-2-HR		MRI-Esm^2-0	
		Before Bias	After Bias	Before Bias	After Bias	Before Bias	After Bias	Before Bias	After Bias	Before Bias	After Bias
905	NSE	-1.06	1	-1.09	1	-0.89	1	-1.06	1	-0.98	1
	PBIAS	21.4	0	21.7	0	20.5	0	21.6	0	21	0
	R^2	0.91	1	0.94	1	0.93	1	0.93	1	0.94	1

Table 5.4 NSE, PBIAS and R^2 of minimum temperature (Tmin) before and after applying bias correction

Station	Tool	ACCESS-Cm^2		EC-EARTH3		MIROC6		MPI-ESM1-2-HR		MRI-Esm^2-0	
		Before Bias	After Bias	Before Bias	After Bias	Before Bias	After Bias	Before Bias	After Bias	Before Bias	After Bias
905	NSE	0.53	1	0.54	1	0.58	1	0.56	1	0.55	1
	PBIAS	24.7	0	24.1	0	22.6	0.1	24.2	0.1	23.5	0
	R^2	1	1	1	1	1	1	1	1	1	1

Bias Correction for precipitation

After analysis of family of QM methods, it was concluded that RQUANT method was best for correction of precipitation (Enayati et al., 2021). So the method RQUANT was used for bias correction as shown in table for the future GCM outputs under SP245 scenario. NSE ranging from -7.68 and 0.99 has been corrected to value between 0.63 and 1. PBIAS ranging from -9 to 48.5 has been corrected to value from 0.2 and 40. The parameter R^2 has been corrected from ranging between 0.1 and 0.99 to 0.7 to 0.99

Bias Correction for Temperature

Unlike precipitation, all the bias correction methods excluding SSPLIN and PTF: scale worked well for the temperature parameter (Enayati et al., 2021). It is because GCM models are better at modeling temperature than rainfall. PTF: linear transfer function was used in our study and the effectiveness of this method can be seen from the table.

5.5   Standard Operating Policy Results
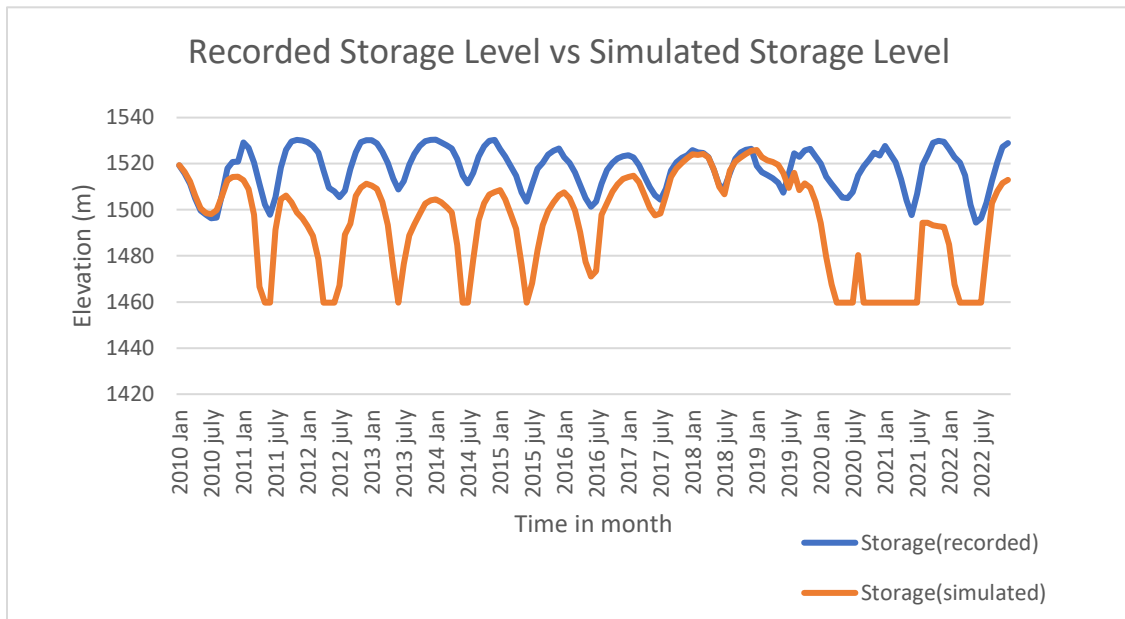
Figure 5.2 Recorded Storage Level vs Simulated Storage Level (Refer Table B-2)
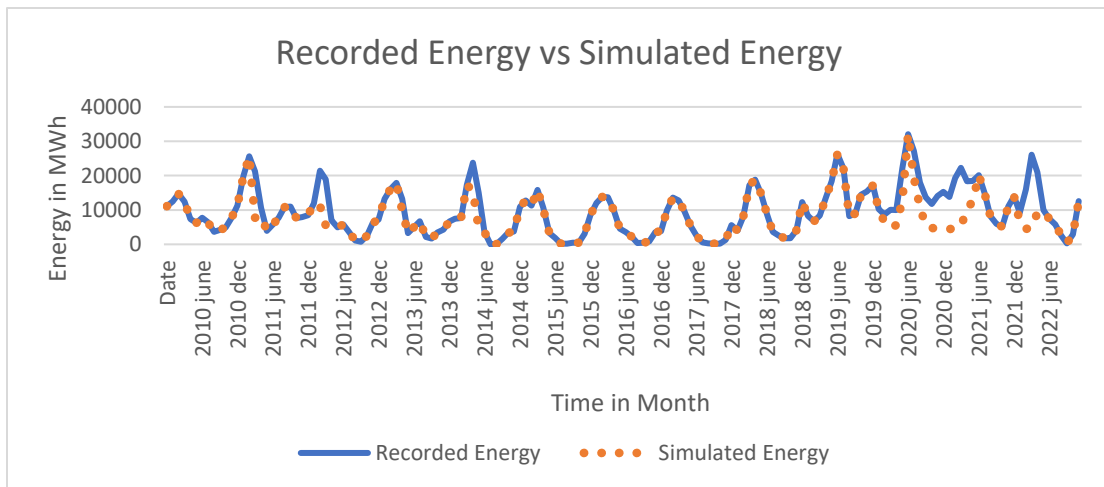
Figure 5.3 Recorded Energy vs Simulated Energy (Refer Table 5.5)

The obtained plot shows that the recorded storage level and simulated storage level is highly correlated. Also, the energy demand is fulfilled for most of the time period using simulation from the SOP output. This shows that our model performs well provided that the input data are highly accurate.

Table 5.5 Output of Standard Operating Policy Algorithm from 2010-2012

Month	Inflow (Mcu.m)	Demand (Mcu.m)	Storage (Mcu.m)	Outflow (Mcu.m)	Generated (MWh)
2010-01	3.576	7.937	41.688	7.937	11092
2010-02	3.587	8.963	37.247	8.963	12465.5
2010-03	3.771	10.638	31.788	10.638	14694
2010-04	3.646	9.098	24.76	9.098	12438
2010-05	3.891	5.473	19.092	5.473	7410.4
2010-06	4.435	4.616	17.293	4.616	6227.9
2010-07	7.217	5.744	16.972	5.744	7745
2010-08	10.978	4.754	18.395	4.754	6428.5
2010-09	10.551	2.684	24.562	2.684	3668
2010-10	4.896	3.023	32.363	3.023	4179.5
2010-11	3.845	3.517	34.139	3.517	4873
2010-12	3.632	5.587	34.382	5.587	7743
2011-01	3.586	8.161	32.365	8.161	11281.5
2011-02	3.595	14.521	27.724	14.521	19941.5
2011-03	3.593	19.012	16.738	19.012	25621
2011-04	4.88	16.683	1.247	6.093	7770.1

Month	Inflow (Mcu.m)	Demand (Mcu.m)	Storage (Mcu.m)	Outflow (Mcu.m)	Generated (MWh)
2011-05	6.646	8.456	0	6.627	8346.2
2011-06	15.338	3.09	0	3.09	3891
2011-07	15.319	4.331	12.185	4.331	5772
2011-08	7.286	5.664	23.124	5.664	7722.5
2011-09	4.933	7.915	24.686	7.915	10819.5
2011-10	4.051	8.102	21.647	8.102	11020.5
2011-11	3.734	5.641	17.531	5.641	7614.5
2011-12	3.607	5.881	15.574	5.881	7905
2012-01	3.592	6.318	13.266	6.318	8444.5
2012-02	3.608	8.964	10.506	8.964	11889
2012-03	3.579	16.459	5.119	8.663	11287.32
2012-04	4.398	15.029	0	4.382	5517.99
2012-05	3.797	5.587	0	3.778	4757.6
2012-06	5.353	3.964	0	3.964	4991.5
2012-07	13.999	4.509	1.363	4.509	5756
2012-08	5.665	2.595	10.827	2.595	3445.5
2012-09	11.561	0.824	13.858	0.824	1102.5
2012-10	4.765	0.585	24.545	0.585	799.5
2012-11	3.821	1.855	28.643	1.855	2550.5
2012-12	3.63	4.557	30.534	4.557	6283

5.6 Forecasting

The power generation calculated using Standard Operating Procedure algorithm is plotted as shown in below. The x-axis represents the monthly timeframe and y-axis represents the power generation in MWh. The power generation is very low in some month between 2014 and 2019. It is because of the maintenance work in the reservoir.
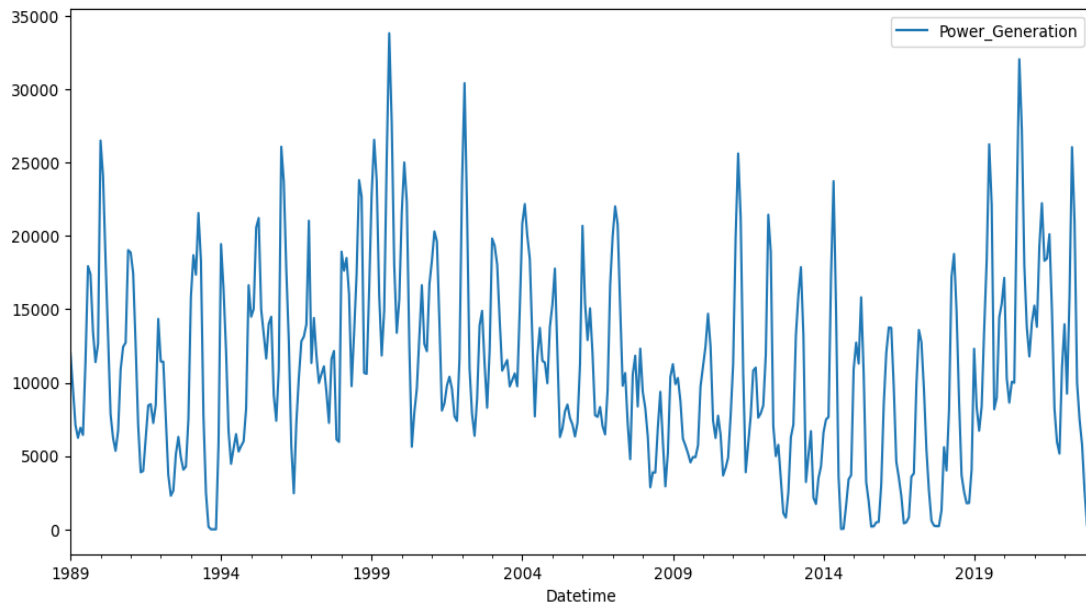
Figure 5.4 Plot of power generation and time in month. (Extracted from Jupyter Notebook)

The non-seasonal order (p, d, q) for SARIMAX is (0, 1, 2) and seasonal order (p, d, q, m) is (1, 2, 2, 12) which is calculated using Akaike Information Criterion (AIC). The minimum value of AIC is selected and best fitted model is selected. The calculation of AIC is shown in Annex-C.

A forecast is carried out from January, 2018 to December, 2022 to compare the trend with real data. The x-axis represents time in month and y-axis represents Energy

generation in MWh. Then, the forecast is carried out till December, 2029. It is shown as:
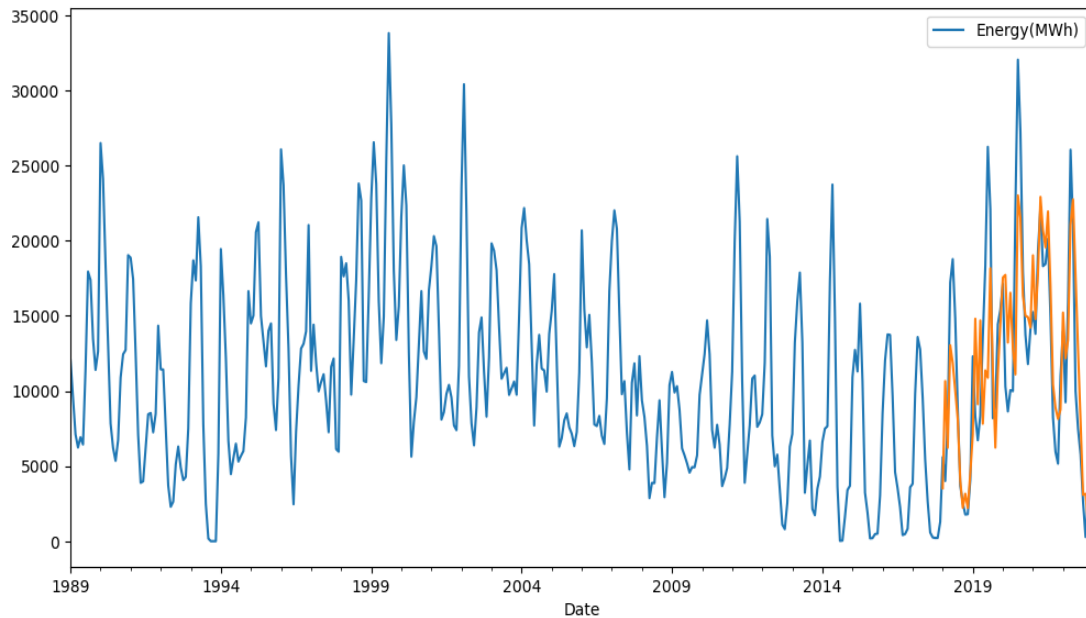
Figure 5.5 Plot on Energy Generation forecasted from January, 2018 to December,2022

The data from January 2018 to December 2022, known as training set, is used to forecast the power generation for the same time period. The graph represents the high correlation of training set.

Result summary:

```
==================================================================
==========
                 coef     std err          z       P>|z|        [0.025
0.975]
------------------------------------------------------------------
----------
ma.L1          -0.0377      0.042      -0.903       0.367       -0.120
0.044
ma.L2          -0.6642      0.039     -16.907       0.000       -0.741
-0.587
ar.S.L12        0.0098      0.059       0.167       0.868       -0.105
0.125
```

```
ma.S.L12     -1.7440      0.050     -34.964      0.000      -1.842
-1.646
ma.S.L24      0.7552      0.045      16.706      0.000       0.667
0.844
sigma2     1.235e+07    1.89e-09    6.52e+15     0.000      1.23e+07
1.23e+07
================================================================
==========
```

The attribute results from the output of SARIMAX gives a significant volume of information. The coefficient column shows the weight of each feature and how each one impacts the time series. The P>|z| column informs us of the significance of each feature weight. Here, most of the weight has a p-value lower or close to 0.05. So, it is reasonable to retain all of them in our model.

Plot diagnostics:

The plot diagnostics object allows us to quickly generate model diagnostics and investigate for any unusual behavior.
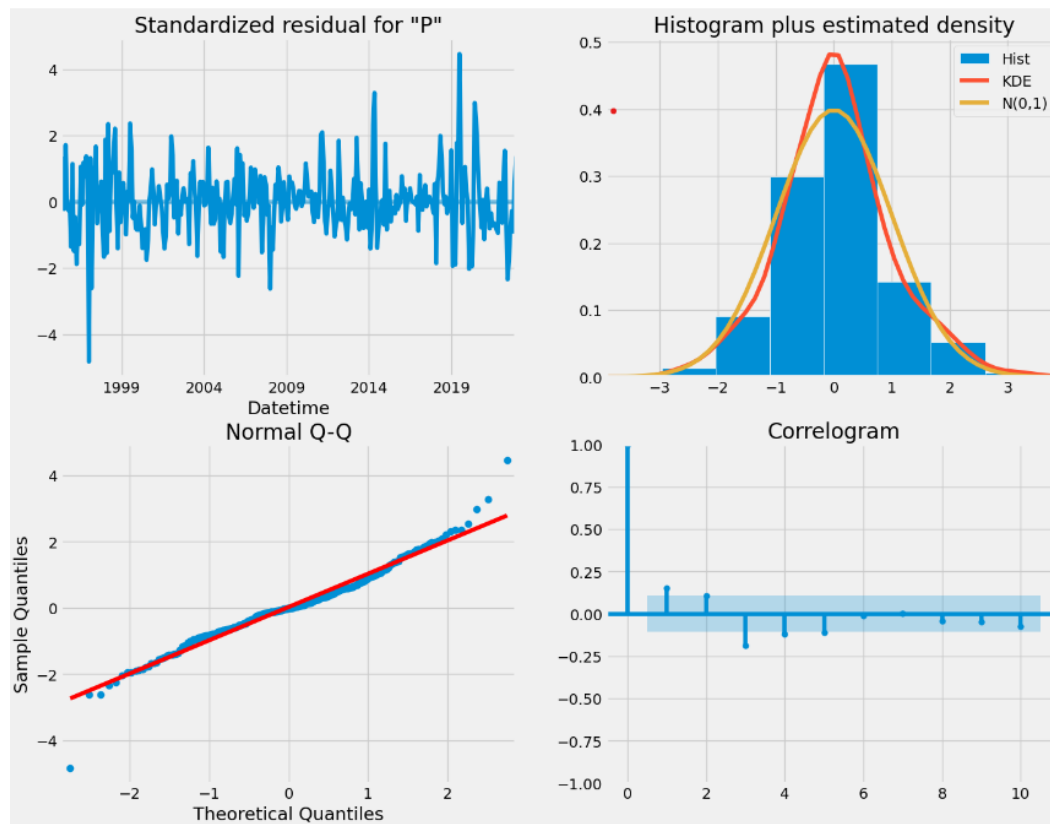
Figure 5.6 Model diagnostics of SARIMAX model

Our model diagnostics suggests that the model residuals are normally distributed based on the following:

1. In the top right plot, we see that the red KDE line follows closely with the N(0,1) line (where N(0,1) is the standard notation for a normal distribution with a mean 0 and standard deviation of 1). This is a good indication that the residuals are normally distributed.

2. The qq-plot on the bottom left shows that the ordered distribution of residuals (blue dots) follows the linear, trend of the samples taken from a standard normal distribution with N (0,1). Again, this is a strong indication that the residuals are normally distributed.

3. The residuals over time don't display any obvious seasonality and appear to be white

noise. This is confirmed by the autocorrelation (i.e correlogram) plot on the bottom right, which shows that the time series residuals have low correlation with lagged version of itself.
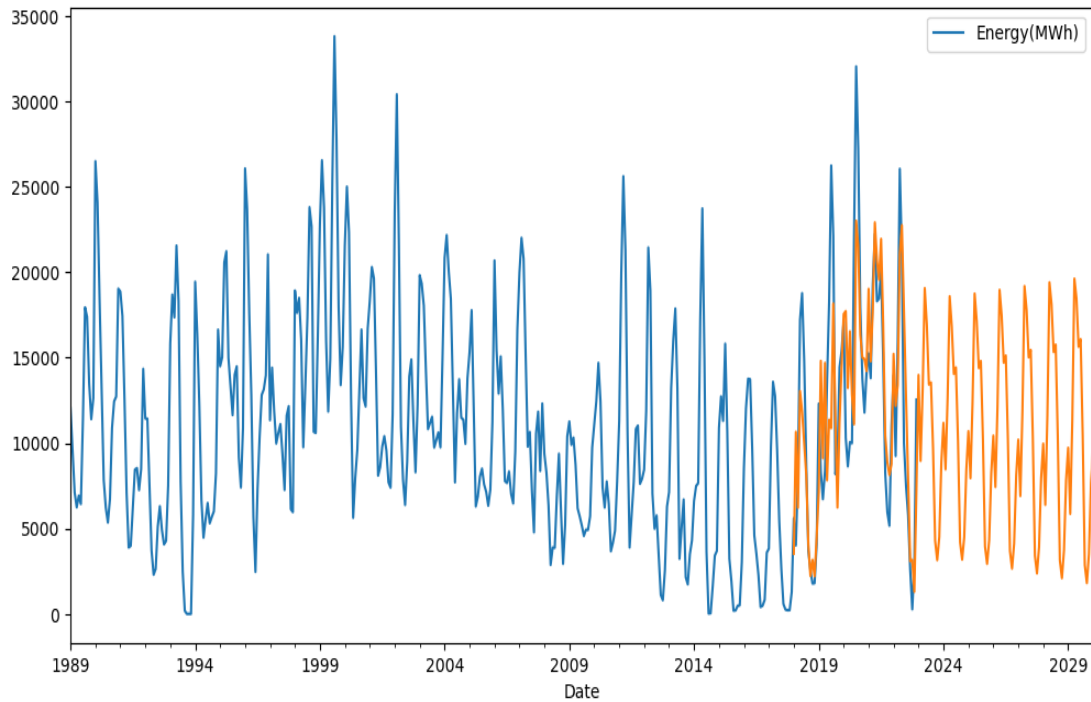
Figure 5.7 Plot on Energy Generation forecasted from January, 2018 to December, 2029

Overall, our forecasts align with the true values very well. As we forecast further out into the future, it is natural for us to become less confident in our values.
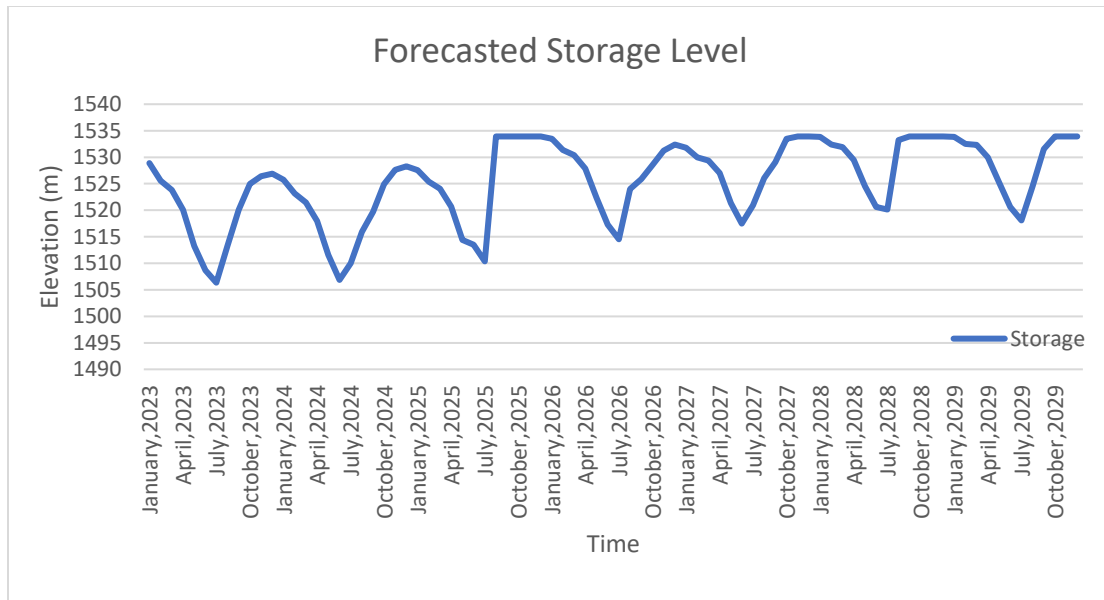
Figure 5.8 Plot of Storage Level forecasted from January, 2023 to December, 2029

The forecasted energy generation and the forecasted discharge into the reservoir were input into the SOP algorithm to simulate storage level from 2023-2029. The forecast shows that there is no significant trend in the change in storage level. However, the storage level is predicted to be high during the time period.

5.7 Discussion

From the results above, we can see that the energy generation depend upon the demand and the available water rather than the dry and wet season. Also, the energy generation is minimum during some months. It is because of the maintenance and the shutdown of reservoir operation. Our model for SOP performed very well for the given datasets by incorporating the evaporation losses. This shows that it can be used for the simulation of reservoir operation if inflow, demand and operation hour of the reservoir is recorded accurately. Also, the forecast showed that there is no significant trend in the change in storage level. However, the storage level is predicted to be high from 2023-2029.

6 Conclusion

Standard Operating Policy program was developed to observe the change in head level of the reservoir. The program was developed to simulate reservoir capacity from 2010 to 2022. Non-linear regression model was used for the discharge calculation. The simulated discharge was compared with recorded data and then was calibrated and validated. CMIP6 tool was used to forecast the precipitation under scenario SSP 245 using 5 models. Average values from all models were used as the precipitation. SARIMAX model was used for power forecast from the years 2022-2029. The model can be used for the optimization of the reservoir after overcoming all the limitations mentioned.

7 Recommendation

Better hydrological model can be used for better analysis of the reservoir operation. The operation hour of the turbine was unrecorded for the time period. Our model could perform better if the operation hour was incorporated into the algorithm. Also, the energy generation data was recorded in Nepali calendar, so there might have been some discrepancy while converting the data into the English calendar.

The obtained results can be used for the optimization of reservoir operation by incorporating the SOP programming model into it. Moreover, the SOP programming model can be further redefined to use as a GIS plugin for simulation of reservoir operation. Also, the machine learning modules, neural network modules etc. can be used for more accurate forecasting of the power generation.

A-1 Annex

Check for Homogeneity

Table A-1: Homogeneity check from cumulative deviation method

Year	Yearly cumulative			
	Daman	Chisapani Gadhi	Markhu	Dhunibesi
1993	1932	2698.4	1936.8	1539.1
1994	1078.5	1909.2	1176.2	1819.7
1995	1619.6	2186.7	1683.7	1645.1
1996	1803.8	2272	1298	1596.3
1997	1252.7	2661.4	1473.4	2120.5
1998	1680.6	2418.2	1592.9	3032.7
1999	2576.6	2930.2	2032.2	2014.9
2000	2186.6	2687.1	1498.4	1415.9
2001	1716.7	1725.8	1365.1	1782
2002	2427.2	2955.8	1940.3	2090.2
2003	1352.3	2712.8	1484.3	1556.4
2004	1880.6	2214.4	1405.6	1319.6
2005	1381.6	2243.3	1286.2	1443.2
2006	1621.7	391.2	1266.7	1498.7
2007	1902	3246.5	1548	1413.3
2008	892.8	1068.9	943	1149.2
2009	1071	1214.9	1152.7	1375.2
2010	1000.7	1349.5	1232.3	1772.8
2011	1903.5	1901.4	1485.7	1683.9
2012	1519.9	1641.4	1133.5	1748.1
2013	1479.9	1890.2	1235.3	1333.2
2014	852.2	1614.9	751.4	1004.4
2015	1150.4	1434	895.5	1135.6
2016	1128.1	1646.6	1012	1179.3
2017	1357.6	1933.4	1136.1	1405.8
2018	1488.9	1905.5	1092.3	1781.7
2019	1721.1	2181	1633.1	1688.1
2020	1987.3	2432.5	1675	1530.1
2021	2193.8	2309.9	1516.6	1721.3

2022	1734.6	2254.4	1337.8	1362.1
n =	30			
Average:	1596.5	2067.7	1374	1605.3
Standard Deviation	442.1	621.6	308.2	384.7

Table i: Y calculation

	Y			
Year	Daman	Chisapani Gadhi	Markhu	Dhunibesi
1993	249.7	1173.1	180.3	-140.3
1994	-603.8	383.9	-580.3	140.3
1995	-62.7	661.4	-72.8	-34.3
1996	121.5	746.7	-458.5	-83.1
1997	-429.6	1136.1	-283.1	441.1
1998	-1.7	892.9	-163.6	1353.3
1999	894.3	1404.9	275.7	335.5
2000	504.3	1161.8	-258.1	-263.5
2001	34.4	200.5	-391.4	102.6
2002	744.9	1430.5	183.8	410.8
2003	-330.0	1187.5	-272.2	-123.0
2004	198.3	689.1	-350.9	-359.8
2005	-300.7	718.0	-470.3	-236.2
2006	-60.6	-1134.1	-489.8	-180.7
2007	219.7	1721.2	-208.5	-266.1
2008	-789.5	-456.4	-813.5	-530.2
2009	-611.3	-310.4	-603.8	-304.2
2010	-681.6	-175.8	-524.2	93.4
2011	221.2	376.1	-270.8	4.5
2012	-162.4	116.1	-623.0	68.7
2013	-202.4	364.9	-521.2	-346.2
2014	-830.1	89.6	-1005.1	-675.0
2015	-531.9	-91.3	-861.0	-543.8
2016	-554.2	121.3	-744.5	-500.1
2017	-324.7	408.1	-620.4	-273.6
2018	-193.4	380.2	-664.2	102.3
2019	38.8	655.7	-123.4	8.7
2020	305.0	907.2	-81.5	-149.3
2021	511.5	784.7	-239.9	41.9
2022	52.3	729.1	-418.7	-317.3

	-85.9	542.5	-382.5	-74.1

Y$_{avg}$ =

Then $(Y_i - Yavg)$ is calculated as follows:

	Y$_i$-Y$_{avg}$			
Year	Daman	Chisapani Gadhi	Markhu	Dhunibesi
1993	335.5	630.7	562.8	-66.2
1994	-518.0	-158.5	-197.8	214.4
1995	23.1	119.0	309.7	39.8
1996	207.3	204.3	-76.0	-9.0
1997	-343.8	593.7	99.4	515.2
1998	84.1	350.5	218.9	1427.4
1999	980.1	862.5	658.2	409.6
2000	590.1	619.4	124.4	-189.4
2001	120.2	-341.9	-8.9	176.7
2002	830.7	888.1	566.3	484.9
2003	-244.2	645.1	110.3	-48.9
2004	284.1	146.7	31.6	-285.7
2005	-214.9	175.6	-87.8	-162.1
2006	25.2	-1676.5	-107.3	-106.6
2007	305.5	1178.8	174.0	-192.0
2008	-703.7	-998.8	-431.0	-456.1
2009	-525.5	-852.8	-221.3	-230.1
2010	-595.8	-718.2	-141.7	167.5
2011	307.0	-166.3	111.7	78.6
2012	-76.5	-426.3	-240.5	142.8
2013	-116.6	-177.5	-138.7	-272.1
2014	-744.3	-452.8	-622.6	-600.9
2015	-446.1	-633.7	-478.5	-469.7
2016	-468.4	-421.1	-362.0	-426.0
2017	-238.9	-134.3	-237.9	-199.5
2018	-107.6	-162.2	-281.7	176.4
2019	124.6	113.3	259.1	82.8
2020	390.8	364.8	301.0	-75.2
2021	597.3	242.2	142.6	116.0
2022	138.1	186.6	-36.3	-243.2
D$_Y$ =	434.69	611.16	303.03	378.25

Cumulative sum S_k^* is obtained as:

Year	S*			
	Daman	Chisapani Gadhi	Markhu	Dhunibesi
1993	335.5	630.7	562.8	-66.2
1994	-182.5	472.2	365.0	148.2
1995	-159.3	591.2	674.7	188.1
1996	48.0	795.4	598.7	179.1
1997	-295.8	1389.1	698.1	694.3
1998	-211.7	1739.6	917.0	2121.7
1999	768.4	2602.1	1575.2	2531.3
2000	1358.6	3221.5	1699.6	2342.0
2001	1478.8	2879.6	1690.7	2518.7
2002	2309.5	3767.6	2257.0	3003.6
2003	2065.3	4412.7	2367.3	2954.7
2004	2349.4	4559.4	2398.9	2669.0
2005	2134.6	4735.0	2311.1	2507.0
2006	2159.8	3058.5	2203.8	2400.4
2007	2465.3	4237.3	2377.8	2208.4
2008	1761.7	3238.4	1946.8	1752.3
2009	1236.2	2385.6	1725.5	1522.2
2010	640.4	1667.4	1583.8	1689.8
2011	947.4	1501.1	1695.5	1768.4
2012	870.9	1074.8	1455.0	1911.2
2013	754.3	897.3	1316.3	1639.1
2014	10.0	444.5	693.7	1038.2
2015	-436.1	-189.3	215.2	568.6
2016	-904.4	-610.4	-146.8	142.6
2017	-1143.3	-744.7	-384.7	-56.9
2018	-1250.9	-906.9	-666.4	119.5
2019	-1126.3	-793.6	-407.3	202.3
2020	-735.4	-428.8	-106.3	127.2
2021	-138.1	-186.6	36.3	243.2
2022	0.0	0.0	0.0	0.0

Design Flood Estimation

Table A-2 Rainfall Analysis of Chisapani Gadhi Station using Log-excel Method

Station	Year	Extreme rainfall(mm)	extreme rainfall in descending order (mm)	Rank(m)	Frequency f=m/(n+1)	Return period T=1/f	Predicted value from curve (mm)
Chisapani Gadhi	1993	295.0	459.5	1	0.0312	32	469.83
	1994	96.4	442.5	2	0.0625	16	386.48
	1995	116.0	344.2	3	0.0937	10.666	337.72
	1996	150.2	295.0	4	0.125	8	303.13
	1997	146.0	262.1	5	0.1562	6.4	276.29
	1998	98.3	227.5	6	0.1875	5.333	254.37
	1999	262.1	219.5	7	0.2187	4.542	235.83
	2000	162.0	216.5	8	0.25	4	219.78
	2001	192.8	194.1	9	0.2812	3.555	205.61
	2002	442.5	192.8	10	0.3125	3.2	192.94
	2003	344.2	162.5	11	0.3437	2.909	181.48
	2004	156.0	162.0	12	0.375	2.666	171.02
	2005	219.5	156.0	13	0.4062	2.461	161.39
	2006	42.0	150.2	14	0.4375	2.285	152.48
	2007	104.0	146.0	15	0.4687	2.133	144.19
	2008	45.0	136.5	16	0.5	2	136.42
	2009	102.3	135.5	17	0.5312	1.882	129.13
	2010	77.4	135.5	18	0.5625	1.777	122.26
	2011	135.5	123.0	19	0.5937	1.684	115.76
	2012	87.3	116.0	20	0.625	1.6	109.59

Year	Extreme rainfall(mm)	extreme rainfall in descending order (mm)	Rank(m)	Frequency f=m/(n+1)	Return period T=1/f	Predicted value from curve (mm)
2013	135.5	104.0	21	0.6562	1.523	103.72
2014	136.5	102.3	22	0.6875	1.454	98.13
2015	54.5	98.3	23	0.7187	1.391	92.79
2016	162.5	96.4	24	0.75	1.333	87.67
2017	459.5	95.5	25	0.7812	1.28	82.76
2018	94.5	94.5	26	0.8125	1.231	78.04
2019	216.5	87.3	27	0.8437	1.185	73.50
2020	123.0	77.4	28	0.875	1.142	69.13
2021	194.1	54.5	29	0.9062	1.103	64.91
2022	95.5	45.0	30	0.9375	1.066	60.83
2023	227.5	42.0	31	0.9687	1.032	56.89
Design Rainfall with return Period					10	329.96
					50	523.49
					100	606.85
					200	690.20
					500	800.38
					1000	883.73

Rainfall Analysis of Daman Station using Log-excel Method

Station	Year	Extreme rainfall(mm)	extreme rainfall in descending order (mm)	Rank(m)	Frequency f=m/(n+1)	Return period T=1/f	Predicted value from curve (mm)
	1993	373.2	373.2	1	0.0312	32	357.82
	1994	74.5	369.0	2	0.0625	16	293.93
	1995	101.0	319.3	3	0.0937	10.666	256.55
	1996	113.0	170.0	4	0.125	8	230.03
	1997	96.5	168.0	5	0.1562	6.4	209.46
	1998	140.4	165.5	6	0.1875	5.333	192.66
	1999	126.2	140.4	7	0.2187	4.5714	178.45
	2000	319.3	129.0	8	0.25	4	166.14
	2001	120.0	128.0	9	0.2812	3.555	155.28
	2002	369.0	126.2	10	0.3125	3.2	145.57
Daman	2003	129.0	122.0	11	0.3437	2.909	136.79
	2004	168.0	120.0	12	0.375	2.6666	128.76
	2005	90.0	113.0	13	0.4062	2.4615	121.39
	2006	71.0	111.6	14	0.4375	2.2857	114.56
	2007	170.0	101.0	15	0.4687	2.1333	108.20
	2008	39.2	100.9	16	0.5	2	102.25
	2009	100.9	100.0	17	0.5312	1.8823	96.66
	2010	85.0	96.5	18	0.5625	1.7777	91.39
	2011	100.0	94.0	19	0.5937	1.6842	86.41
	2012	111.6	93.0	20	0.625	1.6	81.68
	2013	72.3	90.0	21	0.6562	1.5238	77.18
	2014	64.5	85.0	22	0.6875	1.4545	72.89

	Year	Extreme rainfall(mm)	extreme rainfall in descending order (mm)	Rank(m)	Frequency f=m/(n+1)	Return period T=1/f	Predicted value from curve (mm)
	2015	32.6	83.1	23	0.7187	1.3913	68.80
	2016	83.1	76.0	24	0.75	1.3333	64.87
	2017	93.0	74.5	25	0.7812	1.28	61.11
	2018	76.0	72.3	26	0.8125	1.2307	57.49
	2019	94.0	71.0	27	0.8437	1.1851	54.01
	2020	128.0	65.2	28	0.8751	1.1428	50.66
	2021	165.5	64.5	29	0.9062	1.1034	47.43
	2022	65.2	39.2	30	0.9375	1.0666	44.30
	2023	122.0	32.6	31	0.9687	1.0322	41.28
Design Rainfall with return Period						10	250.60
						50	398.96
						100	462.85
						200	526.74
						500	611.20
						1000	675.10

Rainfall Analysis of Markhu Gaun Station using Log-excel Method

Station	Year	Extreme rainfall(mm)	extreme rainfall in decending order (mm)	Rank(m)	Frequency f=m/(n+1)	Return period T=1/f	Predicted value from curve (mm)
Markhu Gaun	1993	385.6	385.6	1	0.03125	32	302.17
	1994	70.3	275.0	2	0.0625	16	250.97
	1995	138.5	192.5	3	0.09375	10.6666	221.02
	1996	80.4	165.4	4	0.125	8	199.76
	1997	89.0	138.5	5	0.15625	6.4	183.28
	1998	110.0	130.0	6	0.1875	5.3333	169.81
	1999	192.5	130.0	7	0.21875	4.5714	158.42
	2000	130.0	120.0	8	0.25	4	148.56
	2001	110.0	118.0	9	0.28125	3.5556	139.86
	2002	275.0	110.4	14	0.4375	2.2857	107.22
	2003	120.0	110.0	14	0.4375	2.2857	107.22
	2004	118.0	110.0	14	0.4375	2.2857	107.22
	2005	84.4	110.0	14	0.4375	2.2857	107.22
	2006	110.0	110.0	14	0.4375	2.2857	107.22
	2007	75.0	105.3	15	0.46875	2.133	102.12
	2008	66.0	102.0	16	0.5	2	97.36
	2009	83.3	98.0	17	0.53125	1.8823	92.88
	2010	102.0	89.2	18	0.5625	1.777	88.66
	2011	165.4	89.0	19	0.59375	1.6842	84.66
	2012	69.2	84.4	20	0.625	1.6	80.87
	2013	89.2	83.3	21	0.65625	1.523	77.27
	2014	65.3	82.2	22	0.6875	1.454	73.83
	2015	47.0	80.4	23	0.71875	1.3913	70.55

Year	Extreme rainfall(mm)	extreme rainfall in descending order (mm)	Rank(m)	Frequency f=m/(n+1)	Return period T=1/f	Predicted value from curve (mm)
2016	98.0	75.0	24	0.75	1.3333	67.40
2017	66.5	70.3	25	0.78125	1.28	64.39
2018	60.5	69.2	26	0.8125	1.2307	61.49
2019	130.0	66.5	27	0.84375	1.1851	58.70
2020	110.0	66.0	28	0.875	1.142	56.02
2021	105.3	65.3	29	0.90625	1.103	53.42
2022	82.2	60.5	30	0.9375	1.0666	50.92
2023	110.4	47.0	31	0.96875	1.0322	48.50
Design Rainfall with return Period					10	216.25
					50	335.14
					100	386.35
					200	437.55
					500	505.24
					1000	556.44

Rainfall Analysis of Dhunibesi Station using Log-excel Method

Station	Year	Extreme rainfall(mm)	extreme rainfall in descending order (mm)	Rank(m)	Frequency f=m/(n+1)	Return period T=1/f	Predicted value from curve (mm)
Dhunibesi	1993	88.3	313.0	1	0.03125	32	259.42
	1994	98.0	198.0	2	0.0625	16	216.15
	1995	72.6	185.5	3	0.09375	10.6667	190.83
	1996	79.2	169.2	4	0.125	8	172.87
	1997	185.5	152.1	5	0.15625	6.4	158.94
	1998	109.4	136.7	6	0.1875	5.3333	147.55
	1999	103.4	110.2	7	0.21875	4.5719	137.93
	2000	51.2	109.4	8	0.25	4	129.59
	2001	169.2	103.4	9	0.28125	3.5556	122.24
	2002	98.0	98.0	14	0.4375	2.2857	94.65
	2003	85.0	98.0	14	0.4375	2.2857	94.65
	2004	90.6	90.6	14	0.4375	2.2857	94.65
	2005	110.2	88.3	14	0.4375	2.2857	94.65
	2006	61.2	87.4	14	0.4375	2.2857	94.65
	2007	84.6	87.2	15	0.46875	2.1333	90.34
	2008	79.4	85.0	16	0.5	2	86.31
	2009	74.0	84.6	17	0.53125	1.8823	82.53
	2010	70.2	84.2	18	0.5625	1.7777	78.96
	2011	87.4	79.4	19	0.59375	1.6842	75.58
	2012	313.0	79.2	20	0.625	1.6	72.38
	2013	87.2	74.0	21	0.65625	1.523	69.33
	2014	47.8	72.6	22	0.6875	1.4545	66.43
	2015	65.4	70.2	23	0.71875	1.3913	63.65

2016	198.0	65.4	24	0.75	1.333	61.00
2017	63.8	64.8	25	0.78125	1.28	58.45
2018	152.1	63.8	26	0.8125	1.2307	56.00
2019	58.2	61.2	27	0.84375	1.1851	53.64
2020	84.2	58.2	28	0.875	1.1428	51.37
2021	64.8	51.2	29	0.90625	1.1034	49.18
2022	48.4	48.4	30	0.9375	1.0666	47.07
2023	136.7	47.8	31	0.96875	1.0328	45.02
Design Rainfall with return Period					10	186.80
					50	287.29
					100	330.56
					200	373.84
					500	431.05
					1000	474.33

Calibration and Validation using Regression Equation

Table A-3: Calibration of the discharge using regression equation

Date	Precipitation (mm)	Observed Discharge (m³/s)	Simulated Discharge (m³/s)	Error	Sum of Errors
January,1972	1.927	1.72			
February,1972	51.416	1.78	1.48	0.3	0.09
March,1972	18.43	1.62	1.458	0.162	0.026
April,1972	21.424	1.41	1.434	-0.024	0.001
May,1972	57.78	1.38	1.424	-0.044	0.002
June,1972	258.689	1.45	2.917	-1.467	2.153
July,1972	819.538	26.3	27.356	-1.056	1.114
August,1972	145.78	5.6	3.239	2.361	5.576
September,1972	246.872	7.92	3.301	4.619	21.335
October,1972	93.515	3.51	2.23	1.28	1.639
November,1972	18.592	1.15	1.722	-0.572	0.327
December,1972	0	1.58	1.321	0.259	0.067
January,1973	62.667	1.38	1.47	-0.09	0.008
February,1973	50.632	1.24	1.406	-0.166	0.028
March,1973	58.555	1.58	1.385	0.195	0.038
April,1973	67.765	0.96	1.48	-0.52	0.27
May,1973	147.023	1.29	1.654	-0.364	0.132
June,1973	506.033	10.2	9.324	0.876	0.767
July,1973	271.736	7.34	3.978	3.362	11.304
August,1973	235.745	7.95	3.289	4.661	21.727

Date	Precipitation (mm)	Observed Discharge (m³/s)	Simulated Discharge (m³/s)	Error	Sum of Errors
September,1973	447.787	9.51	8.009	1.501	2.252
October,1973	220.526	9.51	3.243	6.267	39.276
November,1973	10.668	5.14	2.202	2.938	8.63
December,1973	0.807	2.74	1.888	0.852	0.727
January,1974	8.388	1.59	1.62	-0.03	0.001
February,1974	23.695	1.33	1.428	-0.098	0.01
March,1974	33.428	1.14	1.376	-0.236	0.056
April,1974	59.553	1.16	1.361	-0.201	0.04
May,1974	131.246	1.26	1.616	-0.356	0.127
June,1974	169.437	1.66	1.895	-0.235	0.055
July,1974	452.668	7.15	7.502	-0.352	0.124
August,1974	628.704	15.6	15.61	-0.01	0
September,1974	453.343	3.5	8.584	-5.084	25.85
October,1974	57.017	3.5	1.756	1.744	3.042
November,1974	13.643	1.96	1.719	0.241	0.058
December,1974	15.211	1.5	1.497	0.003	0
January,1975	32.58	1.28	1.414	-0.134	0.018
February,1975	19.591	1.18	1.357	-0.177	0.031
March,1975	9.004	0.88	1.33	-0.45	0.202
April,1975	53.259	0.76	1.276	-0.516	0.266
May,1975	186.514	1.07	1.894	-0.824	0.679
June,1975	251.485	2.11	2.736	-0.626	0.392
July,1975	616.751	14.8	14.46	0.34	0.116

Date	Precipitation (mm)	Observed Discharge (m³/s)	Simulated Discharge (m³/s)	Error	Sum of Errors
August,1975	427.143	11	7.725	3.275	10.727
September,1975	340.751	4.7	5.308	-0.608	0.37
October,1975	56.263	4.7	1.883	2.817	7.935
November,1975	12.97	2.35	1.847	0.503	0.253
December,1975	3.84	1.67	1.561	0.109	0.012
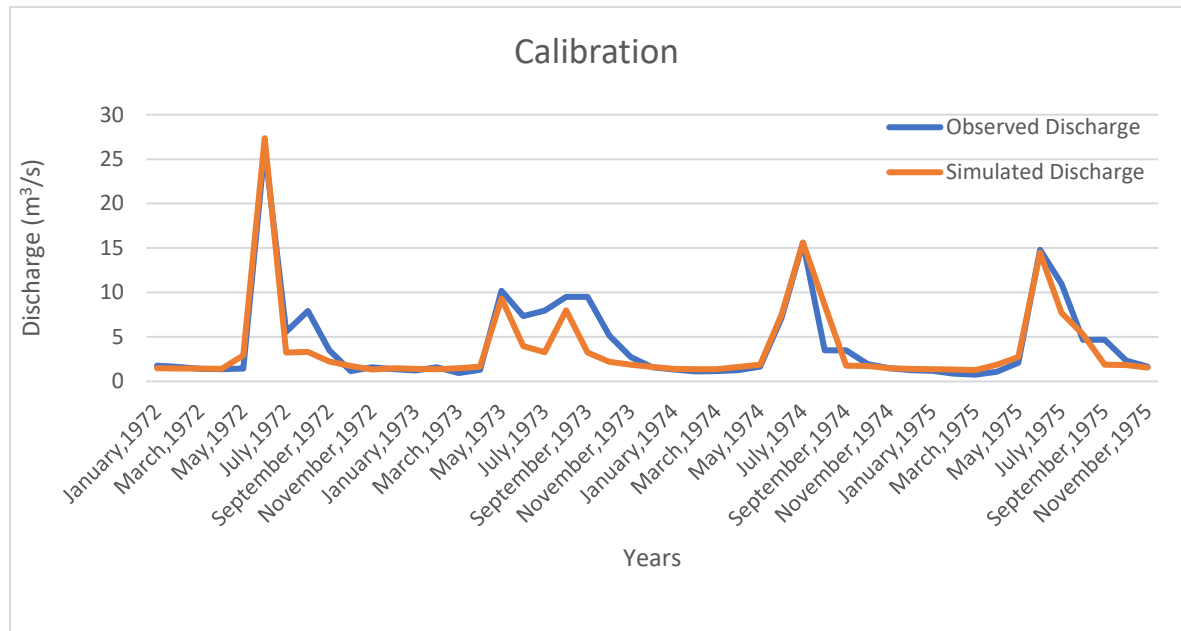
Figure A-1: Calibration plot of observed discharge versus simulated discharge

Table A-4: Validation of the discharge using regression equation

Date	Precipitation (mm)	Observed Discharge (m³/s)	Simulated Discharge (m³/s)
January,1976	42.056	1.46	1.436
February,1976	9.628	1.25	1.391
March,1976	0.205	1.02	1.380
April,1976	66.885	1.09	1.434
May,1976	181.766	1.44	2.039
June,1976	552.336	7.96	11.383
July,1976	441.542	6.04	8.010
August,1976	284.699	4.75	4.055
September,1976	191.371	2.3	2.516
October,1976	21.965	2.3	1.591
November,1976	7.297	1.75	1.424
December,1976	1.149	1.45	1.388
January,1977	5.431	1.28	1.380
February,1977	17.082	1.22	1.380
March,1977	32.564	1.07	1.387
April,1977	167.510	1.39	1.910
May,1977	167.384	1.64	2.016
June,1977	197.749	1.57	2.303
July,1977	276.447	3.16	3.365

Date	Precipitation (mm)	Observed Discharge (m³/s)	Simulated Discharge (m³/s)
August,1977	315.322	3.47	4.202
September,1977	121.790	1.8	2.040
October,1977	66.271	1.8	1.564
November,1977	44.021	1.6	1.439
December,1977	65.251	1.63	1.444
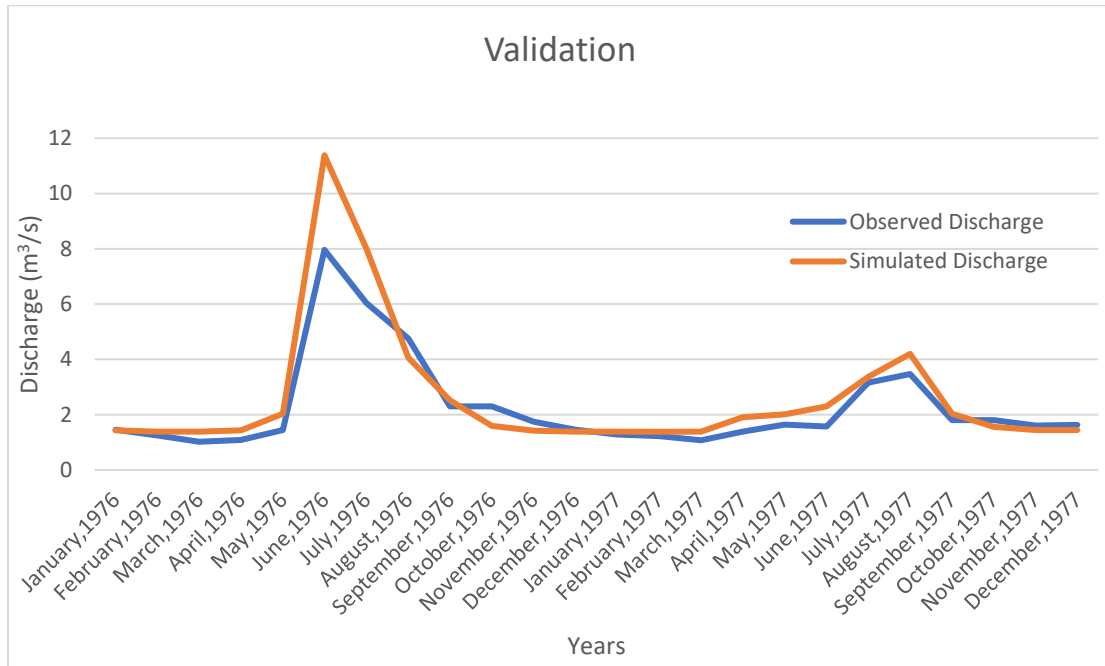
Figure A-2: Validation plot of observed discharge versus simulated discharge

Observation of change in storage of Kulekhani Reservoir using Standard Operating Policy
by Alija, Biplov, Dip Sagar, Hemanta, Kabindra, Saurab

90

B-1　　Annex

Power and Head Correlation and Standard Operating Policy

Table B-1: Volume Elevation & Area Calculation

Elevation (m)	Reference	Surface Area in (ha)	Volume in million cu.m
1534	BELOW	189.5	67.5
1533	BELOW	188.84	65.61
1532	BELOW	188.14	63.73
1531	BELOW	187.25	61.85
1530	BELOW	185.66	59.98
1529	BELOW	183.62	58.14
1528	BELOW	181.58	56.31
1527	BELOW	179.25	54.5
1526	BELOW	176.2	52.73
1525	BELOW	172.29	50.83
1524	BELOW	168.87	49.28
1523	BELOW	165.93	47.6
1522	BELOW	162.95	45.96
1521	BELOW	159.79	43.43
1520	BELOW	155.81	42.76
1519	BELOW	151.96	41.22
1518	BELOW	148.83	39.72
1517	BELOW	145.58	38.25
1516	BELOW	142.2	36.81
1515	BELOW	138.41	35.41
1514	BELOW	134.67	34.04
1513	BELOW	131.21	32.71
1512	BELOW	128.12	31.42
1511	BELOW	124.82	30.15
1510	BELOW	120.89	28.92
1509	BELOW	116.57	27.73
1508	BELOW	112.73	26.59
1507	BELOW	109.19	25.48
1506	BELOW	105.68	24.41
1505	BELOW	101.75	23.37
1504	BELOW	98	22.37

Observation of change in storage of Kulekhani Reservoir using Standard Operating Policy
by Alija, Biplov, Dip Sagar, Hemanta, Kabindra, Saurab

91

Elevation (m)	Reference	Surface Area in (ha)	Volume in million cu.m
1503	BELOW	95.19	21.4
1502	BELOW	92.54	20.47
1501	BELOW	89.78	19.56
1500	BELOW	86.31	18.67
1499	BELOW	82.94	17.83
1498	BELOW	80.59	17.01
1497	BELOW	78.24	16.22
1496	BELOW	76.25	15.45
1495	BELOW	73.87	14.69
1494	BELOW	71.59	13.97
1493	BELOW	69.58	13.26
1492	BELOW	67.55	12.58
1491	BELOW	65.39	11.91
1490	BELOW	63.23	11.27
1489	BELOW	61.2	10.65
1488	BELOW	59.28	10.04
1487	BELOW	57.29	9.46
1486	BELOW	55.57	8.9
1485	BELOW	53.68	8.35
1484	BELOW	51.72	7.82
1483	BELOW	50.2	6.95
1482	BELOW	48.78	6.82
1481	BELOW	47.39	6.34
1480	BELOW	45.85	5.87
1479	BELOW	44.12	5.42
1478	BELOW	42.53	4.99
1477	BELOW	41.05	4.57
1476	BELOW	39.59	4.17
1475	BELOW	37.95	3.78
1474	BELOW	36.29	3.41
1473	BELOW	34.74	3.06
1472	BELOW	33.21	2.72
1471	BELOW	31.62	2.39
1470	BELOW	29.76	1.86
1469	BELOW	27.79	1.8
1468	BELOW	26.14	1.53

Elevation (m)	Reference	Surface Area in (ha)	Volume in million cu.m
1467	BELOW	24.52	1.28
1466	BELOW	22.76	1.04
1465	BELOW	20.39	0.02
1464	BELOW	17.15	0.64
1463	BELOW	15.14	0.48
1462	BELOW	13.2	0.03
1461	BELOW	11.16	0.21
1460	BELOW	8.24	0.11
1459	BELOW	4.22	0.06

Table B-2: Computation of Recorded and Simulated Storage Level using SOP

Date	Recorded Storage Level (m)	Simulated Storage Level (m)
2010 Jan	1519.156	1519.333
2010 Feb	1515.756	1516.439
2010 Mar	1511.266	1512.337
2010 Apr	1504.896	1506.204
2010 May	1499.691	1500.560
2010 june	1497.851	1498.487
2010 july	1496.278	1498.096
2010 august	1496.59	1499.779
2010 sep	1506.655	1506.021
2010 oct	1517.92	1512.802
2010 nov	1520.79	1514.189
2010 dec	1520.823	1514.373
2011 Jan	1529.185	1512.803
2011 Feb	1526.895	1508.880
2011 march	1520.52	1497.805
2011 april	1511.145	1466.608
2011 may	1502.22	1459.702
2011 june	1497.805	1459.702
2011 july	1505.525	1491.380
2011 august	1518.325	1504.668
2011 sep	1526.055	1506.135
2011 oct	1529.625	1503.229

Date	Recorded Storage Level (m)	Simulated Storage Level (m)
2011 nov	1530.35	1498.772
2011 dec	1530.06	1496.309
2012 Jan	1529.37	1493.044
2012 Feb	1527.68	1488.636
2012 mar	1524.72	1478.523
2012 april	1517.095	1459.702
2012 may	1509.515	1459.702
2012 june	1507.98	1459.702
2012 july	1505.535	1467.135
2012 aug	1508.305	1489.175
2012 sep	1517.675	1493.919
2012 oct	1524.905	1506.005
2012 nov	1529.33	1509.685
2012 dec	1530.18	1511.301
2013 Jan	1530.195	1510.467
2013 Feb	1528.83	1509.027
2013 mar	1525.255	1503.413
2013 april	1520.355	1493.463
2013 may	1513.505	1475.125
2013 june	1508.77	1459.702
2013 july	1512.475	1476.451
2013 aug	1519.47	1488.743
2013 sep	1524.215	1493.660
2013 oct	1527.695	1498.268
2013 nov	1529.805	1502.712
2013 dec	1530.33	1504.022
2014 Jan	1530.42	1504.466
2014 Feb	1529.265	1503.187
2014 mar	1527.98	1501.147
2014 april	1526.64	1498.849
2014 may	1521.93	1484.666
2014 june	1514.96	1459.702
2014 july	1511.44	1459.702
2014 aug	1516.085	1478.401
2014 sep	1523.16	1495.431
2014 oct	1527.57	1502.846
2014 nov	1529.975	1506.534
2014 dec	1530.385	1507.738
2015 Jan	1526.335	1508.551

Date	Recorded Storage Level (m)	Simulated Storage Level (m)
2015 Feb	1523.055	1504.492
2015 mar	1519.01	1498.299
2015 april	1514.765	1491.715
2015 may	1507.555	1476.359
2015 june	1503.495	1459.702
2015 july	1510.835	1468.075
2015 aug	1517.85	1482.374
2015 sep	1520.28	1493.314
2015 oct	1523.87	1499.465
2015 nov	1525.565	1503.220
2015 dec	1526.545	1506.337
2016 Jan	1522.825	1507.548
2016 Feb	1520.325	1505.063
2016 mar	1516.22	1499.597
2016 april	1510.795	1490.323
2016 may	1505.01	1477.482
2016 june	1501.265	1471.038
2016 july	1503.525	1473.349
2016 aug	1511.295	1497.824
2016 sep	1517.315	1502.904
2016 oct	1520.3	1507.892
2016 nov	1522.32	1511.001
2016 dec	1523.235	1513.439
2017 Jan	1523.675	1514.163
2017 Feb	1522.68	1514.748
2017 mar	1519.355	1511.947
2017 april	1514.52	1506.431
2017 may	1509.78	1500.776
2017 june	1506.255	1497.507
2017 july	1504.35	1498.370
2017 aug	1509.08	1506.119
2017 sep	1516.995	1514.212
2017 oct	1520.57	1517.986
2017 nov	1522.585	1520.337
2017 dec	1523.635	1522.454
2018 Jan	1525.865	1524.073
2018 Feb	1524.935	1523.771
2018 mar	1524.69	1524.155
2018 april	1522.82	1522.658

Observation of change in storage of Kulekhani Reservoir using Standard Operating Policy
by Alija, Biplov, Dip Sagar, Hemanta, Kabindra, Saurab

Date	Recorded Storage Level (m)	Simulated Storage Level (m)
2018 may	1517.23	1517.427
2018 june	1510.445	1509.895
2018 july	1509.545	1506.730
2018 aug	1515.91	1516.991
2018 sep	1522.175	1520.877
2018 oct	1524.96	1522.684
2018 nov	1525.99	1524.205
2018 dec	1526.425	1525.566
2019 Jan	1519.08	1525.932
2019 Feb	1516.28	1522.806
2019 mar	1515.12	1521.461
2019 april	1513.715	1520.720
2019 may	1511.695	1519.438
2019 june	1507.41	1515.894
2019 july	1515.585	1509.484
2019 aug	1524.535	1516.069
2019 sep	1522.945	1508.494
2019 oct	1525.755	1511.421
2019 nov	1526.4	1509.631
2019 dec	1523.13	1503.360
2020 Jan	1520.025	1494.246
2020 Feb	1514.305	1479.507
2020 mar	1511.21	1467.517
2020 april	1508.365	1459.702
2020 may	1505.275	1459.702
2020 june	1505.08	1459.702
2020 july	1507.715	1459.702
2020 aug	1514.965	1480.331
2020 sep	1518.855	1459.702
2020 oct	1521.725	1459.702
2020 nov	1524.815	1459.702
2020 dec	1523.455	1459.702
2021 Jan	1527.65	1459.702
2021 Feb	1524.175	1459.702
2021 mar	1520.615	1459.702
2021 april	1513.22	1459.702
2021 may	1504.105	1459.702
2021 june	1497.74	1459.702
2021 july	1506.915	1459.702

Observation of change in storage of Kulekhani Reservoir using Standard Operating Policy
by Alija, Biplov, Dip Sagar, Hemanta, Kabindra, Saurab

Date	Recorded Storage Level (m)	Simulated Storage Level (m)
2021 aug	1519.385	1494.339
2021 sep	1523.845	1494.405
2021 oct	1529.03	1493.314
2021 nov	1529.89	1492.897
2021 dec	1529.47	1492.603
2022 Jan	1526.385	1484.964
2022 Feb	1522.765	1467.546
2022 mar	1520.44	1459.702
2022 april	1514.87	1459.702
2022 may	1502.11	1459.702
2022 june	1494.42	1459.702
2022 july	1496.255	1459.702
2022 aug	1503.14	1481.723
2022 sep	1512.525	1502.828
2022 oct	1520.795	1508.072
2022 nov	1527.235	1511.549
2022 dec	1528.96	1512.973

Computer code for Standard Operating Policy

```
import pandas as pd

import numpy as np

import sys

daily_df=pd.read_excel('inflow2.xlsx')

curve_df = pd.read_excel('VEA.xlsx')

def convert_cms_to_mcm(val):

    result = val*30.*24.*60.*60./1.e6

    return result

def predict_y_from_x(dataframe, x_column, y_column, degree, x_to_predict):
    x_values = dataframe[x_column].values
    y_values = dataframe[y_column].values
    coefficients = np.polyfit(x_values, y_values, degree)
```

```
    poly_equation = np.poly1d(coefficients)

    y_predicted = poly_equation(x_to_predict)

    return y_predicted

x_column = 'Volume'

y_column = 'Elevation'

degree = 10

def predict_a_from_h(dataframe, x1_column, y1_column, degree1, x1_to_predict):

    x1_values = dataframe[x1_column].values

    y1_values = dataframe[y1_column].values

    coefficients = np.polyfit(x1_values, y1_values, degree1)

    poly_equation = np.poly1d(coefficients)

    a_predicted = poly_equation(x1_to_predict)

    return a_predicted

x1_column = 'Elevation'

y1_column = 'Area'

degree1=6

def predict_a_from_v(dataframe, x2_column, y2_column, degree2, x2_to_predict):

    x2_values = dataframe[x2_column].values

    y2_values = dataframe[y2_column].values

    coefficients = np.polyfit(x2_values, y2_values, degree2)

    poly_equation = np.poly1d(coefficients)

    a_predicted = poly_equation(x2_to_predict)

    return a_predicted

x2_column = 'Volume'

y2_column = 'Area'

degree2=10

def predict_v_from_h(dataframe, x3_column, y3_column, degree3, x3_to_predict):

    x3_values=dataframe[x3_column].values
```

```
    y3_values= dataframe[y3_column].values
    coefficients = np.polyfit(x3_values, y3_values, degree3)
    poly_equation = np.poly1d(coefficients)
    v_predicted = poly_equation(x3_to_predict)
    return v_predicted

x3_to_predict = float(input ("Enter initial water level:  "))

initial_storage = predict_v_from_h(curve_df, x3_column, y3_column, degree3,
x3_to_predict)

def convert_eg_to_demand(energy , elevation):

    head = elevation- 918
    result = energy/(0.85*9810*head)
    return result

daily_df['Inflow']= convert_cms_to_mcm(daily_df['Discharge(m3/s)'].to_numpy())

def reservoir_simulation(df, initial_storage, storage_capacity):

    inflow=df['Inflow'].to_numpy()
    Energy=df['Energy'].to_numpy()
    K=df['Ke'].to_numpy()
    N=len(inflow)
    demand=np.zeros(N)
    storage=np.zeros(N)
    height=np.zeros(N)
    area=np.zeros(N)
    trial_evaporation=np.zeros(N)
    evap=np.zeros(N)
    delivery=np.zeros(N)
    spill=np.zeros(N)
    outflow=np.zeros(N)
```

```
    energy_generated=np.zeros(N)
storage[0]=initial_storage
  for i in range(N):
    x_to_predict =storage[i]
    height[i] = predict_y_from_x(curve_df, x_column, y_column, degree,
x_to_predict)
    x2_to_predict = storage[i]
    area[i]= predict_a_from_v(curve_df, x2_column, y2_column, degree2,
x2_to_predict)
    elevation = height[i]
    energy= Energy[i]
    demand[i]= convert_eg_to_demand (energy , elevation)
        trial_evaporation[i] = (K[i] * area[i])/1.e6
      available_water=inflow[i]+storage[i]-trial_evaporation[i]
    if available_water>demand[i]:
      delivery[i]=demand[i]
    else:
      delivery[i]=available_water
    delivery[i] = max(0, delivery[i])
    trial_storage=storage[i]+inflow[i]-delivery[i]-trial_evaporation[i]
    trial_storage = max(0, min(trial_storage, storage_capacity))
    if trial_storage>storage_capacity:
      spill[i]= trial_storage-storage_capacity
      if i< N-1:
        storage[i+1]=storage_capacity
    else:
      spill[i]=0
      if i<N-1:
        storage[i+1]=trial_storage
```

```
area[i]=predict_a_from_v(curve_df, x2_column, y2_column, degree2,
storage[i])

    if i<N-1:

      x2_to_predict=storage[i+1]

      area[i+1]=predict_a_from_v(curve_df, x2_column, y2_column, degree2,
x2_to_predict)

    if i<N-1:

      while True:

        a=area[i]

        b=area[i+1]

        c=(a+b)*0.5

        evap[i] = K[i]*c/1.e6

        available_water=inflow[i]+storage[i]- evap[i]

        if available_water>demand[i]:

          delivery[i]=demand[i]

        else:

          delivery[i]=available_water

        delivery[i] = max(0, delivery[i])

        trial_storage=storage[i]+inflow[i]-delivery[i]-evap[i]

        trial_storage = max(0, trial_storage)

        if trial_storage>storage_capacity:

          spill[i]= trial_storage-storage_capacity

          storage[i+1]=storage_capacity

        else:

          spill[i]=0

          storage[i+1]=trial_storage

        area[i+1]=predict_a_from_v(curve_df,x2_column, y2_column, degree2,
storage[i+1])
```

```
            if abs(b-area[i+1])<0.0001:
                break
        outflow[i]=spill[i]+delivery[i]
        energy_generated[i]=(0.85*9810*delivery[i]*(height[i]-916))/3600
    df['demand']=demand
    df['storage']=storage
    df['Height']=height
    df['Area']=area
    df['Evap Loss']=trial_evaporation
    df['Evap']=evap
    df['Delivery']=delivery
    df['Spill']=spill
    df['Outflow']=outflow
    df['Generated'] = energy_generated
    return df
maximum_capacity=67.5
daily_df=reservoir_simulation(daily_df, initial_storage, maximum_capacity)
```

Observation of change in storage of Kulekhani Reservoir using Standard Operating Policy
by Alija, Biplov, Dip Sagar, Hemanta, Kabindra, Saurab

102

C-1   Annex

Best fitting of seasonal and non-seasonal order

Table C-1: Calculation of Minimum Akaike Information Criterion (AIC)

Non-seasonal order (p,d,q)	Seasonal Order (p,d,q,m)	AIC
(0, 0, 0)	(0, 0, 0, 12)	8325.9151
(0, 0, 0)	(0, 0, 1, 12)	7812.4354
(0, 0, 0)	(0, 0, 2, 12)	7574.932
(0, 0, 0)	(0, 1, 0, 12)	7507.6949
(0, 0, 0)	(0, 1, 1, 12)	7220.2801
(0, 0, 0)	(0, 1, 2, 12)	6957.1829
(0, 0, 0)	(0, 2, 0, 12)	7609.4099
(0, 0, 0)	(0, 2, 1, 12)	7091.0816
(0, 0, 0)	(0, 2, 2, 12)	6807.3896
(0, 0, 0)	(1, 0, 0, 12)	7510.9491
(0, 0, 0)	(1, 0, 1, 12)	7450.7502
(0, 0, 0)	(1, 0, 2, 12)	7219.4285
(0, 0, 0)	(1, 1, 0, 12)	7260.7635
(0, 0, 0)	(1, 1, 1, 12)	7216.683
(0, 0, 0)	(1, 1, 2, 12)	6959.127
(0, 0, 0)	(1, 2, 0, 12)	7225.7073
(0, 0, 0)	(1, 2, 1, 12)	7056.5772
(0, 0, 0)	(1, 2, 2, 12)	6780.8911
(0, 0, 0)	(2, 0, 0, 12)	7255.1861
(0, 0, 0)	(2, 0, 1, 12)	7237.0192
(0, 0, 0)	(2, 0, 2, 12)	7221.1828
(0, 0, 0)	(2, 1, 0, 12)	6989.7492
(0, 0, 0)	(2, 1, 1, 12)	6977.951
(0, 0, 0)	(2, 1, 2, 12)	6960.0638
(0, 0, 0)	(2, 2, 0, 12)	6916.5717
(0, 0, 0)	(2, 2, 1, 12)	6815.9991
(0, 0, 0)	(2, 2, 2, 12)	6773.3656
(0, 0, 1)	(0, 0, 0, 12)	7988.9102
(0, 0, 1)	(0, 0, 1, 12)	7684.5872
(0, 0, 1)	(0, 0, 2, 12)	7417.3343
(0, 0, 1)	(0, 1, 0, 12)	7271.5442

(0, 0, 1)	(0, 1, 1, 12)	6951.1634
(0, 0, 1)	(0, 1, 2, 12)	6715.2581
(0, 0, 1)	(0, 2, 0, 12)	7408.0265
(0, 0, 1)	(0, 2, 1, 12)	6963.1484
(0, 0, 1)	(0, 2, 2, 12)	6689.8014
(0, 0, 1)	(1, 0, 0, 12)	7689.9335
(0, 0, 1)	(1, 0, 1, 12)	7160.4712
(0, 0, 1)	(1, 0, 2, 12)	7393.9686
(0, 0, 1)	(1, 1, 0, 12)	7017.629
(0, 0, 1)	(1, 1, 1, 12)	6953.1374
(0, 0, 1)	(1, 1, 2, 12)	6717.0676
(0, 0, 1)	(1, 2, 0, 12)	7061.5711
(0, 0, 1)	(1, 2, 1, 12)	6941.898
(0, 0, 1)	(1, 2, 2, 12)	6691.7796
(0, 0, 1)	(2, 0, 0, 12)	7436.2116
(0, 0, 1)	(2, 0, 1, 12)	6973.6116
(0, 0, 1)	(2, 0, 2, 12)	6934.7464
(0, 0, 1)	(2, 1, 0, 12)	6744.3627
(0, 0, 1)	(2, 1, 1, 12)	6731.0747
(0, 0, 1)	(2, 1, 2, 12)	6718.6947
(0, 0, 1)	(2, 2, 0, 12)	6691.3253
(0, 0, 1)	(2, 2, 1, 12)	6569.054
(0, 0, 1)	(2, 2, 2, 12)	6693.1188
(0, 0, 2)	(0, 0, 0, 12)	8006.003
(0, 0, 2)	(0, 0, 1, 12)	7311.1674
(0, 0, 2)	(0, 0, 2, 12)	7008.9621
(0, 0, 2)	(0, 1, 0, 12)	7227.7804
(0, 0, 2)	(0, 1, 1, 12)	6885.3681
(0, 0, 2)	(0, 1, 2, 12)	6651.943
(0, 0, 2)	(0, 2, 0, 12)	7374.3214
(0, 0, 2)	(0, 2, 1, 12)	6805.5237
(0, 0, 2)	(0, 2, 2, 12)	6643.281
(0, 0, 2)	(1, 0, 0, 12)	7255.9707
(0, 0, 2)	(1, 0, 1, 12)	7088.0019
(0, 0, 2)	(1, 0, 2, 12)	7347.1385
(0, 0, 2)	(1, 1, 0, 12)	6976.895
(0, 0, 2)	(1, 1, 1, 12)	6885.554

(0, 0, 2)	(1, 1, 2, 12)	6653.9316
(0, 0, 2)	(1, 2, 0, 12)	7038.6822
(0, 0, 2)	(1, 2, 1, 12)	6721.4174
(0, 0, 2)	(1, 2, 2, 12)	6644.4988
(0, 0, 2)	(2, 0, 0, 12)	6953.2377
(0, 0, 2)	(2, 0, 1, 12)	6921.7391
(0, 0, 2)	(2, 0, 2, 12)	6863.6559
(0, 0, 2)	(2, 1, 0, 12)	6721.6958
(0, 0, 2)	(2, 1, 1, 12)	6711.5356
(0, 0, 2)	(2, 1, 2, 12)	6655.7526
(0, 0, 2)	(2, 2, 0, 12)	6752.3031
(0, 0, 2)	(2, 2, 1, 12)	6527.3408
(0, 0, 2)	(2, 2, 2, 12)	6445.7762
(0, 1, 0)	(0, 0, 0, 12)	7500.3067
(0, 1, 0)	(0, 0, 1, 12)	7239.1064
(0, 1, 0)	(0, 0, 2, 12)	6990.559
(0, 1, 0)	(0, 1, 0, 12)	7350.871
(0, 1, 0)	(0, 1, 1, 12)	6961.5551
(0, 1, 0)	(0, 1, 2, 12)	6723.6869
(0, 1, 0)	(0, 2, 0, 12)	7505.3219
(0, 1, 0)	(0, 2, 1, 12)	6939.1827
(0, 1, 0)	(0, 2, 2, 12)	6580.6406
(0, 1, 0)	(1, 0, 0, 12)	7238.1582
(0, 1, 0)	(1, 0, 1, 12)	7175.9907
(0, 1, 0)	(1, 0, 2, 12)	6953.5839
(0, 1, 0)	(1, 1, 0, 12)	7045.5092
(0, 1, 0)	(1, 1, 1, 12)	6961.233
(0, 1, 0)	(1, 1, 2, 12)	6723.6417
(0, 1, 0)	(1, 2, 0, 12)	7057.0897
(0, 1, 0)	(1, 2, 1, 12)	6847.4414
(0, 1, 0)	(1, 2, 2, 12)	6555.3751
(0, 1, 0)	(2, 0, 0, 12)	6990.479
(0, 1, 0)	(2, 0, 1, 12)	6972.5054
(0, 1, 0)	(2, 0, 2, 12)	6955.4902
(0, 1, 0)	(2, 1, 0, 12)	6776.9435
(0, 1, 0)	(2, 1, 1, 12)	6744.7292
(0, 1, 0)	(2, 1, 2, 12)	6724.2311

(0, 1, 0)	(2, 2, 0, 12)	6728.0643
(0, 1, 0)	(2, 2, 1, 12)	6607.4131
(0, 1, 0)	(2, 2, 2, 12)	6548.936
(0, 1, 1)	(0, 0, 0, 12)	7403.23
(0, 1, 1)	(0, 0, 1, 12)	7170.6984
(0, 1, 1)	(0, 0, 2, 12)	6931.7283
(0, 1, 1)	(0, 1, 0, 12)	7328.4746
(0, 1, 1)	(0, 1, 1, 12)	6951.5606
(0, 1, 1)	(0, 1, 2, 12)	6717.3114
(0, 1, 1)	(0, 2, 0, 12)	7485.8601
(0, 1, 1)	(0, 2, 1, 12)	6892.3253
(0, 1, 1)	(0, 2, 2, 12)	6734.2523
(0, 1, 1)	(1, 0, 0, 12)	7205.9296
(0, 1, 1)	(1, 0, 1, 12)	7131.2976
(0, 1, 1)	(1, 0, 2, 12)	6907.7804
(0, 1, 1)	(1, 1, 0, 12)	7038.9245
(0, 1, 1)	(1, 1, 1, 12)	6951.5481
(0, 1, 1)	(1, 1, 2, 12)	6672.9388
(0, 1, 1)	(1, 2, 0, 12)	7052.1251
(0, 1, 1)	(1, 2, 1, 12)	6785.2312
(0, 1, 1)	(1, 2, 2, 12)	6735.3155
(0, 1, 1)	(2, 0, 0, 12)	6959.5612
(0, 1, 1)	(2, 0, 1, 12)	6944.9277
(0, 1, 1)	(2, 0, 2, 12)	6909.6916
(0, 1, 1)	(2, 1, 0, 12)	6777.6423
(0, 1, 1)	(2, 1, 1, 12)	6757.7496
(0, 1, 1)	(2, 1, 2, 12)	6719.8806
(0, 1, 1)	(2, 2, 0, 12)	6823.6212
(0, 1, 1)	(2, 2, 1, 12)	6781.0505
(0, 1, 1)	(2, 2, 2, 12)	6737.2259
(0, 1, 2)	(0, 0, 0, 12)	7373.0687
(0, 1, 2)	(0, 0, 1, 12)	7118.7207
(0, 1, 2)	(0, 0, 2, 12)	6871.6064
(0, 1, 2)	(0, 1, 0, 12)	7235.0912
(0, 1, 2)	(0, 1, 1, 12)	6870.9936
(0, 1, 2)	(0, 1, 2, 12)	6639.7618
(0, 1, 2)	(0, 2, 0, 12)	7369.6453

(0, 1, 2)	(0, 2, 1, 12)	6930.3429
(0, 1, 2)	(0, 2, 2, 12)	6405.4744
(0, 1, 2)	(1, 0, 0, 12)	7165.064
(0, 1, 2)	(1, 0, 1, 12)	7067.7261
(0, 1, 2)	(1, 0, 2, 12)	6839.532
(0, 1, 2)	(1, 1, 0, 12)	6984.1357
(0, 1, 2)	(1, 1, 1, 12)	6872.9202
(0, 1, 2)	(1, 1, 2, 12)	6596.4827
(0, 1, 2)	(1, 2, 0, 12)	7046.1881
(0, 1, 2)	(1, 2, 1, 12)	6713.6261
(0, 1, 2)	(1, 2, 2, 12)	6407.4579
(0, 1, 2)	(2, 0, 0, 12)	6920.1222
(0, 1, 2)	(2, 0, 1, 12)	6900.5923
(0, 1, 2)	(2, 0, 2, 12)	6841.531
(0, 1, 2)	(2, 1, 0, 12)	6722.7696
(0, 1, 2)	(2, 1, 1, 12)	6700.0141
(0, 1, 2)	(2, 1, 2, 12)	6598.185
(0, 1, 2)	(2, 2, 0, 12)	6653.4592
(0, 1, 2)	(2, 2, 1, 12)	6505.9414
(0, 1, 2)	(2, 2, 2, 12)	6656.3875
(0, 2, 0)	(0, 0, 0, 12)	7603.1903
(0, 2, 0)	(0, 0, 1, 12)	7366.6276
(0, 2, 0)	(0, 0, 2, 12)	7123.7987
(0, 2, 0)	(0, 1, 0, 12)	7559.1548
(0, 2, 0)	(0, 1, 1, 12)	7126.6347
(0, 2, 0)	(0, 1, 2, 12)	6870.1953
(0, 2, 0)	(0, 2, 0, 12)	7724.0462
(0, 2, 0)	(0, 2, 1, 12)	7162.7949
(0, 2, 0)	(0, 2, 2, 12)	6760.5547
(0, 2, 0)	(1, 0, 0, 12)	7383.3998
(0, 2, 0)	(1, 0, 1, 12)	7334.4542
(0, 2, 0)	(1, 0, 2, 12)	7103.6949
(0, 2, 0)	(1, 1, 0, 12)	7208.3459
(0, 2, 0)	(1, 1, 1, 12)	7111.2165
(0, 2, 0)	(1, 1, 2, 12)	6865.4244
(0, 2, 0)	(1, 2, 0, 12)	7241.7995
(0, 2, 0)	(1, 2, 1, 12)	6971.4624

(0, 2, 0)	(1, 2, 2, 12)	6705.434
(0, 2, 0)	(2, 0, 0, 12)	7134.5987
(0, 2, 0)	(2, 0, 1, 12)	7121.9465
(0, 2, 0)	(2, 0, 2, 12)	7105.9009
(0, 2, 0)	(2, 1, 0, 12)	6923.6958
(0, 2, 0)	(2, 1, 1, 12)	6886.0863
(0, 2, 0)	(2, 1, 2, 12)	6866.6656
(0, 2, 0)	(2, 2, 0, 12)	6881.4539
(0, 2, 0)	(2, 2, 1, 12)	6746.9877
(0, 2, 0)	(2, 2, 2, 12)	6685.6932
(0, 2, 1)	(0, 0, 0, 12)	7508.6353
(0, 2, 1)	(0, 0, 1, 12)	7228.8863
(0, 2, 1)	(0, 0, 2, 12)	6985.525
(0, 2, 1)	(0, 1, 0, 12)	7346.4177
(0, 2, 1)	(0, 1, 1, 12)	7030.513
(0, 2, 1)	(0, 1, 2, 12)	6790.4491
(0, 2, 1)	(0, 2, 0, 12)	7498.0714
(0, 2, 1)	(0, 2, 1, 12)	7105.0804
(0, 2, 1)	(0, 2, 2, 12)	6833.5376
(0, 2, 1)	(1, 0, 0, 12)	7254.435
(0, 2, 1)	(1, 0, 1, 12)	7200.9212
(0, 2, 1)	(1, 0, 2, 12)	6965.162
(0, 2, 1)	(1, 1, 0, 12)	7096.9897
(0, 2, 1)	(1, 1, 1, 12)	7032.4985
(0, 2, 1)	(1, 1, 2, 12)	6792.3691
(0, 2, 1)	(1, 2, 0, 12)	7180.1418
(0, 2, 1)	(1, 2, 1, 12)	7088.4574
(0, 2, 1)	(1, 2, 2, 12)	6835.4884
(0, 2, 1)	(2, 0, 0, 12)	7011.0726
(0, 2, 1)	(2, 0, 1, 12)	7004.3303
(0, 2, 1)	(2, 0, 2, 12)	6967.1322
(0, 2, 1)	(2, 1, 0, 12)	6843.8217
(0, 2, 1)	(2, 1, 1, 12)	6831.3129
(0, 2, 1)	(2, 1, 2, 12)	6793.7496
(0, 2, 1)	(2, 2, 0, 12)	6906.6328
(0, 2, 1)	(2, 2, 1, 12)	6879.2195
(0, 2, 1)	(2, 2, 2, 12)	6837.3214

Observation of change in storage of Kulekhani Reservoir using Standard Operating Policy
by Alija, Biplov, Dip Sagar, Hemanta, Kabindra, Saurab

(0, 2, 2)	(0, 0, 0, 12)	7394.7225
(0, 2, 2)	(0, 0, 1, 12)	7143.9506
(0, 2, 2)	(0, 0, 2, 12)	6902.6283
(0, 2, 2)	(0, 1, 0, 12)	7299.3155
(0, 2, 2)	(0, 1, 1, 12)	6882.0752
(0, 2, 2)	(0, 1, 2, 12)	6703.4848
(0, 2, 2)	(0, 2, 0, 12)	7455.3358
(0, 2, 2)	(0, 2, 1, 12)	7017.5148
(0, 2, 2)	(0, 2, 2, 12)	6735.736
(0, 2, 2)	(1, 0, 0, 12)	7198.1959
(0, 2, 2)	(1, 0, 1, 12)	7120.2039
(0, 2, 2)	(1, 0, 2, 12)	6883.9605
(0, 2, 2)	(1, 1, 0, 12)	7039.4112
(0, 2, 2)	(1, 1, 1, 12)	6942.1978
(0, 2, 2)	(1, 1, 2, 12)	6704.7973
(0, 2, 2)	(1, 2, 0, 12)	7121.3996
(0, 2, 2)	(1, 2, 1, 12)	6990.4417
(0, 2, 2)	(1, 2, 2, 12)	6452.579
(0, 2, 2)	(2, 0, 0, 12)	6952.6402
(0, 2, 2)	(2, 0, 1, 12)	6943.5217
(0, 2, 2)	(2, 0, 2, 12)	6885.954
(0, 2, 2)	(2, 1, 0, 12)	6779.5305
(0, 2, 2)	(2, 1, 1, 12)	6762.6519
(0, 2, 2)	(2, 1, 2, 12)	6706.6171
(0, 2, 2)	(2, 2, 0, 12)	6837.4866
(0, 2, 2)	(2, 2, 1, 12)	6800.7653
(0, 2, 2)	(2, 2, 2, 12)	6716.4972
(1, 0, 0)	(0, 0, 0, 12)	7508.6003
(1, 0, 0)	(0, 0, 1, 12)	7244.5162
(1, 0, 0)	(0, 0, 2, 12)	6994.9326
(1, 0, 0)	(0, 1, 0, 12)	7300.7861
(1, 0, 0)	(0, 1, 1, 12)	6960.3682
(1, 0, 0)	(0, 1, 2, 12)	6724.6019
(1, 0, 0)	(0, 2, 0, 12)	7446.8543
(1, 0, 0)	(0, 2, 1, 12)	6993.9794
(1, 0, 0)	(0, 2, 2, 12)	6508.1695
(1, 0, 0)	(1, 0, 0, 12)	7221.9401

(1, 0, 0)	(1, 0, 1, 12)	7171.9845
(1, 0, 0)	(1, 0, 2, 12)	6949.6154
(1, 0, 0)	(1, 1, 0, 12)	7000.2833
(1, 0, 0)	(1, 1, 1, 12)	6962.3682
(1, 0, 0)	(1, 1, 2, 12)	6726.135
(1, 0, 0)	(1, 2, 0, 12)	6998.0131
(1, 0, 0)	(1, 2, 1, 12)	6969.5578
(1, 0, 0)	(1, 2, 2, 12)	6716.9958
(1, 0, 0)	(2, 0, 0, 12)	6970.4327
(1, 0, 0)	(2, 0, 1, 12)	6949.6227
(1, 0, 0)	(2, 0, 2, 12)	6951.5022
(1, 0, 0)	(2, 1, 0, 12)	6742.9233
(1, 0, 0)	(2, 1, 1, 12)	6726.5832
(1, 0, 0)	(2, 1, 2, 12)	6727.9403
(1, 0, 0)	(2, 2, 0, 12)	6677.8549
(1, 0, 0)	(2, 2, 1, 12)	6721.4489
(1, 0, 0)	(2, 2, 2, 12)	6718.8299
(1, 0, 1)	(0, 0, 0, 12)	7400.7501
(1, 0, 1)	(0, 0, 1, 12)	7166.1251
(1, 0, 1)	(0, 0, 2, 12)	6920.6134
(1, 0, 1)	(0, 1, 0, 12)	7241.7574
(1, 0, 1)	(0, 1, 1, 12)	6887.0277
(1, 0, 1)	(0, 1, 2, 12)	6654.8193
(1, 0, 1)	(0, 2, 0, 12)	7394.1023
(1, 0, 1)	(0, 2, 1, 12)	6942.2478
(1, 0, 1)	(0, 2, 2, 12)	6439.9819
(1, 0, 1)	(1, 0, 0, 12)	7178.4841
(1, 0, 1)	(1, 0, 1, 12)	7093.3225
(1, 0, 1)	(1, 0, 2, 12)	6864.8619
(1, 0, 1)	(1, 1, 0, 12)	6946.0728
(1, 0, 1)	(1, 1, 1, 12)	6853.4595
(1, 0, 1)	(1, 1, 2, 12)	6624.5566
(1, 0, 1)	(1, 2, 0, 12)	7012.0831
(1, 0, 1)	(1, 2, 1, 12)	6728.9695
(1, 0, 1)	(1, 2, 2, 12)	6439.2096
(1, 0, 1)	(2, 0, 0, 12)	6914.1611
(1, 0, 1)	(2, 0, 1, 12)	6886.4012

(1, 0, 1)	(2, 0, 2, 12)	6866.854
(1, 0, 1)	(2, 1, 0, 12)	6688.6601
(1, 0, 1)	(2, 1, 1, 12)	6643.2021
(1, 0, 1)	(2, 1, 2, 12)	6658.4614
(1, 0, 1)	(2, 2, 0, 12)	6725.9469
(1, 0, 1)	(2, 2, 1, 12)	6479.2888
(1, 0, 1)	(2, 2, 2, 12)	6445.4529
(1, 0, 2)	(0, 0, 0, 12)	7380.893
(1, 0, 2)	(0, 0, 1, 12)	7142.4112
(1, 0, 2)	(0, 0, 2, 12)	6893.8601
(1, 0, 2)	(0, 1, 0, 12)	7223.7304
(1, 0, 2)	(0, 1, 1, 12)	6869.5184
(1, 0, 2)	(0, 1, 2, 12)	6637.3761
(1, 0, 2)	(0, 2, 0, 12)	7373.793
(1, 0, 2)	(0, 2, 1, 12)	6923.5156
(1, 0, 2)	(0, 2, 2, 12)	6639.5885
(1, 0, 2)	(1, 0, 0, 12)	7166.445
(1, 0, 2)	(1, 0, 1, 12)	7075.7268
(1, 0, 2)	(1, 0, 2, 12)	6849.5944
(1, 0, 2)	(1, 1, 0, 12)	6947.906
(1, 0, 2)	(1, 1, 1, 12)	6869.0699
(1, 0, 2)	(1, 1, 2, 12)	6639.2299
(1, 0, 2)	(1, 2, 0, 12)	7013.3791
(1, 0, 2)	(1, 2, 1, 12)	6711.7664
(1, 0, 2)	(1, 2, 2, 12)	6640.6024
(1, 0, 2)	(2, 0, 0, 12)	6915.4166
(1, 0, 2)	(2, 0, 1, 12)	6889.2794
(1, 0, 2)	(2, 0, 2, 12)	6851.5929
(1, 0, 2)	(2, 1, 0, 12)	6690.4497
(1, 0, 2)	(2, 1, 1, 12)	6676.8834
(1, 0, 2)	(2, 1, 2, 12)	6609.179
(1, 0, 2)	(2, 2, 0, 12)	6727.1995
(1, 0, 2)	(2, 2, 1, 12)	6481.2751
(1, 0, 2)	(2, 2, 2, 12)	6642.3103
(1, 1, 0)	(0, 0, 0, 12)	7464.4455
(1, 1, 0)	(0, 0, 1, 12)	7219.2561
(1, 1, 0)	(0, 0, 2, 12)	6975.8758

(1, 1, 0)	(0, 1, 0, 12)	7350.5778
(1, 1, 0)	(0, 1, 1, 12)	6981.3766
(1, 1, 0)	(0, 1, 2, 12)	6747.6189
(1, 1, 0)	(0, 2, 0, 12)	7506.2081
(1, 1, 0)	(0, 2, 1, 12)	7042.1695
(1, 1, 0)	(0, 2, 2, 12)	6757.61
(1, 1, 0)	(1, 0, 0, 12)	7208.6228
(1, 1, 0)	(1, 0, 1, 12)	7170.0143
(1, 1, 0)	(1, 0, 2, 12)	6947.4909
(1, 1, 0)	(1, 1, 0, 12)	7018.6334
(1, 1, 0)	(1, 1, 1, 12)	6983.1823
(1, 1, 0)	(1, 1, 2, 12)	6748.418
(1, 1, 0)	(1, 2, 0, 12)	7035.1096
(1, 1, 0)	(1, 2, 1, 12)	7013.595
(1, 1, 0)	(1, 2, 2, 12)	6518.307
(1, 1, 0)	(2, 0, 0, 12)	6961.9787
(1, 1, 0)	(2, 0, 1, 12)	6947.4942
(1, 1, 0)	(2, 0, 2, 12)	6949.4906
(1, 1, 0)	(2, 1, 0, 12)	6769.7836
(1, 1, 0)	(2, 1, 1, 12)	6749.1624
(1, 1, 0)	(2, 1, 2, 12)	6750.1483
(1, 1, 0)	(2, 2, 0, 12)	6807.5323
(1, 1, 0)	(2, 2, 1, 12)	6550.6843
(1, 1, 0)	(2, 2, 2, 12)	6761.4081
(1, 1, 1)	(0, 0, 0, 12)	7400.0409
(1, 1, 1)	(0, 0, 1, 12)	7164.7893
(1, 1, 1)	(0, 0, 2, 12)	6924.3875
(1, 1, 1)	(0, 1, 0, 12)	7298.2827
(1, 1, 1)	(0, 1, 1, 12)	6944.0512
(1, 1, 1)	(0, 1, 2, 12)	6710.6049
(1, 1, 1)	(0, 2, 0, 12)	7421.4227
(1, 1, 1)	(0, 2, 1, 12)	7006.4551
(1, 1, 1)	(0, 2, 2, 12)	6731.9981
(1, 1, 1)	(1, 0, 0, 12)	7175.897
(1, 1, 1)	(1, 0, 1, 12)	7122.622
(1, 1, 1)	(1, 0, 2, 12)	6899.2516
(1, 1, 1)	(1, 1, 0, 12)	7005.2029

(1, 1, 1)	(1, 1, 1, 12)	6894.904
(1, 1, 1)	(1, 1, 2, 12)	6660.8071
(1, 1, 1)	(1, 2, 0, 12)	7069.3568
(1, 1, 1)	(1, 2, 1, 12)	6986.6064
(1, 1, 1)	(1, 2, 2, 12)	6733.0962
(1, 1, 1)	(2, 0, 0, 12)	6932.5807
(1, 1, 1)	(2, 0, 1, 12)	6917.6449
(1, 1, 1)	(2, 0, 2, 12)	6901.1523
(1, 1, 1)	(2, 1, 0, 12)	6750.1797
(1, 1, 1)	(2, 1, 1, 12)	6730.9186
(1, 1, 1)	(2, 1, 2, 12)	6663.1175
(1, 1, 1)	(2, 2, 0, 12)	6794.4154
(1, 1, 1)	(2, 2, 1, 12)	6524.7122
(1, 1, 1)	(2, 2, 2, 12)	6734.9152
(1, 1, 2)	(0, 0, 0, 12)	7314.6325
(1, 1, 2)	(0, 0, 1, 12)	7073.878
(1, 1, 2)	(0, 0, 2, 12)	6831.5515
(1, 1, 2)	(0, 1, 0, 12)	7211.7793
(1, 1, 2)	(0, 1, 1, 12)	6849.3844
(1, 1, 2)	(0, 1, 2, 12)	6620.9638
(1, 1, 2)	(0, 2, 0, 12)	7358.1723
(1, 1, 2)	(0, 2, 1, 12)	6919.18
(1, 1, 2)	(0, 2, 2, 12)	6454.7355
(1, 1, 2)	(1, 0, 0, 12)	7104.946
(1, 1, 2)	(1, 0, 1, 12)	7033.5345
(1, 1, 2)	(1, 0, 2, 12)	6807.7713
(1, 1, 2)	(1, 1, 0, 12)	6938.2936
(1, 1, 2)	(1, 1, 1, 12)	6800.8752
(1, 1, 2)	(1, 1, 2, 12)	6621.164
(1, 1, 2)	(1, 2, 0, 12)	7008.0643
(1, 1, 2)	(1, 2, 1, 12)	6893.4486
(1, 1, 2)	(1, 2, 2, 12)	6641.6733
(1, 1, 2)	(2, 0, 0, 12)	6862.0188
(1, 1, 2)	(2, 0, 1, 12)	6848.2946
(1, 1, 2)	(2, 0, 2, 12)	6809.7631
(1, 1, 2)	(2, 1, 0, 12)	6681.0487
(1, 1, 2)	(2, 1, 1, 12)	6613.9498

(1, 1, 2)	(2, 1, 2, 12)	6623.1534
(1, 1, 2)	(2, 2, 0, 12)	6726.0159
(1, 1, 2)	(2, 2, 1, 12)	6685.757
(1, 1, 2)	(2, 2, 2, 12)	6442.4133
(1, 2, 0)	(0, 0, 0, 12)	7602.1236
(1, 2, 0)	(0, 0, 1, 12)	7362.8591
(1, 2, 0)	(0, 0, 2, 12)	7118.9318
(1, 2, 0)	(0, 1, 0, 12)	7529.3688
(1, 2, 0)	(0, 1, 1, 12)	7100.611
(1, 2, 0)	(0, 1, 2, 12)	6901.1906
(1, 2, 0)	(0, 2, 0, 12)	7686.0913
(1, 2, 0)	(0, 2, 1, 12)	7071.2363
(1, 2, 0)	(0, 2, 2, 12)	6915.9251
(1, 2, 0)	(1, 0, 0, 12)	7358.317
(1, 2, 0)	(1, 0, 1, 12)	7326.7295
(1, 2, 0)	(1, 0, 2, 12)	7097.3463
(1, 2, 0)	(1, 1, 0, 12)	7176.607
(1, 2, 0)	(1, 1, 1, 12)	7101.5355
(1, 2, 0)	(1, 1, 2, 12)	6901.8328
(1, 2, 0)	(1, 2, 0, 12)	7199.1387
(1, 2, 0)	(1, 2, 1, 12)	7177.3651
(1, 2, 0)	(1, 2, 2, 12)	6917.2335
(1, 2, 0)	(2, 0, 0, 12)	7109.0374
(1, 2, 0)	(2, 0, 1, 12)	7097.2521
(1, 2, 0)	(2, 0, 2, 12)	7099.2302
(1, 2, 0)	(2, 1, 0, 12)	6897.2889
(1, 2, 0)	(2, 1, 1, 12)	6858.6488
(1, 2, 0)	(2, 1, 2, 12)	6860.2055
(1, 2, 0)	(2, 2, 0, 12)	6849.5097
(1, 2, 0)	(2, 2, 1, 12)	6921.128
(1, 2, 0)	(2, 2, 2, 12)	6919.1936
(1, 2, 1)	(0, 0, 0, 12)	7475.3385
(1, 2, 1)	(0, 0, 1, 12)	7212.9728
(1, 2, 1)	(0, 0, 2, 12)	6972.4793
(1, 2, 1)	(0, 1, 0, 12)	7342.2553
(1, 2, 1)	(0, 1, 1, 12)	7019.4366
(1, 2, 1)	(0, 1, 2, 12)	6780.2228

(1, 2, 1)	(0, 2, 0, 12)	7496.171
(1, 2, 1)	(0, 2, 1, 12)	7098.386
(1, 2, 1)	(0, 2, 2, 12)	6824.8962
(1, 2, 1)	(1, 0, 0, 12)	7224.5751
(1, 2, 1)	(1, 0, 1, 12)	7190.4151
(1, 2, 1)	(1, 0, 2, 12)	6955.5139
(1, 2, 1)	(1, 1, 0, 12)	7006.0397
(1, 2, 1)	(1, 1, 1, 12)	7021.276
(1, 2, 1)	(1, 1, 2, 12)	6781.8492
(1, 2, 1)	(1, 2, 0, 12)	7021.3719
(1, 2, 1)	(1, 2, 1, 12)	7079.608
(1, 2, 1)	(1, 2, 2, 12)	6492.3282
(1, 2, 1)	(2, 0, 0, 12)	6981.8527
(1, 2, 1)	(2, 0, 1, 12)	6975.6988
(1, 2, 1)	(2, 0, 2, 12)	6957.5122
(1, 2, 1)	(2, 1, 0, 12)	6813.7929
(1, 2, 1)	(2, 1, 1, 12)	6801.3592
(1, 2, 1)	(2, 1, 2, 12)	6783.4661
(1, 2, 1)	(2, 2, 0, 12)	6877.7463
(1, 2, 1)	(2, 2, 1, 12)	6849.1545
(1, 2, 1)	(2, 2, 2, 12)	6828.4253
(1, 2, 2)	(0, 0, 0, 12)	7392.5409
(1, 2, 2)	(0, 0, 1, 12)	7138.792
(1, 2, 2)	(0, 0, 2, 12)	6896.9977
(1, 2, 2)	(0, 1, 0, 12)	7266.5062
(1, 2, 2)	(0, 1, 1, 12)	6931.1095
(1, 2, 2)	(0, 1, 2, 12)	6693.2795
(1, 2, 2)	(0, 2, 0, 12)	7416.4425
(1, 2, 2)	(0, 2, 1, 12)	6998.3157
(1, 2, 2)	(0, 2, 2, 12)	6723.2075
(1, 2, 2)	(1, 0, 0, 12)	7167.8784
(1, 2, 2)	(1, 0, 1, 12)	7110.0129
(1, 2, 2)	(1, 0, 2, 12)	6876.0484
(1, 2, 2)	(1, 1, 0, 12)	7003.7075
(1, 2, 2)	(1, 1, 1, 12)	6932.4233
(1, 2, 2)	(1, 1, 2, 12)	6695.1063
(1, 2, 2)	(1, 2, 0, 12)	7078.2751

Observation of change in storage of Kulekhani Reservoir using Standard Operating Policy
by Alija, Biplov, Dip Sagar, Hemanta, Kabindra, Saurab

115

(1, 2, 2)	(1, 2, 1, 12)	6976.5273
(1, 2, 2)	(1, 2, 2, 12)	6724.5785
(1, 2, 2)	(2, 0, 0, 12)	6925.8938
(1, 2, 2)	(2, 0, 1, 12)	6916.4777
(1, 2, 2)	(2, 0, 2, 12)	6877.9865
(1, 2, 2)	(2, 1, 0, 12)	6750.4319
(1, 2, 2)	(2, 1, 1, 12)	6734.1831
(1, 2, 2)	(2, 1, 2, 12)	6631.8858
(1, 2, 2)	(2, 2, 0, 12)	6801.0842
(1, 2, 2)	(2, 2, 1, 12)	6768.3187
(1, 2, 2)	(2, 2, 2, 12)	6726.4527
(2, 0, 0)	(0, 0, 0, 12)	7443.0407
(2, 0, 0)	(0, 0, 1, 12)	7215.4909
(2, 0, 0)	(0, 0, 2, 12)	6967.835
(2, 0, 0)	(0, 1, 0, 12)	7249.853
(2, 0, 0)	(0, 1, 1, 12)	6922.9683
(2, 0, 0)	(0, 1, 2, 12)	6689.4206
(2, 0, 0)	(0, 2, 0, 12)	7399.7806
(2, 0, 0)	(0, 2, 1, 12)	6967.9078
(2, 0, 0)	(0, 2, 2, 12)	6685.9495
(2, 0, 0)	(1, 0, 0, 12)	7180.518
(2, 0, 0)	(1, 0, 1, 12)	7114.1223
(2, 0, 0)	(1, 0, 2, 12)	6910.5412
(2, 0, 0)	(1, 1, 0, 12)	6939.3016
(2, 0, 0)	(1, 1, 1, 12)	6876.0578
(2, 0, 0)	(1, 1, 2, 12)	6691.1737
(2, 0, 0)	(1, 2, 0, 12)	6998.2273
(2, 0, 0)	(1, 2, 1, 12)	6744.3371
(2, 0, 0)	(1, 2, 2, 12)	6687.6
(2, 0, 0)	(2, 0, 0, 12)	6916.8995
(2, 0, 0)	(2, 0, 1, 12)	6890.9636
(2, 0, 0)	(2, 0, 2, 12)	6892.9197
(2, 0, 0)	(2, 1, 0, 12)	6665.3627
(2, 0, 0)	(2, 1, 1, 12)	6672.3977
(2, 0, 0)	(2, 1, 2, 12)	6674.2999
(2, 0, 0)	(2, 2, 0, 12)	6714.7628
(2, 0, 0)	(2, 2, 1, 12)	6476.9584

(2, 0, 0)	(2, 2, 2, 12)	6669.1712
(2, 0, 1)	(0, 0, 0, 12)	7455.236
(2, 0, 1)	(0, 0, 1, 12)	7170.4782
(2, 0, 1)	(0, 0, 2, 12)	6918.6429
(2, 0, 1)	(0, 1, 0, 12)	7243.7074
(2, 0, 1)	(0, 1, 1, 12)	6888.6587
(2, 0, 1)	(0, 1, 2, 12)	6624.9096
(2, 0, 1)	(0, 2, 0, 12)	7395.9975
(2, 0, 1)	(0, 2, 1, 12)	6813.9087
(2, 0, 1)	(0, 2, 2, 12)	6659.9814
(2, 0, 1)	(1, 0, 0, 12)	7150.4908
(2, 0, 1)	(1, 0, 1, 12)	7091.613
(2, 0, 1)	(1, 0, 2, 12)	6863.0389
(2, 0, 1)	(1, 1, 0, 12)	6928.8139
(2, 0, 1)	(1, 1, 1, 12)	6888.0014
(2, 0, 1)	(1, 1, 2, 12)	6658.3906
(2, 0, 1)	(1, 2, 0, 12)	6992.0687
(2, 0, 1)	(1, 2, 1, 12)	6783.5178
(2, 0, 1)	(1, 2, 2, 12)	6478.9349
(2, 0, 1)	(2, 0, 0, 12)	6895.0085
(2, 0, 1)	(2, 0, 1, 12)	6863.1377
(2, 0, 1)	(2, 0, 2, 12)	6865.0376
(2, 0, 1)	(2, 1, 0, 12)	6670.8418
(2, 0, 1)	(2, 1, 1, 12)	6626.5372
(2, 0, 1)	(2, 1, 2, 12)	6660.2259
(2, 0, 1)	(2, 2, 0, 12)	6707.2773
(2, 0, 1)	(2, 2, 1, 12)	6461.2944
(2, 0, 1)	(2, 2, 2, 12)	6451.8852
(2, 0, 2)	(0, 0, 0, 12)	7347.4282
(2, 0, 2)	(0, 0, 1, 12)	7091.0663
(2, 0, 2)	(0, 0, 2, 12)	6854.1468
(2, 0, 2)	(0, 1, 0, 12)	7206.1629
(2, 0, 2)	(0, 1, 1, 12)	6870.6935
(2, 0, 2)	(0, 1, 2, 12)	6636.5376
(2, 0, 2)	(0, 2, 0, 12)	7347.5084
(2, 0, 2)	(0, 2, 1, 12)	6920.7967
(2, 0, 2)	(0, 2, 2, 12)	6639.9204

Observation of change in storage of Kulekhani Reservoir using Standard Operating Policy
by Alija, Biplov, Dip Sagar, Hemanta, Kabindra, Saurab

117

(2, 0, 2)	(1, 0, 0, 12)	7107.5145
(2, 0, 2)	(1, 0, 1, 12)	7052.9474
(2, 0, 2)	(1, 0, 2, 12)	6828.6661
(2, 0, 2)	(1, 1, 0, 12)	6919.7926
(2, 0, 2)	(1, 1, 1, 12)	6870.4662
(2, 0, 2)	(1, 1, 2, 12)	6637.134
(2, 0, 2)	(1, 2, 0, 12)	6982.9464
(2, 0, 2)	(1, 2, 1, 12)	6843.9444
(2, 0, 2)	(1, 2, 2, 12)	6642.5483
(2, 0, 2)	(2, 0, 0, 12)	6862.4327
(2, 0, 2)	(2, 0, 1, 12)	6846.5881
(2, 0, 2)	(2, 0, 2, 12)	6830.1509
(2, 0, 2)	(2, 1, 0, 12)	6665.6067
(2, 0, 2)	(2, 1, 1, 12)	6656.6444
(2, 0, 2)	(2, 1, 2, 12)	6638.9929
(2, 0, 2)	(2, 2, 0, 12)	6702.8729
(2, 0, 2)	(2, 2, 1, 12)	6465.5796
(2, 0, 2)	(2, 2, 2, 12)	6640.6865
(2, 1, 0)	(0, 0, 0, 12)	7383.5003
(2, 1, 0)	(0, 0, 1, 12)	7168.2593
(2, 1, 0)	(0, 0, 2, 12)	6924.9891
(2, 1, 0)	(0, 1, 0, 12)	7291.0629
(2, 1, 0)	(0, 1, 1, 12)	6934.1452
(2, 1, 0)	(0, 1, 2, 12)	6699.8324
(2, 1, 0)	(0, 2, 0, 12)	7448.5296
(2, 1, 0)	(0, 2, 1, 12)	7005.5601
(2, 1, 0)	(0, 2, 2, 12)	6719.4961
(2, 1, 0)	(1, 0, 0, 12)	7141.8319
(2, 1, 0)	(1, 0, 1, 12)	7096.5138
(2, 1, 0)	(1, 0, 2, 12)	6893.1835
(2, 1, 0)	(1, 1, 0, 12)	6964.8575
(2, 1, 0)	(1, 1, 1, 12)	6875.1749
(2, 1, 0)	(1, 1, 2, 12)	6658.0907
(2, 1, 0)	(1, 2, 0, 12)	7033.9711
(2, 1, 0)	(1, 2, 1, 12)	6752.1469
(2, 1, 0)	(1, 2, 2, 12)	6720.8914
(2, 1, 0)	(2, 0, 0, 12)	6892.8578

(2, 1, 0)	(2, 0, 1, 12)	6874.5135
(2, 1, 0)	(2, 0, 2, 12)	6876.5114
(2, 1, 0)	(2, 1, 0, 12)	6701.7612
(2, 1, 0)	(2, 1, 1, 12)	6682.186
(2, 1, 0)	(2, 1, 2, 12)	6641.336
(2, 1, 0)	(2, 2, 0, 12)	6634.4917
(2, 1, 0)	(2, 2, 1, 12)	6478.2968
(2, 1, 0)	(2, 2, 2, 12)	6603.5387
(2, 1, 1)	(0, 0, 0, 12)	7343.6011
(2, 1, 1)	(0, 0, 1, 12)	7097.9554
(2, 1, 1)	(0, 0, 2, 12)	6864.9825
(2, 1, 1)	(0, 1, 0, 12)	7243.6492
(2, 1, 1)	(0, 1, 1, 12)	6832.9727
(2, 1, 1)	(0, 1, 2, 12)	6660.1985
(2, 1, 1)	(0, 2, 0, 12)	7391.1968
(2, 1, 1)	(0, 2, 1, 12)	6970.6574
(2, 1, 1)	(0, 2, 2, 12)	6691.5224
(2, 1, 1)	(1, 0, 0, 12)	7093.9549
(2, 1, 1)	(1, 0, 1, 12)	7063.865
(2, 1, 1)	(1, 0, 2, 12)	6842.2851
(2, 1, 1)	(1, 1, 0, 12)	6939.4899
(2, 1, 1)	(1, 1, 1, 12)	6892.7443
(2, 1, 1)	(1, 1, 2, 12)	6660.3535
(2, 1, 1)	(1, 2, 0, 12)	7014.4633
(2, 1, 1)	(1, 2, 1, 12)	6725.3117
(2, 1, 1)	(1, 2, 2, 12)	6693.2101
(2, 1, 1)	(2, 0, 0, 12)	6856.273
(2, 1, 1)	(2, 0, 1, 12)	6842.0687
(2, 1, 1)	(2, 0, 2, 12)	6843.4992
(2, 1, 1)	(2, 1, 0, 12)	6681.3565
(2, 1, 1)	(2, 1, 1, 12)	6603.7056
(2, 1, 1)	(2, 1, 2, 12)	6662.3081
(2, 1, 1)	(2, 2, 0, 12)	6603.5448
(2, 1, 1)	(2, 2, 1, 12)	6697.2163
(2, 1, 1)	(2, 2, 2, 12)	6695.0126
(2, 1, 2)	(0, 0, 0, 12)	7308.8328
(2, 1, 2)	(0, 0, 1, 12)	7073.1805

(2, 1, 2)	(0, 0, 2, 12)	6834.1099
(2, 1, 2)	(0, 1, 0, 12)	7213.5118
(2, 1, 2)	(0, 1, 1, 12)	6849.1267
(2, 1, 2)	(0, 1, 2, 12)	6620.8831
(2, 1, 2)	(0, 2, 0, 12)	7359.7787
(2, 1, 2)	(0, 2, 1, 12)	6833.1353
(2, 1, 2)	(0, 2, 2, 12)	6638.401
(2, 1, 2)	(1, 0, 0, 12)	7084.3605
(2, 1, 2)	(1, 0, 1, 12)	7033.3142
(2, 1, 2)	(1, 0, 2, 12)	6814.2328
(2, 1, 2)	(1, 1, 0, 12)	6920.2502
(2, 1, 2)	(1, 1, 1, 12)	6800.5418
(2, 1, 2)	(1, 1, 2, 12)	6573.7474
(2, 1, 2)	(1, 2, 0, 12)	6987.9834
(2, 1, 2)	(1, 2, 1, 12)	6747.9716
(2, 1, 2)	(1, 2, 2, 12)	6639.8757
(2, 1, 2)	(2, 0, 0, 12)	6844.0808
(2, 1, 2)	(2, 0, 1, 12)	6836.7421
(2, 1, 2)	(2, 0, 2, 12)	6816.1754
(2, 1, 2)	(2, 1, 0, 12)	6662.9326
(2, 1, 2)	(2, 1, 1, 12)	6595.4988
(2, 1, 2)	(2, 1, 2, 12)	6575.7765
(2, 1, 2)	(2, 2, 0, 12)	6705.4118
(2, 1, 2)	(2, 2, 1, 12)	6664.2539
(2, 1, 2)	(2, 2, 2, 12)	6641.6505
(2, 2, 0)	(0, 0, 0, 12)	7518.6983
(2, 2, 0)	(0, 0, 1, 12)	7299.5481
(2, 2, 0)	(0, 0, 2, 12)	7055.9203
(2, 2, 0)	(0, 1, 0, 12)	7437.7449
(2, 2, 0)	(0, 1, 1, 12)	7074.4265
(2, 2, 0)	(0, 1, 2, 12)	6835.3764
(2, 2, 0)	(0, 2, 0, 12)	7593.2696
(2, 2, 0)	(0, 2, 1, 12)	7141.3485
(2, 2, 0)	(0, 2, 2, 12)	6850.0518
(2, 2, 0)	(1, 0, 0, 12)	7275.7132
(2, 2, 0)	(1, 0, 1, 12)	7238.3278
(2, 2, 0)	(1, 0, 2, 12)	7028.8864

(2, 2, 0)	(1, 1, 0, 12)	7104.3608
(2, 2, 0)	(1, 1, 1, 12)	7055.3
(2, 2, 0)	(1, 1, 2, 12)	6836.1202
(2, 2, 0)	(1, 2, 0, 12)	7171.2977
(2, 2, 0)	(1, 2, 1, 12)	7088.7826
(2, 2, 0)	(1, 2, 2, 12)	6851.1377
(2, 2, 0)	(2, 0, 0, 12)	7024.6634
(2, 2, 0)	(2, 0, 1, 12)	7009.5847
(2, 2, 0)	(2, 0, 2, 12)	7011.4337
(2, 2, 0)	(2, 1, 0, 12)	6836.6774
(2, 2, 0)	(2, 1, 1, 12)	6815.5065
(2, 2, 0)	(2, 1, 2, 12)	6817.1014
(2, 2, 0)	(2, 2, 0, 12)	6766.45
(2, 2, 0)	(2, 2, 1, 12)	6835.2934
(2, 2, 0)	(2, 2, 2, 12)	6832.7511
(2, 2, 1)	(0, 0, 0, 12)	7422.8133
(2, 2, 1)	(0, 0, 1, 12)	7160.8971
(2, 2, 1)	(0, 0, 2, 12)	6921.7061
(2, 2, 1)	(0, 1, 0, 12)	7306.612
(2, 2, 1)	(0, 1, 1, 12)	6866.5795
(2, 2, 1)	(0, 1, 2, 12)	6740.6967
(2, 2, 1)	(0, 2, 0, 12)	7463.149
(2, 2, 1)	(0, 2, 1, 12)	7069.9211
(2, 2, 1)	(0, 2, 2, 12)	6797.3268
(2, 2, 1)	(1, 0, 0, 12)	7156.4653
(2, 2, 1)	(1, 0, 1, 12)	7139.9057
(2, 2, 1)	(1, 0, 2, 12)	6901.0226
(2, 2, 1)	(1, 1, 0, 12)	7005.8594
(2, 2, 1)	(1, 1, 1, 12)	6866.4772
(2, 2, 1)	(1, 1, 2, 12)	6626.5899
(2, 2, 1)	(1, 2, 0, 12)	7099.2547
(2, 2, 1)	(1, 2, 1, 12)	6738.9871
(2, 2, 1)	(1, 2, 2, 12)	6524.8377
(2, 2, 1)	(2, 0, 0, 12)	6910.8027
(2, 2, 1)	(2, 0, 1, 12)	6901.2211
(2, 2, 1)	(2, 0, 2, 12)	6903.0196
(2, 2, 1)	(2, 1, 0, 12)	6754.4963

Observation of change in storage of Kulekhani Reservoir using Standard Operating Policy
by Alija, Biplov, Dip Sagar, Hemanta, Kabindra, Saurab

121

(2, 2, 1)	(2, 1, 1, 12)	6626.5663
(2, 2, 1)	(2, 1, 2, 12)	6744.1144
(2, 2, 1)	(2, 2, 0, 12)	6827.5084
(2, 2, 1)	(2, 2, 1, 12)	6469.1393
(2, 2, 1)	(2, 2, 2, 12)	6800.723
(2, 2, 2)	(0, 0, 0, 12)	7329.6623
(2, 2, 2)	(0, 0, 1, 12)	7090.4433
(2, 2, 2)	(0, 0, 2, 12)	6856.8335
(2, 2, 2)	(0, 1, 0, 12)	7241.7967
(2, 2, 2)	(0, 1, 1, 12)	6899.0795
(2, 2, 2)	(0, 1, 2, 12)	6668.2079
(2, 2, 2)	(0, 2, 0, 12)	7381.3949
(2, 2, 2)	(0, 2, 1, 12)	6999.1423
(2, 2, 2)	(0, 2, 2, 12)	6715.41
(2, 2, 2)	(1, 0, 0, 12)	7106.671
(2, 2, 2)	(1, 0, 1, 12)	7071.3873
(2, 2, 2)	(1, 0, 2, 12)	6840.4038
(2, 2, 2)	(1, 1, 0, 12)	6953.7999
(2, 2, 2)	(1, 1, 1, 12)	6900.4154
(2, 2, 2)	(1, 1, 2, 12)	6667.5262
(2, 2, 2)	(1, 2, 0, 12)	7044.563
(2, 2, 2)	(1, 2, 1, 12)	6970.8805
(2, 2, 2)	(1, 2, 2, 12)	6716.9702
(2, 2, 2)	(2, 0, 0, 12)	6868.633
(2, 2, 2)	(2, 0, 1, 12)	6859.1342
(2, 2, 2)	(2, 0, 2, 12)	6843.1324
(2, 2, 2)	(2, 1, 0, 12)	6706.3179
(2, 2, 2)	(2, 1, 1, 12)	6688.901
(2, 2, 2)	(2, 1, 2, 12)	6669.5245
(2, 2, 2)	(2, 2, 0, 12)	6772.087
(2, 2, 2)	(2, 2, 1, 12)	6741.414
(2, 2, 2)	(2, 2, 2, 12)	6718.8039

8 References

Bevans, R. (2023, june 22). *scribbr*. Retrieved from Akaike Information Criterion | When & How to Use It: https://www.scribbr.com/statistics/akaike-information-criterion/

Bourdeau-Goulet, S.-C. H. (2021). Comparisons between CMIP5 and CMIP6 models: Simulations of climate indices influencing food security, infrastructure resilience, and human health in Canada. *Earth's Future*, e2021EF001995.

Chalid, A. a. (2020). Utilization of a pond in East Jakarta for a sustainable urban drainage system model. *IOP Conference Series: Earth and Environmental Science, 437*, 012018.

DhavalDwivedi. (2019). *Flood discharge at various return periods using Gumbel's extreme value distribution | Hydrology*. Retrieved from youtube: https://www.youtube.com/watch?v=RE7Q4NDVPQQ&t=521s&ab_channel=DhavalDwivedi

gpt, c. (2024). *open AI*. Retrieved from https://chat.openai.com/

JICA. (1993). *Disaster Prevention Study in the Central Development Region of Nepal.*

JICA. (2003). *JICA KULEKHANI III HPP.* JICA.

K. Srinivasan, T. N. (1999). Mixed-integer programming model for reservoir performance optimization. *Journal of Water Resources Planning and Management*, 298-301.

K.N. Dulal, B. (2015). *Engineering Hydrology.* Apex Educational Academy.

Kirpich, Z. (1940). In *Time of Concentration in small agricultural watersheds* (p. 362).

Montgomery DC, P. E. (2012). Introduction to linear regression analysis. *John Wiley & Sons,*.

Moriasi, D. e. (2007). Model Evaluation Guidelines for Systematic Quantification of Accuracy in Watershed Simulations. *Transactions of the ASABE*, 885-900.

Nepal, D. o. (2024). Retrieved from Hydrological Stations: https://www.dhm.gov.np/hydology/hydrological-stations

Omar M. A. Mahmood Agha, S. Ç. (2017). Homogeneity Analysis of Precipitation Series in North Iraq. *IOSR Journal of Applied Geology and Geophysics (IOSR-JAGG)*, 57-63.

Rijal, K. (2014). Comparative Study of Flood Calculation Approaches, a Case Study of East Rapti River Basin, Nepal. *Hydro Nepal: Journal of Water, Energy and Environment*.

Saephan, S. (2022, February 26). *Open GIS Lab*. Retrieved from Creating Contours From DEM using QGIS: https://opengislab.com/blog/tag/SRTM-Downloader+plugin+QGIS

Stedinger, J. (1984). Performance of LDR models for preliminary design and reservoir operation. *Water Resources Research*, 215-224.

Berg, P., Feldmann, H., & Panitz, H.-J. (2012). Bias correction of high resolution regional climate model data. *Journal of Hydrology*, *448–449*, 80–92.

Hamed, M. M., Nashwan, M. S., & Shahid, S. (2022). A novel selection method of CMIP6 GCMs for robust climate projection. *International Journal of Climatology*, *42*(8), 4258–4272.

Jakob Themeßl, M., Gobiet, A., & Leuprecht, A. (2011). Empirical-statistical downscaling and error correction of daily precipitation from regional climate models. *International Journal of Climatology*, *31*(10), 1530–1544.

Jolliff, J. K., Kindle, J. C., Shulman, I., Penta, B., Friedrichs, M. A. M., Helber, R., & Arnone, R. A. (2009). Summary diagrams for coupled hydrodynamic-ecosystem model skill assessment. *Journal of Marine Systems*, *76*(1), 64–82.

Liang, Z., Tang, T., Li, B., Liu, T., Wang, J., & Hu, Y. (2017). Long-term streamflow forecasting using SWAT through the integration of the random forests precipitation generator: Case study of Danjiangkou Reservoir. *Hydrology Research*, *49*(5), 1513–1527.

Nyunt, C. T., Koike, T., & Yamamoto, A. (2016). Statistical bias correction for climate change impact on the basin scale precipitation in Sri Lanka, Philippines, Japan and Tunisia [Preprint].

Willmott, C. J., & Matsuura, K. (2005). Advantages of the mean absolute error (MAE) over the root mean square error (RMSE) in assessing average model performance. *Climate Research*, *30*(1), 79–82.

O'Neill, B. C., Kriegler, E., Riahi, K., Ebi, K. L., Hallegatte, S., Carter, T. R., Mathur, R., & van Vuuren, D. P. (2014). A new scenario framework for climate change research: The concept of shared socioeconomic pathways. *Climatic Change*, *122*(3), 387–400.

Wayne, G. (2013). The Beginner's Guide to Representative Concentration Pathways. 25.